UC Berkeley
UC Berkeley Electronic Theses and Dissertations

Title
Intersections of Nutrient Availability, Heterochromatic Silencing, Growth, Aging and DNA Damage Repair in Saccharomyces cerevisiae

Permalink
https://escholarship.org/uc/item/9ft2m3hv

Author
McCleary, David Frankel

Publication Date
2016

Peer reviewed|Thesis/dissertation

eScholarship.org Powered by the California Digital Library
University of California

Intersections of Nutrient Availability, Heterochromatic Silencing, Growth, Aging and DNA Damage Repair in *Saccharomyces cerevisiae*

By

David Frankel McCleary

A dissertation submitted in partial satisfaction of the

requirements for the degree of

Doctor of Philosophy

In

Molecular and Cell Biology

in the

Graduate Division

of the

University of California, Berkeley

Committee in charge:

Professor Jasper D. Rine, Chair
Professor Michael B. Eisen
Professor Andrew Dillin
Professor John E. Dueber

Fall 2016

Abstract

Intersections of Nutrient Availability, Heterochromatic Silencing, Growth, Aging and DNA Damage Repair in *Saccharomyces cerevisiae*

By

David Frankel McCleary

Doctor of Philosophy in Molecular and Cell Biology

University of California, Berkeley

Professor Jasper D. Rine, Chair

Calorie restriction extends lifespan in organisms as diverse as yeast and mammals through incompletely understood mechanism(s). The role of NAD^+-dependent deacetylases, known as Sirtuins, in this process, particularly in the yeast *S. cerevisiae* is controversial.

In Chapter 1, I measured chronological lifespan of wild-type and *sir2Δ* strains over a higher glucose range than typically used for studying yeast calorie restriction. *sir2Δ* extended lifespan in high-glucose synthetic complete medium, and had little effect in low-glucose medium, revealing a partial role for Sir2 in the calorie restriction response under these conditions. I measured growth, glucose consumption, and pH of these cultures and revealed a mild effect of *sir2Δ* that inhibited growth, lowered glucose consumption, and increased extracellular pH. Buffering of growth medium eliminated the *sir2Δ*-dependent extension of chronological lifespan, as did replacing stationary-phase media with water. Replacing medium with water at stationary phase actually led to a *sir2Δ*-dependent reduction in lifespan in high-glucose. Growth on high levels of other fermentable sugars still resulted in the *sir2Δ*-dependent extension of lifespan, whereas growth on high levels of glycerol, a non-fermentable carbon source, did not allow for *sir2Δ*-dependent lifespan extension. When cells were grown in high- or low-glucose yeast peptone medium, large amounts of stationary-phase adaptive regrowth were observed, especially in high-glucose cultures. This regrowth complicated analysis of chronological aging. Interestingly, high-glucose yeast peptone cultures had dramatically decreased initial viability as compared to low-glucose yeast peptone or any other media tested. Also of interest, adaptively regrown cells from high-glucose yeast peptone cultures displayed enhanced growth, a trait that was heritable.

In Chapter 2, I measured chronological lifespan of wild-type and *sir2Δ* strains in rich yeast peptone medium with a newly-developed genetic strategy. This approach revealed that *sir2Δ* shortened lifespan in low glucose while having little effect in

high glucose, revealing a partial role for Sir2 in calorie restriction-mediated lifespan extension in yeast peptone medium. In complete minimal media like synthetic complete, Sir2 shortened lifespan as glucose levels increased, whereas in rich media, Sir2 extended lifespan as glucose levels decreased. Both of these phenotypes are consistent with roll(s) for Sir2 in the calorie restriction response. Using a second genetic strategy to measure the strength of gene silencing at *HML*, I determined increasing glucose stabilized Sir2-based silencing during growth on complete minimal media. Conversely, increasing glucose destabilized Sir-based silencing during growth on rich media, specifically during late cell divisions. In rich medium, silencing was far less stable in high glucose than in low glucose during stationary phase. Therefore, Sir2 is involved in a response to nutrient cues including glucose that regulates chronological aging, possibly through Sir2-dependent modification of chromatin or deacetylation of a non-histone protein.

In Chapter 3, I investigated the origins of a color change of the growth medium at stationary phase when *sir2Δ* cells were grown on 3% glycerol synthetic complete medium. *sir2Δ* cultures eventually turned a yellow-brown color while wild-type cultures remained near-white throughout stationary phase. To determine whether the color change was caused by wild-type and *sir2Δ* cells having different levels of anabolism or catabolism of any small molecules, I performed gas chromatography and mass spectroscopy on filtered medium from wild-type and *sir2Δ* stationary-phase cultures. Quinoline and several chemical derivatives were highly enriched in filtered *sir2Δ* medium relative to wild-type. These molecules in solution are reported to have a yellow-brown color, consistent with my observations. GC-MS analysis of fresh 3% glycerol synthetic complete medium revealed that these quinoline compounds were present before cultures were seeded. Thus, wild-type cultures catabolized these molecules at a higher rate than *sir2Δ* cultures, removing them from the extracellular environment. The quinoline compounds identified here are biosynthesized from tryptophan in some organisms, and are closely related to known UV-degradation products of tryptophan. Closely related compounds including kynurenine and quinolinic acid are also chemical intermediates of the yeast kynurenine pathway, which generates NAD^+ from tryptophan. Since sirtuins including Sir2 are the only enzymes that consume NAD^+ in yeast, loss of Sir2 could lead to less kynurenine pathway activity, limiting consumption of quinoline compounds that formed either through UV-degradation or catabolism of tryptophan.

In Chapter 4, I exploited a microfluidics approach to investigate yeast replicative lifespan using the same calorie restriction paradigm used to investigate chronological lifespan in past chapters. I used a microfluidics chip, provided by Dr. Hao Li, which was designed to trap aging mother cells while washing away smaller, newborn daughter cells. By filming multiple positions on the chip over the course of a single experiment, I was able to count the number of offspring given off by dozens of cells at once. Surprisingly, wild-type cells had the same replicative lifespan in high- and low-glucose, defying the logic of calorie restriction and the results of past

studies of the effects of calorie restriction on replicative lifespan. Since classical replicative lifespan experiments involve micromanipulating daughter cells away from a stationary mother cell growing on solid media, that mother cell is experiencing a changing environment as it metabolizes essential nutrients locally and generates waste. In the case of my microfluidics approach, mother cells are experiencing a static environment, since fresh media is constantly flowing through the chip. Therefore, a changing extracellular environment is likely necessary for calorie restriction to increase replicative lifespan. Additional experiments will be necessary to determine this with certainty.

Finally, in Chapter 5, we investigate a report claiming Sir2 protein was recruited to dicentric chromosomes under tension, and such chromosomes are reported to be especially vulnerable to breakage in *sir2Δ* mutants. We found that the loss of viability in such mutants was an indirect effect of the repression of non-homologous end joining in Sir- mutants, and that the apparent recruitment of Sir2 protein to chromosomes under tension was likely due to methodological weakness in early chromatin immunoprecipitation studies.

To Sara, my partner

To Jasper, my advisor

To workers everywhere, my comrades

Table of Contents:

Introduction iii

Acknowledgements x

Part I: Intersections of nutrient availability, growth, aging, and heterochromatic silencing 1

Chapter 1: Impact of Sir2 on yeast chronological lifespan and growth across different carbon sources and concentrations 2

Chapter 2: Nutritional control of chronological aging and heterochromatin in *Saccharomyces cerevisiae* 25

Chapter 3: Sir-dependent metabolism of quinolone derivatives during growth on a non-fermentable carbon source 57

Chapter 4: Microfluidic analysis of yeast replicative lifespan during growth on high and low glucose media 67

Part II: Sir silencing and mating-type control of DNA damage repair 78

Chapter 5: Sir protein-independent repair of dicentric chromosomes in *Saccharomyces cerevisiae* 79

References 94

Introduction

Sirtuins

Sirtuins are NAD^+-dependent protein deacetylases (Landry *et al.,* 2000a; Smith *et al.,* 2000; Imai *et al.,* 2000) conserved from bacteria to humans (Brachmann, *et al*., 1995). In the budding yeast *Saccharomyces cerevisiae*, Sir proteins are necessary for both the establishment and maintenance of heterochromatic gene silencing (Rusche *et al.,* 2003; Kueng *et al.,* 2013). Sir2, the founding member of the Sirtuin protein family, removes acetyl modifications from N-terminal tails of histones H3 and H4, with acetylated Lysine 16 on H4 being its primary target (Imai, *et al*., 2000). These deacetylated histone tails serve as high-affinity binding sites for Sir3 and Sir4 proteins at both the telomeres and the silent mating-type loci (Hecht *et al.,* 1995), where Sir2, Sir3, and Sir4 assemble into a functional complex known as the Sir2/3/4 complex or Sir complex (Moazed *et al.,* 1997). Sir2 also deacetylates histone tails as part of the RENT complex with Net1 and Cdc14 to repress PolII transcription and recombination in the rDNA (Gottlieb and Esposito, 1989; Smith and Boeke, 1997; Shou, *et al*., 1999; Straight, *et al.*, 1999). Formation of Sir-mediated heterochromatin represses transcription and recombination through the occlusion of necessary factors involved in these processes (Loo and Rine, 1994; Singh and Klar, 1992; Gottschling, 1992; Steakley and Rine, 2015). In addition to acetylated H3 and H4 histones, non-histone substrates of Sir2, including Pck1 (Phosphoenolpyruvate Carboxykinase 1; Lin, *et al*., 2009) and Ifh1 (Downey, *et al*., 2013), have been identified. Pck1 is a conserved enzyme that catalyzes the rate-limiting step in gluconeogenesis (Valdés-Hevia, *et al*., 1989; Jiang, *et al*., 2011), whereas Ifh1 is a ribosomal protein transcription factor (Wade, *et al*., 2004). Sirtuins in other organisms have many non-histone substrates (Martínez-Redondo and Vaquero, 2013).

Beyond Sir2, *S. cerevisiae* has four additional NAD^+-dependent deacetylases belonging to the Sirtuin family, named Hst1-4. The only known substrates of Hst1-4 are acetylated H3 and H4 histones. Hst1 deacetylates histones at specific promoters as part of the Sum1 complex with Sum1 and Rfm1 (McCord, *et al.*, 2003), repressing α-mating-type genes (Zill and Rine, 2008), as well as genes involved in middle sporulation (Xie, *et al*., 1999) and de novo NAD^+ synthesis (Bedalov, *et al*., 2003). Hst2 deacetylates Lysine 16 on histone H4, but only during mitosis (Vaquero, *et al*., 2006) when it is transported into the nucleus from the cytoplasm, where it is otherwise found (Wilson, *et al*., 2006). Hst3 and Hst4 are necessary for preservation of genome integrity through deacetylation of Lysine 56 of histone H3 (Celic, *et al*., 2006). Production of Hst3 and Hst4 protein is restricted to late S-phase and early mitosis, where they remove acetyl marks from newly deposited histones in recently replicated DNA (Maas, *et al*., 2006).

Aging

Biological aging is a complex process, occurring in most if not all organisms (Rose, 1991), that involves changes in physiology over time (Rose, *et al.* 2012). Although symmetrically dividing organisms, including most bacteria, have long been thought to be immortal, recent research has challenged this assumption (Gómez, 2010; Książek, 2010). Late in life, especially once an organism has passed its peak in reproductive fitness, these physiological changes are often unfavorable for survival, eventually leading to death (Rose, *et al.* 2012). Aging in humans is associated with the onset of chronic diseases like heart disease, cancer, and neurodegenerative disorders. Lifespan is a measure of the absolute length of life, from birth to death, of an organism, while healthspan, especially in humans, is used to describe the period of lifespan where biological processes are still functioning at optimal or close to optimal levels (Tatar, 2009). The budding yeast *Saccharomyces cerevisiae* has been useful in the study of cellular aging, with many genes important in mammalian aging having been first identified in studies of yeast aging (Longo, *et al.* 2012)

There have been two main approaches to the study of yeast lifespan (Longo, *et al.* 2012). The first focuses on replicative lifespan, defined as the number of progeny an individual yeast mother cell can produce through mitosis before it can no longer divide, entering senescence (Mortimer and Johnston, 1959). Replicative lifespan serves as a model of aging in actively dividing cell-types, such as germ line stem cells (Jazwinski, 1990). The second measure of yeast lifespan, chronological lifespan, is defined as the length of time that cells in a stationary phase culture remain viable and able to reenter the cell cycle upon introduction to fresh culture medium (Fabrizio and Longo, 2007). Chronological lifespan serves as a model of aging in post-mitotic cell-types, such as terminally differentiated cells (Longo, *et al.* 2012). Sir2 regulates aging in both of these yeast-aging paradigms. For replicative aging, deletion of *SIR2* shortens lifespan, and overexpression of *SIR2* extends it (Kaeberlein, *et al.* 1999). For chronological aging, deletion of *SIR2* dramatically extends lifespan under conditions of extreme nutrient depletion (Fabrizio, *et al*., 2005). Sirtuins also regulate aging in other organisms (Wątroba and Szukiewicz, 2016).

Calorie Restriction

Calorie restriction, where calorie intake is reduced without a reduction in essential nutrients, extends lifespan and healthspan in organisms as diverse as yeast (Lin, *et al.* 2002), invertebrates (Klass, 1977), fish (Comfort, 1963), and mammals (McCay, 1935), through incompletely understood mechanism(s). Both replicative and chronological yeast lifespan is increased with calorie restriction (Kaeberlein, *et al.* 2004; Lin, *et al.* 2000; Smith, *et al.* 2007). Nutrient sensing and signaling pathways such as Insulin/IGF, Tor and AMP Kinase pathways have been implicated as effectors in calorie-restriction-mediated longevity in various organisms (Anderson and Weindruch, 2010), although exactly how they mediate the beneficial aging effects of calorie restriction requires further investigation. Changes in

mitochondrial function (Anderson and Weindruch, 2007; Zahn, *et al.* 2007), fat usage and storage (Zhu, *et al.* 2004; Zhu, *et al.* 2007), and insulin signaling (Chiba, *et al.* 2007; Mair and Dillin, 2008) are thought to play downstream roles in some organisms.

Controversial Role of Sirtuins in Calorie Restriction

In addition to the nutrient sensing pathways discussed above, Sirtuins have been implicated in calorie restriction-mediated longevity (Guarente and Picard, 2005). The work connecting Sirtuins to life extension via calorie restriction originally came from replicative aging studies of *S. cerevisiae*. *S. cerevisiae* grown on 0.5% glucose, considered by some as a calorie-restricted diet, have significantly longer replicative lifespans than cells grown on 2% glucose, typically considered a calorically unrestricted diet. The longevity of 0.5% glucose-grown cells was initially shown to be dependent on Sir2: *sir2Δ* cells experienced no lifespan extension with calorie restriction (Lin, *et al.* 2002). The authors argued that calorie content of the growth medium could influence NAD^+ levels by affecting the redox balance of the cell. Since Sir2 depends on NAD^+ for its enzymatic function, changing NAD^+ levels could activate or inhibit Sir2, leading to downstream changes in aging and lifespan. In addition to being activated by NAD^+, Sir2 is inhibited by nicotinamide (NAM), a compound produced when Sir2 consumes a molecule of NAD^+ as part of the deacetylation reaction (Bitterman, *et al.* 2002). A network of enzymes recycles NAM back to NAD^+, preventing NAM-induced inactivation of Sir2 (Sandmeier, *et al.* 2002). Several of these enzymes are influenced by the levels of a variety of nutrients, including nitrogen (Medvedik, *et al.* 2007), phosphorus (Lu, *et al.* 2011), and carbon (Gasch, *et al.* 2000), providing an alternate mechanism for nutrient sensing by Sir2.

Although observations linking Sir2 and calorie restriction were later supported by studies in other organisms (Tissenbaum and Guarente, 2001; Rogina and Helfand, 2004; Bordone, *et al.* 2007), the original yeast conclusions (Kaeberlein, *et al.* 2004), as well as related work in worms and flies (Burnett, *et al.* 2011) has since been questioned. Additionally, studies of yeast chronological lifespan have revealed no role for Sir2 in the calorie-restriction aging response (Smith, *et al.* 2007; Kaeberlein, *et al.* 2006) despite Sir2's ability to regulate chronological lifespan under some conditions (Fabrizio, *et al*. 2005). The discrepancies in the literature, particularly with respect to replicative aging, have been attributed to differences in strain background and media composition (Couzin-Frankel, 2011), leaving the role of Sir2 in calorie restriction, particularly in yeast, uncertain.

Media Composition

Concerns over slight differences in media composition are not without logic. The mechanism(s) of calorie restriction-mediated longevity points to evolutionarily conserved nutrient sensing and signaling pathways like Insulin/IGF1 (Gesing, *et al.* 2014), AMPK (Greer, *et al.* 2007), RAS/PKA (Wei, *et al.* 2008), Tor/Sch9 (Kaeberlein, 2005), and possibly Sir2 (Guarente and Picard, 2005; Kaeberlein and Powers, 2007).

The activities of these pathways are modified not just by sugar concentration, but also by the levels of many other nutrients. The levels of these nutrients, and likely others, could in principle affect aging characteristics including the response to calorie restriction. Aging and the effect of calorie restriction in one type of growth medium might look quite different than it does elsewhere.

Yeast replicative aging is generally studied on yeast peptone medium (YP), while yeast chronological aging is studied almost exclusively on synthetic complete minimal medium (SC) (Longo, *et al*., 2012). SC has high ammonium sulfate levels, and is weakly buffered against changes in pH compared to natural yeast substrates (Oliva, *et al.* 2011; Garde-Cerdán, *et al.* 2011; Sanchez, 2008; Coghe, *et al.* 2005) and YP (Weinberger, *et al.* 2010). SC medium is used in chronological aging studies because yeast grown to saturation in this medium arrest efficiently in stationary phase, with most if not all cells remaining quiescent until plated to fresh medium (Longo and Fabrizio, 2012). A molecular mechanism linked to pH in yeast has been proposed for chronological aging broadly and the calorie restriction response specifically (Burtner, *et al.* 2009), but it is unclear if this applies to cells grown in well-buffered environments.

A New Calorie Restriction Paradigm

It is important to note that there is no universally agreed upon calorie restriction protocol. The full-calorie, ad libitum, diet used is somewhat arbitrary, and varies from organism to organism (Koubova and Guarente, 2003; Taormina and Mirisola, 2014; Piper and Bartke, 2008). The calorie-restricted diet used is a function of where lifespan extension is observed for that specific organism, and can vary from a 25% reduction to a 75% or more reduction (Koubova and Guarente, 2003). In worms, calorie restriction is often implemented through a 10-fold or higher dilution of bacteria used for feeding (Taormina and Mirisola, 2014). In flies, absolute restriction of feeding is difficult and so manipulations in the ratio of protein to carbohydrate are used to extend lifespan, and different labs study a variety of different paradigms (Piper and Bartke, 2008). In mice, a 30-40% reduction below an ad libitum diet is used (Piper and Bartke, 2008).

The arbitrary nature of calorie restriction protocols is especially evident in replicative and chronological aging studies with *S. cerevisiae.* Both protocols use 2% glucose as the ad libitum, high calorie diet[4]. But in nature, *S. cerevisiae* seems particularly well-adapted to high-sugar environments, with many yeast substrates containing well over 10% sugar by weight. For reference, brewing wort typically ranges from 8-12% w/v sugar (Coghe, *et al.* 2005), tree saps contain as much as 16% sugar (Sanchez, 2008), and grapes can contain over 20% sugar (Oliva, *et al.* 2011; Garde-Cerdán, 2011). All of these substrates are favored environments of *S. cerevisiae*.

There is also evolutionary evidence pointing to *S. cerevisiae* being adapted specifically to high-sugar environments. An ancestor of *S. cerevisiae* underwent a whole-genome duplication roughly 40 million years ago (Wolfe and Shields, 1997; Kellis, *et al.*, 2004). Since then, one of two ohnologs (gene paralogs resulting from a

whole genome duplication) has been lost for ~90% of all genes (Byrne and Wolfe, 2005). Interestingly, half of the ten enzymes involved in glycolysis, the first step in sugar catabolism, have been retained in duplicate in *S. cerevisiae*, hinting at an outsized importance of glycolysis in *S. cerevisiae's* evolutionary history (Conant and Wolfe, 2007). This conservation would make sense if *S. cerevisiae* spent a lot of time in high sugar environments, where glycolysis, rather than oxidative phosphorylation, would be the primary mode of energy production. Increased fermentative capacity would confer a growth advantage in high sugar environments, and could explain why these glycolytic enzymes were preferentially retained in duplicate (Conant and Wolfe, 2007).

Despite this ecological and evolutionary evidence, 2% glucose has been the standard sugar concentration in the majority of *S. cerevisiae* laboratory research papers over the last 100 years. The choice of 2% glucose is practical, as the growth rate of yeast is fairly constant between 2% and 20% or more glucose (Slator, 1908; White, 1955). Rather than 2% glucose being calorically relevant, especially in studies of calorie restriction, it instead seems to be a relic of laboratory economic history. It is possible the discrepancies in the literature over Sir2's role in calorie restriction-mediated longevity is due to the "full-calorie" diet itself being on the edge of calorie restriction for *S. cerevisiae*. If true, using a higher concentration of sugar for the full-calorie diet could expand the dynamic range of phenotypic measurement, allowing previously missed effects of Sir2 on lifespan to be revealed.

Sirtuins, Mating Type, and DNA Damage Repair

The Sir2/3/4 complex is essential for the proper regulation of cell type. Haploid yeast express a single mating-type locus allele, designated either *MATa* or *MATα*. Yeast also has additional copies of *MATa* and *MATα* genes at the *HMRa* and *HMLα* loci, respectively, which are transcriptionally silenced by the Sir proteins (Rine *et al.,* 1979; Klar *et al*., 1981; Rine and Herskowitz, 1987). Yeast strains with the *HO* allele can switch their mating-type by undergoing a double-stranded DNA break at the *MAT* locus followed by gene conversion, with *MAT* being the recipient of genetic information from one of these silenced donor loci. *MATa* and *MATα* haploid cells can mate, producing an a/α diploid. Two proteins encoded by the *MAT* alleles, a1 and α2, form a heterodimer that represses haploid-specific genes including some of those responsible for non-homologous end joining (Aström *et al*., 1999; Haber, 2012).

In many organisms, including the fission yeast *S. pombe* and most eukaryotes, heterochromatin forms near and at the centromere where it contributes to the fidelity of chromosome segregation (Allshire and Karpen, 2008; Allshire and Ekwall, 2015). *S. cerevisiae* centromeres have stood out as an exception due to their lack of heterochromatin. However, there is a report of a role for *S*. *cerevisiae* Sir2 in maintaining chromatin compaction when a chromosome is under artificial tension (Thrower and Bloom, 2001). This study used a strain with a second centromere, whose function was made conditional by being under the control of the *GAL1* promoter (hereafter *GALCEN3* after Thrower and Bloom), 45kb to the left of the

endogenous centromere on chromosome III. In cells grown in medium containing glucose, the promoter is inactive and the conditional centromere is functional. In cells grown in medium containing galactose, the promoter is active, significantly inhibiting the function of this second centromere. The strain also contains a 10.1kb *lacO* array between the centromeres, and a *LacI-GFP* fusion gene to allow visualization of chromosome stretching during anaphase (Thrower and Bloom, 2001).

If microtubules emanating from opposite spindle poles attach to two functional centromeres on a single chromosome during mitosis, the chromosome will usually break (Brock and Bloom, 1994). Dramatic stretching of the chromosome is observed by microscopy in *sir2Δ* and *ku70Δ/80Δ* mutants before a break occurs. The extent of stretching was reported as consistent with a near-complete loss of higher-order chromosome structure. In addition to stretching, *sir2Δ* and *ku70Δ/80Δ* mutants also suffered a significant drop in viability when the second centromere was active. Chromatin immunoprecipitation (ChIP) with anti-Sir2 sera using primers complementary to the *lacO* array revealed enrichment of Sir2, but only under conditions in which the second centromere was active. No ChIP signal was observed when the second centromere was inactive, implying that Sir2 bound *lacO* chromatin only when it was under tension (Thrower and Bloom, 2001). This result was potentially of great interest as it raised the possibility of condition-dependent assembly of Sir-protein based heterochromatin at repeated sequences and potentially at yeast centromeres when put under tension.

Overview

In Chapter 1, I investigate the impact of Sir2 on growth and chronological aging across a variety of carbon sources and concentrations. I identify several novel *sir2Δ* growth and aging phenotypes, and establish a new paradigm of yeast calorie restriction where Sir2 is necessary for full life extension via calorie restriction.

In Chapter 2, I identify several breakdown products of tryptophan whose metabolism is regulated by Sir2 during growth and aging in glycerol, a non-fermentable carbon source. These metabolites, related to quinoline, accumulate in aging *sir2Δ* cultures and lead to a yellow-brown coloration of these cultures.

In Chapter 3, I investigate the replicative lifespan of wild-type cells in high- and low-glucose media using a microfluidics approach. I determine that replicative lifespan is nearly identical in these conditions. Since fresh media is constantly flowing through the microfluidic chip, life extension via calorie restriction during replicative aging observed in other experiments is likely due to changes in the external media environment during metabolism.

In Chapter 4, I compare Sir2's effect on chronological lifespan and heterochromatic silencing in high- and low-glucose complete minimal medium to Sir2's effect in high- and low-glucose yeast peptone medium. To accomplish this, I developed a genetic strategy to overcome an obstacle in our ability to study chronological aging in nutrient-rich, well-buffered media like yeast peptone. I revealed seemingly distinct roles for Sir2 in calorie restriction-mediated longevity in

both media environments. I also reveal opposite effects of increasing glucose on Sir-based heterochromatic silencing at the silent mating locus *HML* in complex minimal medium and yeast peptone medium. In high-glucose yeast peptone medium, a large proportion of stationary-phase cells lose silencing, while few cells lose silencing in low-glucose medium.

Finally, in Chapter 5, my co-authors and I follow up on a previous study that claimed a role for Sir2 in preserving chromatin compaction when a chromosome is under tension. Sir2 preserves the viability of a conditionally dicentric strain, specifically when the second centromere is activated, and chromatin precipitation (ChIP) using Sir2 antisera seemed to show Sir2 enrichment in the region between the two centromeres. We revealed that preservation of viability in the dicentric strain was dependent on the Sir2/3/4 complex, and that the viability defect was rescued by deletion of *HML*. Sir2/3/4 regulation of mating type therefore mediates the preservation of viability. We also failed to observe Sir2 enrichment via ChIP as had previously been claimed. Previously-documented mating-type regulation of nonhomologous end joining is the likely explanation for the observed phenotypes, rather than direct binding of Sir proteins to a chromosome under tension.

Acknowledgements

I would first like to thank my dissertation advisor, Jasper Rine, for patiently guiding me through this work for the last 5 years. Jasper has been unbelievably supportive of my career, even while sometimes disagreeing with choices I've made in following my dreams. He allowed me the freedom to pursue the project I wanted, despite his deep skepticism of its prospects for success. He was always there when I needed him, even cutting a vacation short to help me with a grant proposal that was giving me trouble. Despite always being there when I needed him, he never micromanaged my work and let me manage my own time as I saw fit. I am convinced that I never would have made it to this point if I had been working under anyone else.

I would also like to thank the members of the Rine lab who have contributed to the best workplace environment I have ever been part of in my nearly 15 years of laboratory work. My rotation mentor, Dr. David Steakley, deserves special attention for teaching me the basics of working with yeast. Dr. Anne Dodson also deserves special thanks for developing the CRASH assay and helping me to use it with great success to elucidate the effects of nutrient availability on heterochromatic silencing. Past lab members (Dr. Meru Sadhu, Dr. Aisha Ellahi, and Dr. Sarah Bissonnette) and current lab members (Dr. Ryan Janke, Kripa Asrani, Jean Yan, Katie Sieverman, and Gavin Schlissel) have also gone out of their way to provide invaluable help and advice over the years, and I am grateful to have shared the last several years with them.

I would also like to thank my thesis committee members, Dr. Michael Eisen, Dr. Andrew Dillin, and Dr. John Dueber, for their help and advice in shaping my research over the years during formal thesis committee meetings and informal discussions. Their unique skills and knowledge bases have definitely influenced the way that this work has advanced, and the final results are stronger because of them.

Finally, I would like to thank Dr. Dan Gottschling, Dr. Michael Eisen, Dr. Kelly Schiabor, Dr. David Drubin, Dr. Georjana Barnes, Dr. Eric Lewellyn, Dr. Hao Li, Dr. Ke Zou, Dr. Kerry Bloom, and Dr. Arshad Desai for providing strains, materials, reagents, equipment, and training necessary for the completion of this work.

Part I:

Intersections of nutrient availability, growth, aging, and heterochromatic silencing

Chapter 1:

Impact of Sir2 on yeast chronological lifespan and growth across different carbon sources and concentrations

Introduction

The role of the S. cerevisiae NAD+-dependent protein deacetylase Sir2 in calorie restriction-mediated longevity is controversial (Lin, *et al.* 2002; Kaeberlein, *et al.* 2004; Kaeberlein, *et al.* 2006; Smith, *et al.* 2007) despite Sir2's well-defined role in regulating yeast aging (Kaeberlein, *et* al. 1999; Fabrizio, *et al*. 2005). The discrepancies in the published literature have been attributed, without specific evidence, to differences in strain background and media composition (Couzin-Frankel, 2011). The exact role of Sir2 in calorie restriction, particularly in yeast, remains unclear as a result.

Nutrient sensing and signaling pathways like Insulin/IGF1 (Gesing, *et al.* 2014), AMPK (Greer, *et al.* 2007), RAS/PKA (Wei, *et al.* 2008), Tor/Sch9 (Kaeberlein, 2005), and possibly Sir2 (Guarente and Picard, 2005; Kaeberlein and Powers, 2007) have been linked to calorie restriction-mediated longevity in a variety of organisms. The levels of many nutrients, including carbon source and concentration, modulate these pathways. The mechanisms underlying calorie restriction in one type of growth medium might look quite different than in other media environments.

Yeast chronological aging is studied almost exclusively on synthetic complete minimal medium (SC) with glucose as a carbon source (Longo, *et al*., 2012). Studies of yeast calorie restriction have used 2% glucose as the full-calorie diet, and 0.5% or less glucose as the calorie-restricted condition (Fabrizio *et al.* 2005; Smith *et al*. 2007). In nature, *S. cerevisiae* is often found in high-calorie environments made up of a complex mix of sugars, with many yeast substrates containing well over 10% sugar, often little of that being glucose (Coghe, *et al.* 2005; Sanchez, 2008; Garde-Cerdán, 2011; Oliva, *et al.* 2011). *S. cerevisiae* has also retained five out of ten glycolytic enzymes in duplicate following a whole genome duplication, even as most duplicated genes were lost through evolution (Byrne and Wolfe, 2005; Conant and Wolfe, 2007). Increased fermentative capacity should confer a growth advantage in high-sugar media, pointing to high-sugar environments being relevant to studying *S. cerevisiae* biology (Conant and Wolfe, 2007).

It is possible the discrepancies in the literature over Sir2's role in calorie restriction-mediated longevity is due to the "full-calorie" diet itself being on the edge of calorie restriction for *S. cerevisiae*. If true, using a higher concentration of glucose for the full-calorie diet could expand the dynamic range of phenotypic measurement, allowing previously missed effects of Sir2 on lifespan to be revealed. Other aspects of media, such as carbon source, pH, and availability of other nutrients could also impact Sir2's contribution to growth, aging and calorie restriction-mediated longevity. To test these hypotheses, I examined growth and chronological aging in a variety of media environments, using a new calorie restriction paradigm that accounts for *S. cerevisiae*'s preference for high-sugar.

Materials and Methods

Yeast strains and media

Genotypes of strains from this study are given in Table 1.1. JRY10779 was derived from W303 (JRY4012) using standard yeast methodology. Synthetic complete minimal medium was produced according to the standard protocol (Fabrizio and Longo, 2007), with minor changes as described. Media were prepared with either 2% w/v or 12% w/v sugar, with 10% w/v sorbitol added only to 2% media to control for osmolarity differences between 2%- and 12%-sugar cultures, unless otherwise noted. Additionally, synthetic complete media were supplemented with four-fold excesses of leucine, lysine, tryptophan, histidine, and uracil as needed to complement strain auxotrophies, and pH-adjusted to 5.0 with NaOH. SC glycerol medium was made with 3%- or 18%-glycerol instead of sugar, with no sorbitol added. Buffered SC medium was made by adding 64.2 mM Na_2HPO_4 and 17.9 mM citric acid to the typical SC medium recipe and adjusting pH to 6.0. YP medium was produced according to the standard protocol, also with minor changes as described. Media was prepared with either 2% w/v or 12% w/v glucose, with 10% w/v sorbitol added only to 2% media as appropriate. Rather than autoclaving, which causes glucose to caramelize, all media were filter-sterilized using 0.2 μm polyethersulfone filters. Solid media used for counting colony-forming units during chronological lifespan experiments was 2%-glucose yeast peptone medium, made according to the standard protocol.

Measurement of culture cell density, pH and glucose concentration

Cell density was determined by measuring 600nm absorbance using a UV-Vis Spectrophotometer (Shimadzu, UV-1800), with cultures diluted so that the measurement was in the dynamic range of the instrument (0.1-1.0). Culture pH was measured using a Fisher Science Education pH Meter (Fisher Scientific, s90524). Glucose concentration was measured using a portable brix refractometer (WMicro, RHB-32ATC).

Measurement of chronological lifespan

5 mL seed cultures of individual colonies (in appropriate media) were grown overnight, shaking at 200 RPM at 30°C. Flasks with 50 mL of appropriate media were seeded to generate an initial cell concentration of 0.1 OD_{600} units, and incubated at 200 RPM at 30°C until growth ceased for a period of 24 hours as monitored by OD_{600} reading, usually on day 3. At this point, 100 μL aliquots of each culture were removed and the 50 mL cultures were left shaking at 200 RPM at 30°C. A 10-fold serial dilution series was created from the removed 100 μL aliquot, generating 1:10, 1:100, 1:1,000, and 1:10,000 dilutions. 100 μL of 1:10,000 dilution sample was then spread evenly over a fresh 2%-glucose YP plate and incubated at 30°C to determine the colony-forming units (CFU) score for each. Viability at this

time-point is the initial stationary-phase viability of a culture. At subsequent time-points, additional 100 µL aliquots were removed from the still-shaking 50 mL cultures, diluted, plated, and counted as before. The CFU score for each culture decreased as a function of time, generating a lifespan curve for each. CFU scores generated were typically based on counting between 50 and 500 colonies. All experiments were performed in biological triplicate. 250 mL Erlenmeyer flasks (Pyrex No. 4980 Stopper No. 6) with 38 mm silicone sponge closures (Chemglass Life Sciences, CLS-1490-038) were used for all experiments.

Results

Sir2 was required for full extension of chronological lifespan via calorie restriction in glucose synthetic complete media

Previous studies of chronological aging found that calorie restriction extended lifespan independently of Sir2 (Fabrizio, *et al*. 2005; Smith, *et al*. 2007). Those studies used the typical calorie restriction paradigm where 2% glucose is the fully-fed diet. I wanted to see whether the Sir2-independence of chronological life span extension was also true under a more physiologically relevant calorie restriction paradigm. I used 12% glucose as the fully-fed diet, and 2% glucose as the calorie-restricted diet. 12% glucose more closely resembles natural *S. cerevisiae* substrates, making it a more sensible fully-fed diet (Coghe, *et al.* 2005; Sanchez, 2008; Garde-Cerdán, 2011; Oliva, *et al.* 2011). I grew wild-type cells in both 2% and 12% glucose synthetic complete media and performed standard chronological lifespan assays (Fabrizio and Longo, 2007) on both. As expected, growth in 12% glucose decreased lifespan as compared to 2% glucose, which is consistent with the logic of calorie restriction **(Figure 1.1A)**. Interestingly, deleting *SIR2* had no effect in 2% glucose, while dramatically extending lifespan in 12% glucose **(Figure 1.1B)**. This phenotype was consistent with a partial role for Sir2 in lifespan extension via calorie restriction within our higher range of sugar concentrations. 2%-glucose medium was supplemented with sorbitol to achieve a similar osmotic pressure as 12%-glucose medium, although lack of sorbitol did not significantly affect any of these results and in fact slightly extended the lifespan of 2%-glucose cultures independent of Sir2 **(Figure 1.1C)**.

sir2Δ had only mild or no effects on growth, glucose metabolism, and culture pH in synthetic complete media

To elucidate how Sir2 shortened chronological lifespan specifically in 12% glucose, I grew 2%- and 12%-glucose cultures to stationary phase, measuring cell density, culture pH, and glucose concentration throughout. Shockingly, both 2% and 12% cultures had nearly identical log-phase growth-rates and stabilized at nearly identical stationary-phase densities **(Figure 1.2A)**. The only place the growth curves diverged was during the period of the diauxic shift (Werner-Washburne, *et al*. 1993), with 2% cultures seeming to experience a slower shift than 12% cultures.

sir2Δ led to very minor growth defects in both 2% and 12% cultures, emerging at the beginning of the diauxic shift. pH initially dropped at a similar rate in both 2% and 12% cultures, although 12%-culture pH continued to drop as 2%-culture pH stabilized **(Figure 1.2B)**. This led to a modest difference between 2%-culture pH, which dropped to a low of approximately 2.7, and 12%-culture pH, which dropped to a low of 2.4. In both 2%- and 12%-glucose cultures, *sir2Δ* slightly increased pH, although the effect was almost negligible. *sir2Δ* had no effect on the rate of glucose metabolism in 2% cultures **(Figure 1.2C)**. *sir2Δ* slowed the rate of glucose metabolism in 12% cultures, but only very slightly and only later in growth. Interestingly, in 2% cultures, glucose was depleted at almost the exact time that cultures began to transition toward stationary phase. Conversely, 12% cultures began this transition long before glucose was fully depleted from the growth media **(compare Figure 1.2A to Figure 1.2C)**.

Replacing stationary-phase glucose synthetic complete media with water reversed high-glucose *sir2Δ* chronological lifespan phenotype

To disentangle possible Sir2-dependent changes to media composition that impact chronological aging during log-phase from those during stationary phase, I grew wild-type and *sir2Δ* 2% and 12% glucose synthetic complete cultures to stationary phase, replaced spent culture media with water, and performed chronological longevity assays as before. Replacing spent media with water extended the lifespans of both genotypes in both 2%- and 12%-glucose cultures **(compare Figure 1.1B to Figure 1.3)**. *sir2Δ* had no effect on 2%-glucose-grown cultures when stationary-phase medium was replaced with water, similar to cultures where medium was not replaced. Interestingly, the difference in lifespan between 2%- and 12%-glucose-grown wild-type cultures significantly decreased when medium was replaced with water **(compare Figure 1.1B to Figure 1.3)**. Surprisingly, 12%-glucose-grown *sir2Δ* cultures were shorter-lived than wild-type when medium was replaced with water at stationary phase **(Figure 1.3)**. This result contrasts with cultures where the medium was not replaced, where *sir2Δ* instead caused a dramatic extension of lifespan **(Figure 1.1B)**. Thus, a Sir2-dependent change in stationary-phase media composition was responsible for the dramatic extension of lifespan in 12%-glucose-grown *sir2Δ* cultures.

Buffering of high-glucose synthetic complete medium prevented *sir2Δ*-dependent extension of lifespan

Because a Sir2-dependent change in stationary-phase media composition was involved in the high-glucose *sir2Δ* lifespan extension phenotype, I conducted chronological lifespan assays using buffered (pH 6) 12%-glucose synthetic complete media to determine if Sir2-dependent changes in extracellular pH were involved. Buffering of the growth media completely eliminated the *sir2Δ*-dependent extension of chronological lifespan seen in unbuffered 12% glucose medium **(compare Figure 1.1B to Figure 1.4A)**. Whereas Sir2 does not appear to impact growth in buffered

or unbuffered media, buffering high-glucose media led to an increase in stationary-phase cell density, while buffering low-glucose media led to a decrease in stationary-phase cell density **(Figure 1.4B)**. Since buffered media does not allow for lifespan extension of *sir2Δ* cells, the modest Sir2-dependent differences in pH I observed **(Figure 1.2B)** might explain the *sir2Δ* phenotype under these conditions.

sir2Δ increased chronological lifespan of cells grown in high-glucose synthetic complete media with a variety of fermentable sugars

Given that natural *S. cerevisiae* substrates are generally enriched for sugars other than glucose, I wanted to determine whether *sir2Δ* extends lifespan in media with high concentrations of other fermentable sugars, including sucrose, and galactose. Given slight differences in the ways these sugars are metabolized early in glycolysis (van Maris, *et al*. 2006), differences in the *sir2Δ* lifespan phenotype could hint at a mechanism tied to these early glycolytic steps. I grew wild-type and *sir2Δ* cultures in 12% glucose alongside cultures grown in 12% sucrose, and 12% galactose. 12% sucrose and galactose cultures behaved similarly to 12% glucose, implying that the different ways these sugars are metabolized early in glycolysis don't impact Sir2's ability to shorten lifespan in high sugar **(Figure 1.5A-C)**. 2% and 12% cultures of glucose and 12% cultures of sucrose all arrived at a similar maximal stationary-phase cell density, and *sir2Δ* had no effect on this metric **(Figure 1.5D)**. Wild-type 12% galactose-grown cultures, on the other hand, reached a higher stationary-phase cell density, and deleting *SIR2* allowed them to achieve an even greater cell density **(Figure 1.5D)**.

sir2Δ failed to increase chronological lifespan of cells grown in high-calorie non-fermentable synthetic complete medium but had unique affects on growth

Since a variety of fermentable carbon sources have similar *sir2Δ* chronological lifespan phenotypes, I wanted to determine whether *sir2Δ* impacted growth and lifespan similarly when grown in either high- or low-glycerol, a three-carbon molecule that cannot be fermented (Nevoigt and Stahl, 1997). I used 3% glycerol as our low-carbon environment, as this has a nearly identical calorie content to 2% glucose. I therefore used 18% glycerol as our high-carbon environment to remain consistent. Interestingly, wild-type 3%-glycerol cultures reached a stationary-phase density of around 10 OD_{600} units, while *sir2Δ* 3%-glycerol cultures reached a stationary-phase density of only 6 OD_{600} units **(Figure 1.6A)**. This was only the second such example of a Sir2-dependent change in stationary-phase cell density, with the first example being growth in 12% galactose. In 12% galactose, however, *sir2Δ* increases cell density, whereas in 3% glycerol, *sir2Δ* decreases cell density **(compare Figure 1.5D to Figure 1.6A)**. In 18% glycerol, both wild-type and *sir2Δ* cultures reached similar stationary-phase cell densities around 4 OD_{600} units. Surprisingly, however, wild-type cultures experienced a growth lag lasting several days relative to *sir2Δ* cultures **(Figure**

1.6B). As for lifespan, *sir2Δ* seemed to mildly enhance viability during early time points but shorten maximal lifespan relative to wild-type during aging in 3% glycerol medium **(Figure 1.6C)**. As for 18% glycerol medium, *sir2Δ* mildly decreased chronological lifespan, although regrowth of cultures complicates interpretation of this data **(Figure 1.6D)**. Despite this complication, it is clear that *sir2Δ* did not extend lifespan in high-calorie glycerol medium in contrast to its effect in high-calorie fermentable media.

sir2Δ did not affect chronological lifespan in high-glucose yeast peptone medium, but decreased lifespan in low-glucose yeast peptone medium

Having evaluated Sir2's contribution to growth and chronological lifespan in a wide variety of complete minimal media, I wanted to know how Sir2 functioned to regulate growth and aging in high- and low- glucose yeast peptone media. Acidification of the culture medium has been proposed as a mechanism for chronological aging in unbuffered synthetic complete media (Burtner, *et al*. 2009), and Sir2's contribution to chronological lifespan in 12%-glucose was likely dependent on acidification of culture medium, as buffered media eliminated the *sir2Δ*-dependent extension of lifespan **(Figure 1.4A)**. Yeast peptone medium is well-buffered and low in ammonium sulfate, similar to other natural yeast substrates (Weinberger, *et al*. 2010; Garde-Cerdán, *et al*. 2011), making it an important medium to study. I grew wild-type and *sir2Δ* cells to stationary phase in either 2%- or 12%-glucose yeast peptone media and performed chronological lifespan assays as before. As had been seen during experiments with pH-buffered synthetic complete media, 12%-glucose yeast peptone medium supported high levels of stationary-phase regrowth **(Figure 1.7A)**. 2%-glucose medium also allowed for limited regrowth in stationary phase, manifesting as unexpected increases in viability along the lifespan curve **(Figure 1.7B)**. *sir2Δ* clearly decreases lifespan of 2%-glucose cultures, although the fact that stationary-phase regrowth occurs makes it difficult to determine whether this phenotype is due to decreased lifespan or decreased stationary-phase regrowth. Although *sir2Δ* appears to not affect chronological aging in 12%-glucose yeast peptone medium, the large amounts of stationary-phase regrowth in these cultures makes it difficult to know for certain **(Figure 1.7)**. Since Sir2 clearly affects both growth and lifespan under a variety of conditions, it is possible that *sir2Δ* has competing effects on growth and aging here that could hide each other.

Growth in high-glucose yeast peptone medium resulted in a severe decrease in relative initial viability not seen in other media

Initial viability is the viability of a culture at the first time-point in stationary phase. While performing chronological lifespan assays in yeast peptone media, I observed a dramatic Sir2-independent decrease in initial viability of 12%-glucose cultures relative to 2% glucose cultures **(Figure 1.8A)**. I measured viability of log-phase cultures starting from the point of inoculation and discovered that viability of

12% cultures begins dropping relative to 2% cultures almost immediately **(Figure 1.8B)**, even as the cell density of 2% and 12% cultures increases at a similar rate **(Figure 1.7A)**. I calculated the initial viability for wild-type and *sir2Δ* cultures in a variety of conditions previously described and failed to observe any similarly low initial viability **(Figure 1.8C)**. Interestingly, I did observe modest *sir2Δ*-dependent increases in lifespan in both 3%- and 18%-glycerol, and possibly in 12%-sucrose **(Figure 1.8C)**.

Cells isolated from high-glucose yeast peptone cultures following stationary-phase regrowth reached a higher cell density than their parents

I was surprised that 12%-glucose yeast peptone cultures initially arrested with a cell density of around 15 OD_{600} units, given that the cultures could later achieve much higher cell densities. I reasoned that cells in these cultures may have undergone some physiological change that allowed them to continue growing to achieve a higher cell density, and that this change could be heritable. To test this hypothesis, I isolated aliquots of late-stage 12%-glucose yeast peptone cultures (both wild-type and *sir2Δ*) after regrowth had occurred and inoculated fresh 12%-glucose medium with these aliquots to an initial density of 0.1 OD_{600}. I also inoculated fresh 12%-glucose medium to the same initial density with fresh colonies of both strains, and grew all cultures to stationary phase, measuring cell density throughout. Cultures that were inoculated with aliquots from regrown cultures did indeed achieve a greater stationary-phase cell density than cultures inoculated with fresh colonies **(Figure 1.9)**. This was true of both wild-type **(Figure 1.9A)** and *sir2Δ* cultures **(Figure 1.9B)**, which makes sense given that the 12%-glucose regrowth phenotype was Sir2-independent. The inherited increase in stationary-phase cell density, although significant, did not allow cultures to reach as high a cell-density as seen in late-stage 12%-glucose cultures after the period of regrowth **(compare Figure 1.7A to Figure 1.9)**.

Discussion

I have demonstrated that reducing starting sugar concentration of growth medium from 12% to 2% increases lifespan, consistent with the established principle that calorie restriction leads to lifespan extension **(Figure 1.1A)**. Cultures otherwise grew similarly in 2%- and 12%-glucose, establishing these media as reasonable conditions for study **(Figure 1.2A)**. Using this newly-developed calorie restriction paradigm, I identified a role for Sir2 in the extension of chronological lifespan via calorie restriction under these conditions. *sir2Δ* increased lifespan in 12%-glucose synthetic complete medium, while having no effect in 2%-glucose **(Figure 1.1B)**.

Replacing stationary-phase spent media with water eliminated the *sir2Δ*-dependent extension of lifespan in 12% glucose **(Figure 1.3)**. Surprisingly, *sir2Δ* actually decreased lifespan of 12%-glucose cultures when the medium was replaced with water at stationary phase, rather than increasing lifespan when the medium

was not replaced. These results imply that Sir2 might be acting in two opposing pathways to regulate aging, with one shortening lifespan via changes to the external medium and the other extending lifespan independent of the external medium **(compare Figure 1.1B to Figure 1.3)**. Since pH-buffering of 12%-glucose synthetic complete medium or growth in naturally-pH-buffered yeast peptone medium also resulted in a loss of the *sir2Δ* 12%-glucose lifespan phenotype **(Figure 1.4A and Figure 1.7B)**, changes in extracellular pH could mediate Sir2's effect on chronological longevity under these conditions. Consistent with this possibility, *sir2Δ* did mildly increase the pH of unbuffered 12%-glucose cultures **(Figure 1.2B)**.

Replacing glucose with other fermentable sugars did not prevent *sir2Δ*-dependent extension of lifespan in 12%-sugar synthetic complete medium **(Figure 1.5)**. Therefore, differences in metabolism between these sugars, including unique effects on known nutrient sensing and signaling pathways (van Maris, *et al*. 2006), do not impact the *sir2Δ* phenotype. However, replacing glucose with glycerol, a non-fermentable carbon source, prevented *sir2Δ*-dependent lifespan extension in high-calorie synthetic complete medium. In 18%-glycerol medium, which has a similar carbon content to 12%-glucose medium, *sir2Δ* clearly did not extend lifespan, even as regrowth in these conditions complicated interpretation of data **(Figure 1.6D)**. Surprisingly, while *sir2Δ* did not appear to significantly impact chronological aging in high-glycerol, *sir2Δ* did affect aging in 3% glycerol, decreasing viability at early time points and increasing viability at later time-points **(Figure 1.6C)**.

A previous study (Burtner, *et al*. 2009) points to acidification of unbuffered synthetic complete culture medium as a mechanism for chronological aging, and everything I present here is consistent with that mechanism. *sir2Δ* mildly increased the external pH of 12%-glucose-grown cultures (Figure 1.2B), and *sir2Δ*-dependent lifespan extension was seen only in unbuffered media with a high concentration of a fermentable carbon source **(Figure 1.1B and Figure 1.5A-C)**. Glucose, sucrose, and galactose are catabolized via glycolysis, producing ethanol and acetate, the latter of which acidifies external culture medium (Burtner, *et al*. 2009). Conversely, glycerol, a non-fermentable carbon source upon which *sir2Δ* did not extend lifespan **(Figure 1.6D)**, is catabolized via oxidative phosphorylation (Nevoigt and Stahl, 1997). Energy production via oxidative phosphorylation does not lead to increased levels of acetate in the external medium. Sir2 has a previously-defined role in regulating extracellular acetate levels through the deacetylation of Pck1, an enzyme that catalyzes the rate-limiting step in gluconeogenesis (Lin, *et al*. 2009). Additional chronological lifespan experiments using a Pck1 variant that is not subject to deacetylation by Sir2 (Orlandi, *et al*. 2016) will be necessary to determine if Sir2-dependent deacetylation of Pck1 underlies the 12%-glucose *sir2Δ* phenotype.

Beyond Sir2's role as a pro-aging protein in unbuffered, high-sugar media, Sir2 appeared to both positively and negatively regulate growth and aging in other conditions. When stationary-phase medium of 12%-glucose cultures was replaced with water, *sir2Δ* actually decreased lifespan **(Figure 1.3)**. Similarly, *sir2Δ* decreased lifespan in 2%-glucose yeast peptone medium **(Figure 1.7B)** and in 3%-glycerol synthetic complete medium **(Figure 1.6C)**. In fermentable media, *sir2Δ* did

not significantly alter aspects of growth aside from increasing the stationary-phase cell density of 12%-galactose-grown cultures **(Figure 1.2A and Figure 1.5D)**. In non-fermentable glycerol, however, *sir2Δ* limits growth in 3% glycerol while enhancing growth in 18% glycerol **(Figure 1.6A-B)**. Additionally, *sir2Δ* increases the initial viability of both 3%- and 18%-glycerol cultures at the beginning of stationary phase.

Taken together, Sir2's impact on growth and chronological aging differs dramatically depending on media environment. Under certain conditions, Sir2 acts to extend lifespan, while under other conditions, Sir2 acts to shorten lifespan. Similarly, Sir2 enhances growth under certain conditions, while hindering growth under other conditions. These contradictions position Sir2 as a central regulatory hub downstream of a variety of nutrient cues and upstream of growth and aging.

In addition to the wide range of Sir2-dependent effects on growth and aging unearthed in this study, experiments in 12%-glucose yeast peptone medium also revealed interesting and unexpected Sir2-independent growth and viability phenotypes. This decrease in viability began early in log-phase growth **(Figure 1.8B)**. Stationary-phase cultures of 12% yeast peptone medium had dramatically decreased initial viability compared to stationary-phase cultures of any other media tested **(Figure 1.8C)**. Interpretation of chronological lifespan data was difficult due to the extensive and unprecedented amount of regrowth observed, where previously quiescent cells re-entered the cell cycle **(Figure 1.7A)**. This regrowth could have been triggered by the accumulation of a limiting essential nutrient as cells died and lysed, or by the degradation (or evaporation) of a toxic waste product like ethanol. Alternatively, quiescent cells in a 12%-glucose yeast peptone culture could have undergone a physiological change that allowed them to grow under conditions that previously inhibited growth. The ability of these cells to reach a higher stationary-phase cell density was indeed heritable, as all cultures seeded with aliquots of late-stationary-phase cultures reached higher cell density than cultures seeded with fresh colonies **(Figure 1.9)**. That said, cultures seeded with aliquots of regrown cultures did not immediately reach densities similar to late-stationary-phase cultures, implying that the release of a limiting essential nutrient or the depletion of a toxic product is still necessary to achieve maximum cell density. More research is necessary to determine the mechanism underlying the dominant inheritance pattern of the stationary-phase cell density phenotype, as well as the limiting nutrient(s) and/or toxic product(s) that additionally limit cell density in high-glucose yeast peptone medium.

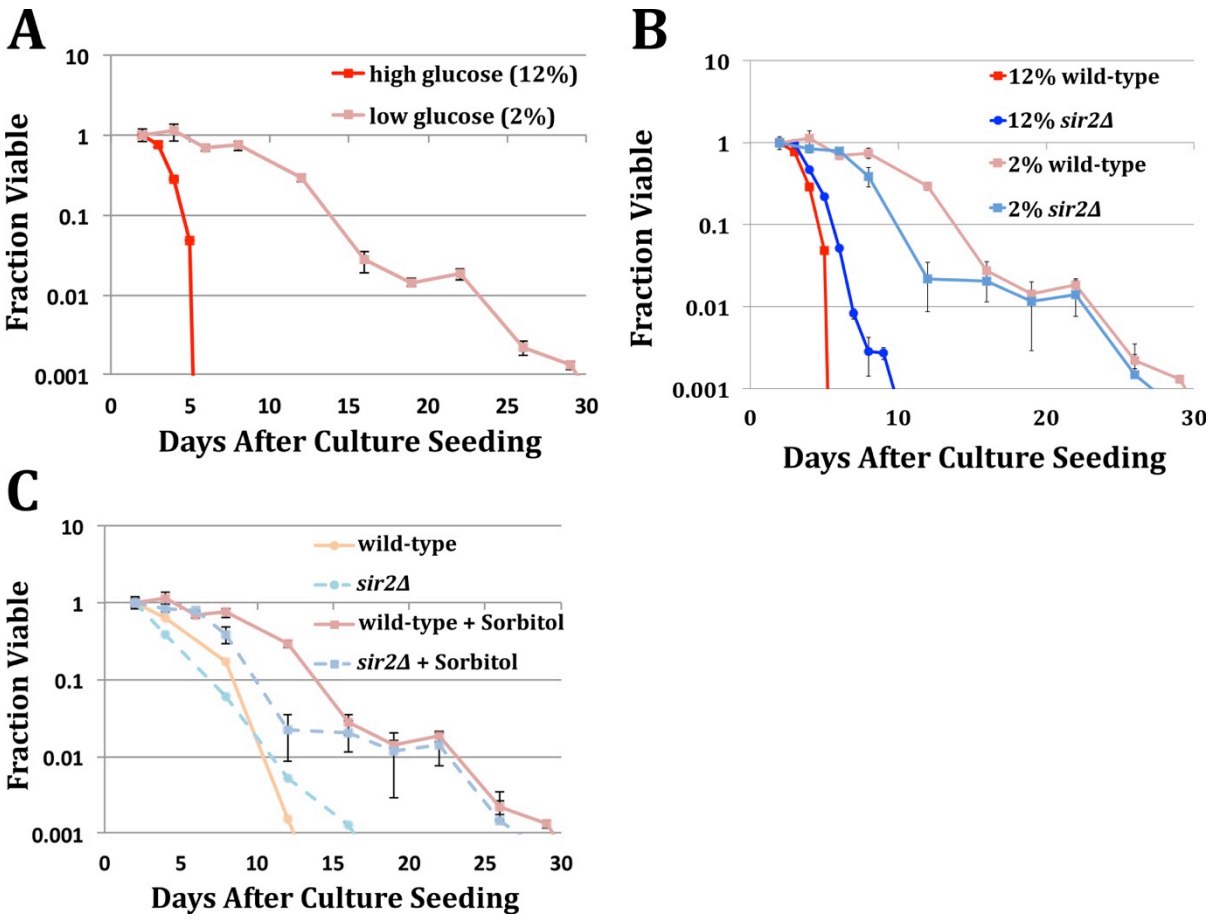


Figure 1.1. Chronological lifespan in high- and low- glucose synthetic complete medium. (A) A wild-type strain was grown to stationary phase in either 2% (low) or 12% (high) glucose and aliquots were removed, diluted, and plated over time. Colonies that grew were counted and the daily total was normalized to the total number of colonies viable at the first timepoint to give the fraction viable. Y-axis is cut off at 0.001 to zoom in on most relevant viability window. (B) *sir2Δ* extends chronological lifespan in 12%-glucose medium but has no significant effect in 2%-glucose medium. (C) Adding sorbitol to increase the osmotic pressure of 2%-glucose cultures to that of 12%-glucose cultures does not decrease lifespan, and instead increases it. The change in lifespan between 2%- and 12%-glucose cultures is therefore not explained by differences in the osmotic pressure of the culture media.

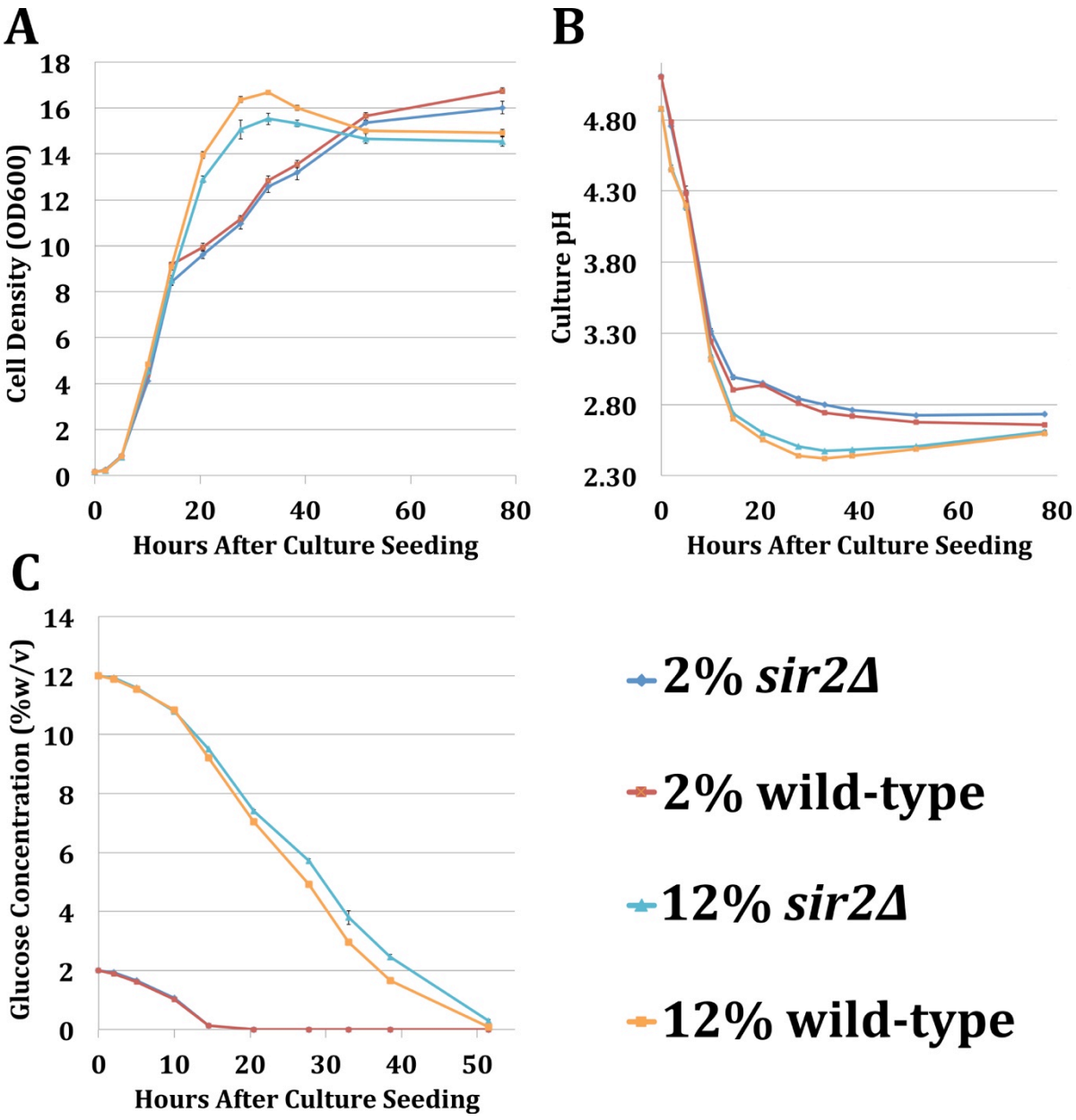


Figure 1.2. Growth, culture pH, and glucose concentration of cultures. (A) Growth kinetics of wild-type and *sir2Δ* 2%- and 12%-glucose synthetic complete cultures over time. 600nm absorbance of cultures was measured with a UV spectrophotometer and used as a proxy for cell density. 2% and 12%-glucose cultures grew similarly and *sir2Δ* mildly inhibited late-stage growth in 12% cultures. (B) pH of wild-type and *sir2Δ* 2%- and 12%-glucose synthetic complete cultures over time. Culture pH was measured using digital pH meter. *sir2Δ* mildly raised pH of cultures at later time-points. (C) Glucose concentration of wild-type and *sir2Δ* 2%- and 12%-glucose synthetic complete cultures over time. Glucose concentration was measured with a portable brix refractometer, normalized to media without glucose. *sir2Δ* mildly slows glucose consumption of 12% cultures.

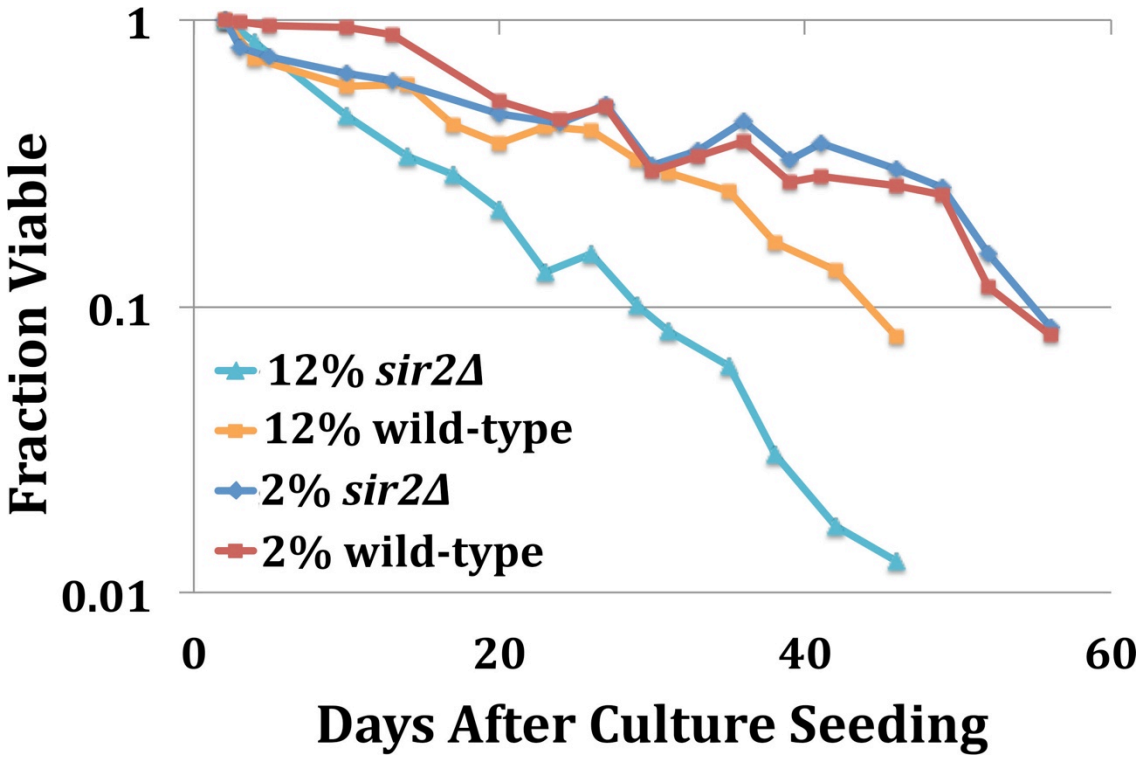


Figure 1.3. Replacing stationary-phase media with water eliminates *sir2Δ*-dependent extension of lifespan in 12%-glucose synthetic complete cultures. Chronological lifespan assays were performed according to the standard protocol except stationary-phase media is replaced by water at the first time-point in stationary phase. Not only does *sir2Δ* no longer extend lifespan, it actually decreases lifespan under these conditions. Each time-point represents two biological replicates.

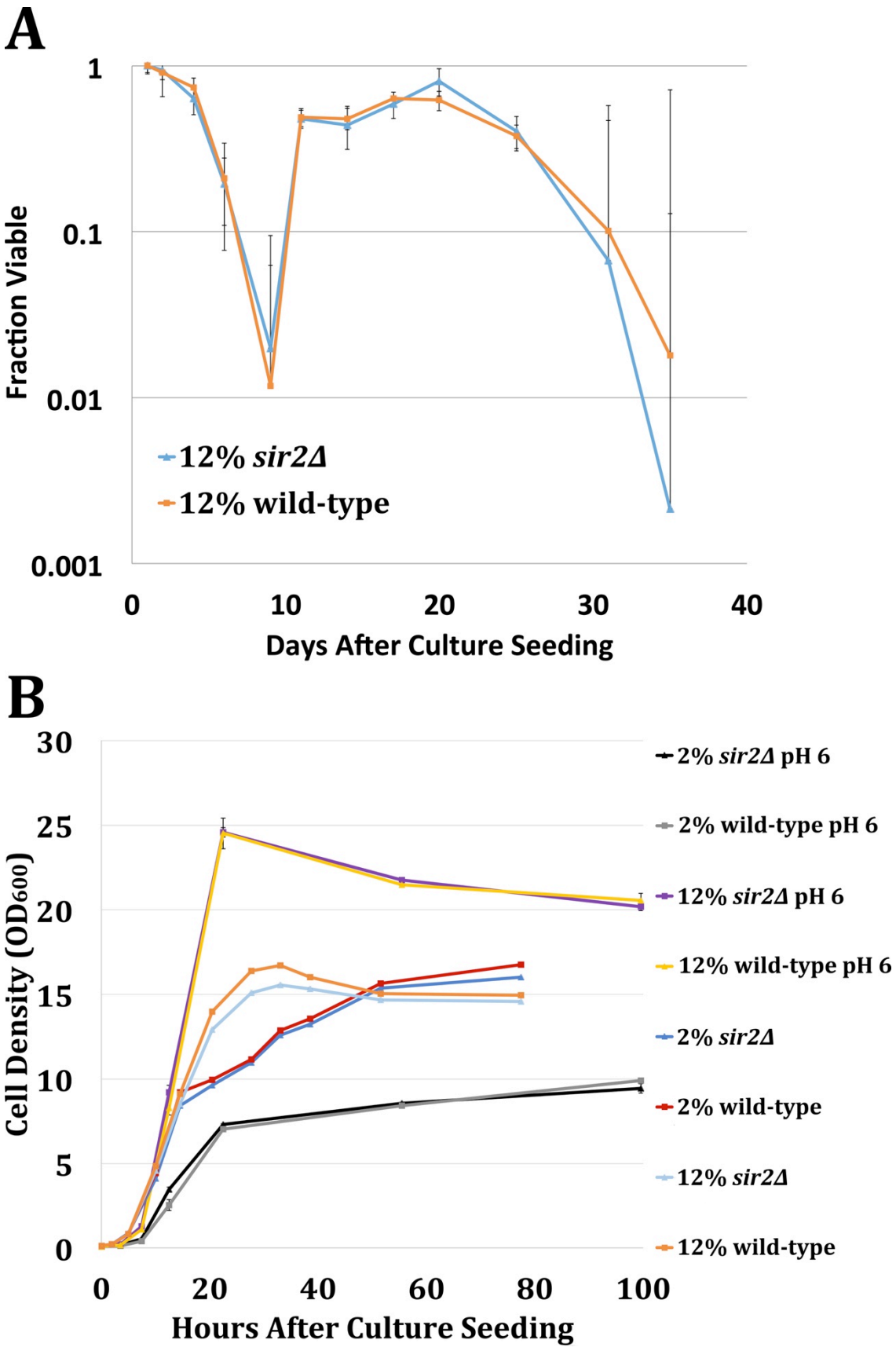

A
1
0.1
0.01
0.001
Fraction Viable
12% sir2Δ
12% wild-type
0
10
20
30
40
Days After Culture Seeding
B
30
25
20
15
10
5
0
Cell Density (OD600)
2% sir2Δ pH 6
2% wild-type pH 6
12% sir2Δ pH 6
12% wild-type pH 6
2% sir2Δ
2% wild-type
12% sir2Δ
12% wild-type
0
20
40
60
80
100
Hours After Culture Seeding

Figure 1.4. Effects of pH-buffering of 12%-glucose synthetic complete medium on chronological aging and growth. (A) Chronological lifespan of wild-type and *sir2Δ* cultures in pH-buffered 12%-glucose medium. Experiment performed exactly as before except with phosphocitrate buffer added to medium and pH adjusted to 6 with NaOH. pH-buffering prevented *sir2Δ*-dependent lifespan extension, although regrowth complicated interpretation of data. (B) Growth kinetics of wild-type and *sir2Δ* in 2%- and 12%-glucose synthetic complete media, buffered and unbuffered. Buffering 12%-glucose medium enhanced growth, independent of Sir2, while buffering 2%-glucose medium inhibited growth, independent of Sir2. Unbuffered data from **Figure 1.2A**.

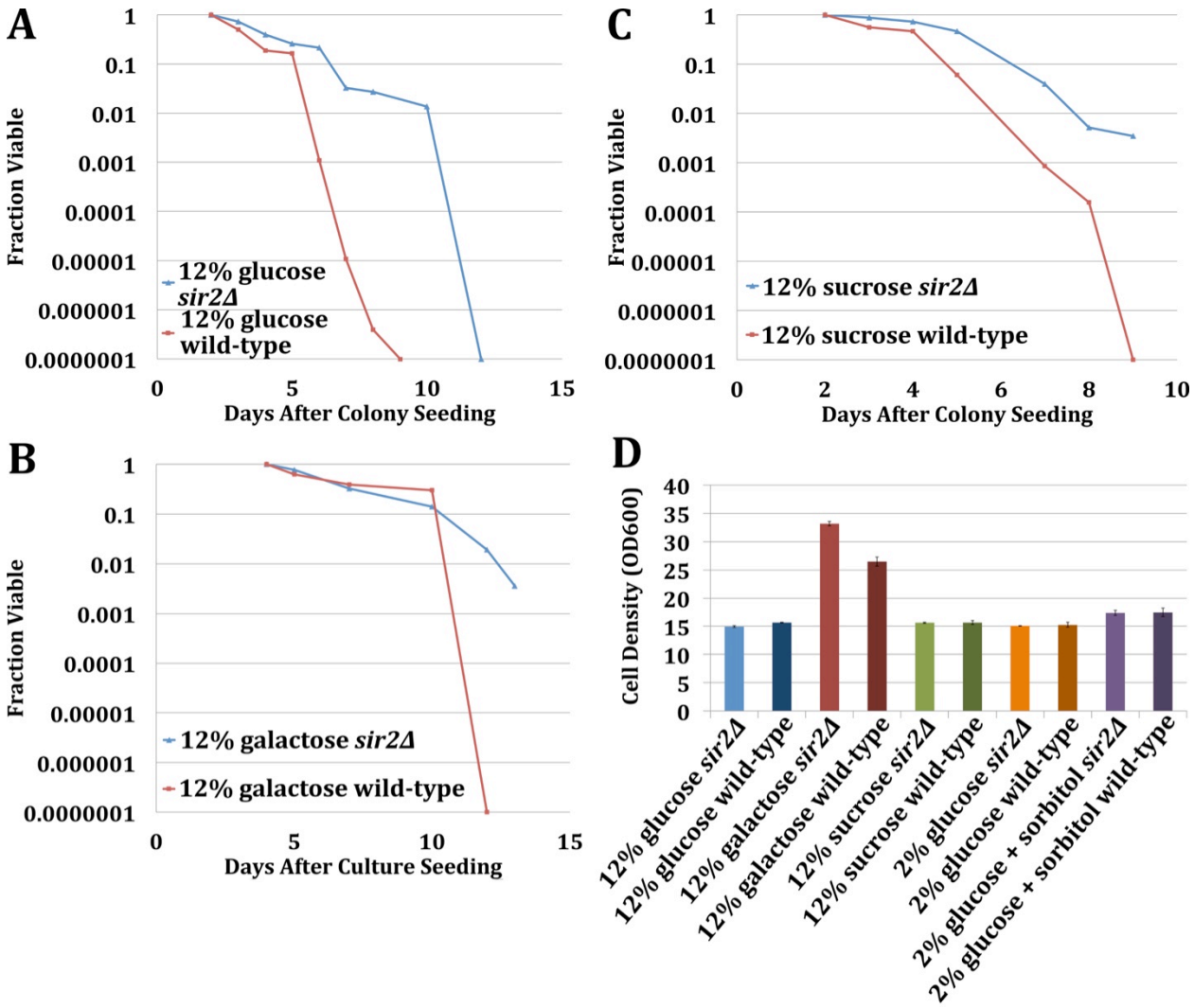


Figure 1.5. Growth and chronological lifespan on alternative fermentable carbon sources. *sir2Δ* extends chronological lifespan in synthetic complete media with (A) 12% glucose, (B) 12% galactose, and (C) 12% sucrose. (D) Stationary-phase cell densities of wild-type and *sir2Δ* cultures with a variety of sugar concentrations and types. Most cultures achieve a final density of around 15 OD_{600} units, independent of *sir2Δ*. Wild-type 12%-galactose-grown cultures, on the other hand, reach a final density of close to 26 OD_{600} units, and *sir2Δ* allows for an even greater cell density of around 33 OD_{600} units.

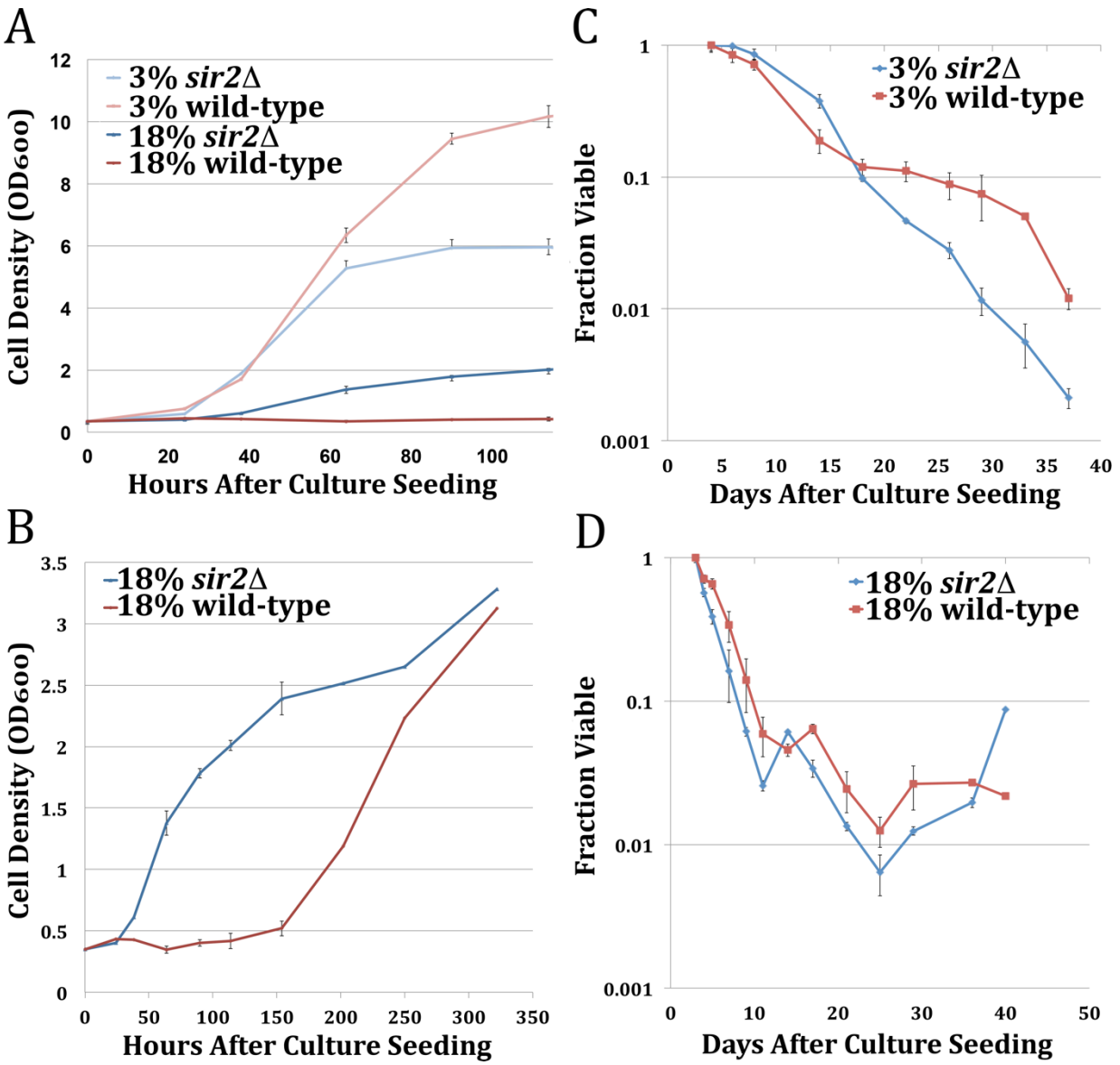


Figure 1.6. Growth and chronological lifespan on a non-fermentable carbon source. (A) Growth kinetics of wild-type and *sir2Δ* on 3%- and 18%-glycerol synthetic complete medium. 600nm absorbance of cultures was measured with a UV spectrophotometer and used as a proxy for cell density. *sir2Δ* inhibited growth in 3% glycerol and enhanced growth in 18% glycerol. (B) Long-term growth kinetics of wild-type and *sir2Δ* on 18% glycerol. Wild-type cultures lagged *sir2Δ* cultures by several days. (C) Chronological lifespan of wild-type and *sir2Δ* cultures in 3%-glycerol synthetic complete medium. Aliquots of stationary-phase cultures were removed, diluted, and plated. Colonies that grew were counted and the daily total was normalized to the total number of colonies viable at the first timepoint to give the fraction viable. *sir2Δ* enhanced viability at early time-points and inhibited viability at later time-points. (D) Chronological lifespan of wild-type and *sir2Δ* cultures in 18%-glycerol synthetic complete medium. *sir2Δ* failed to extend lifespan as was seen in high-calorie fermentable media.

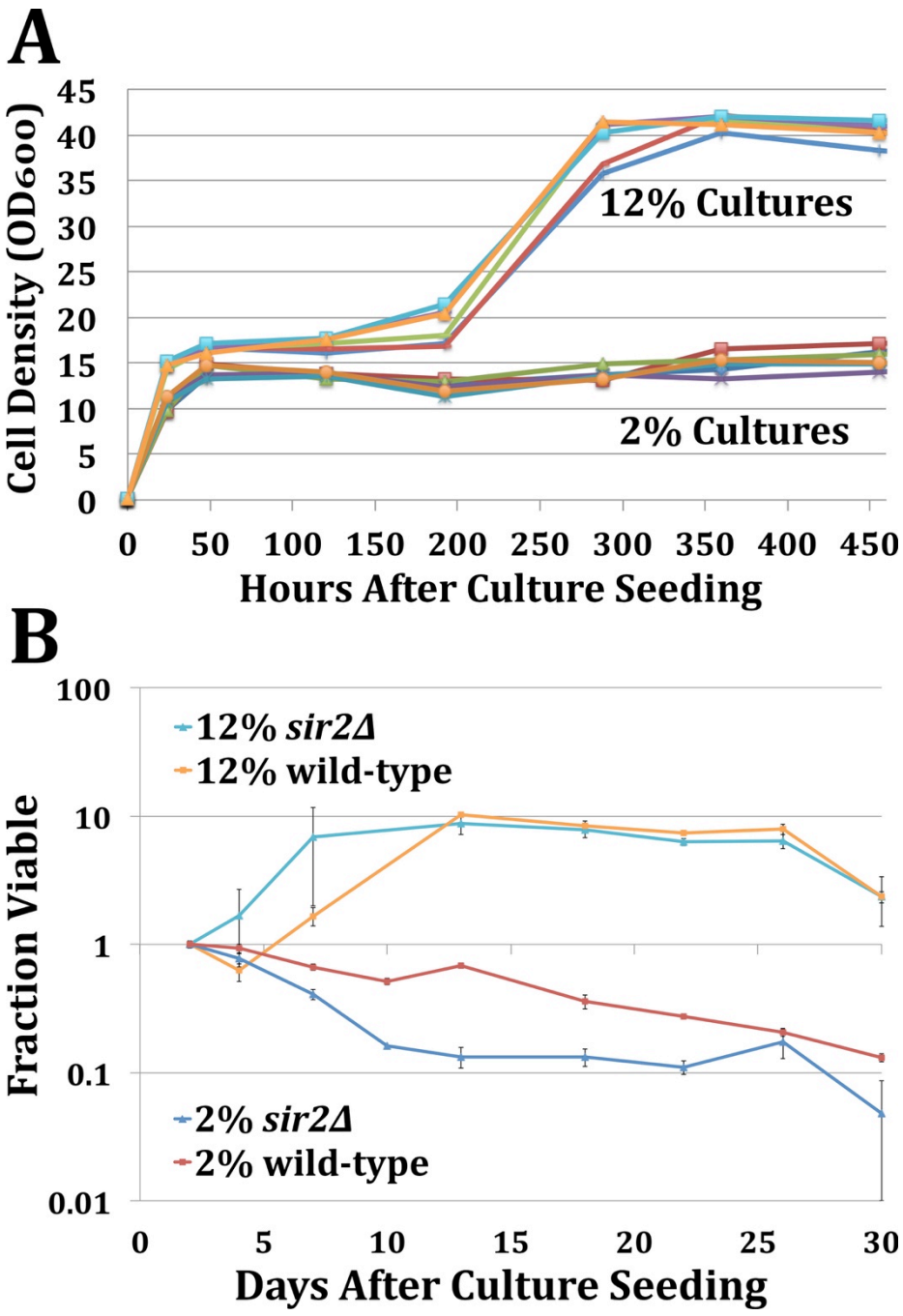


Figure 1.7. Growth and chronological aging on yeast peptone medium. (A) Growth kinetics of individual cultures of wild-type and *sir2Δ* 2%- and 12%-glucose yeast peptone medium. 12% cultures underwent a period of regrowth after arresting for several days. This occurred independent of *sir2Δ*. (B) Chronological lifespan of wild-type and *sir2Δ* in 2%- and 12%-glucose yeast peptone medium. *sir2Δ* decreased lifespan of 2%-glucose-grown cells. *sir2Δ* did not appear to significantly affect lifespan of 12%-glucose-grown cells, although regrowth of 12% cultures complicated interpretation of results.

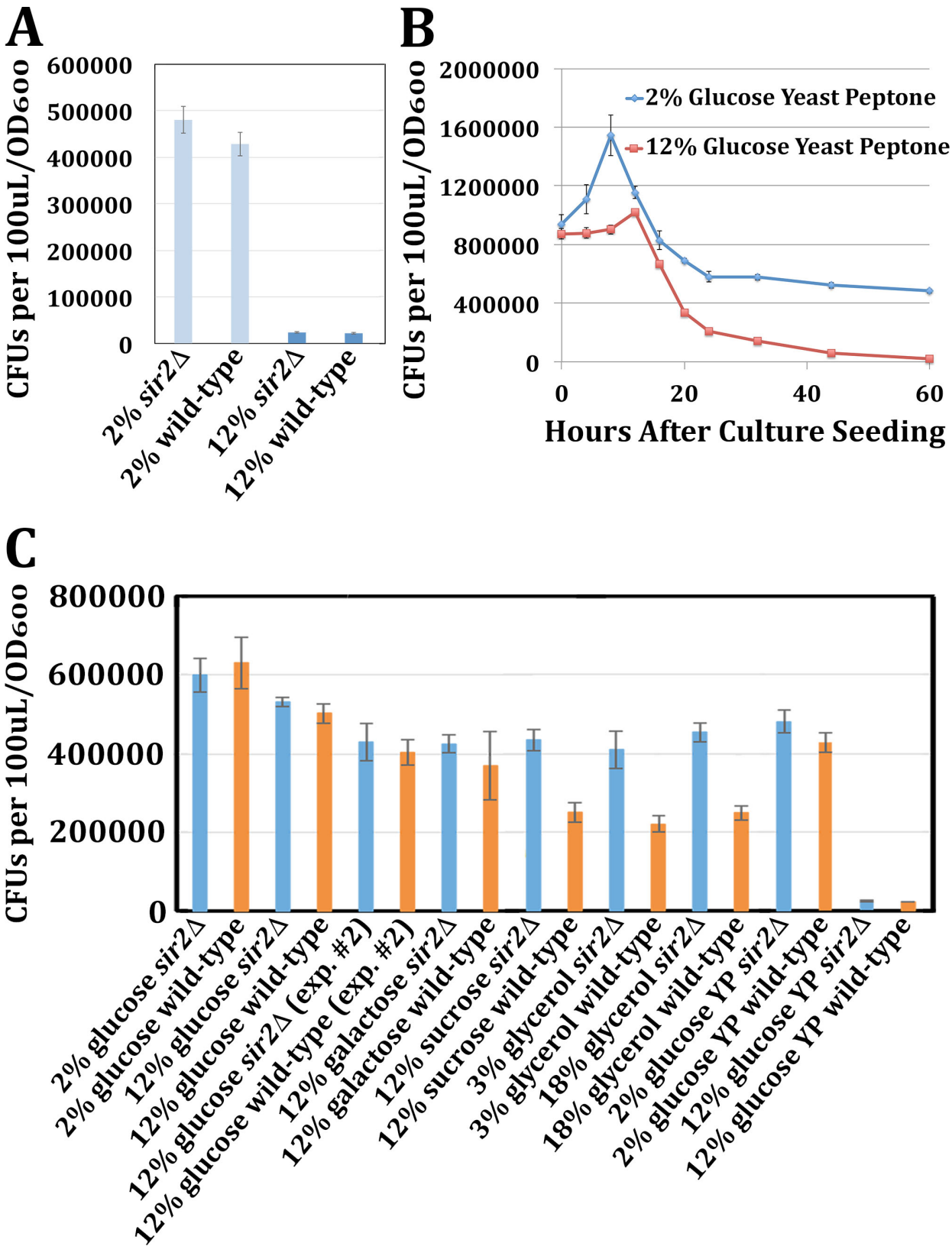

A
CFUs per 100uL/OD600
600000
500000
400000
300000
200000
100000
0
2% sir2Δ
2% wild-type
12% sir2Δ
12% wild-type
B
CFUs per 100uL/OD600
2000000
1600000
1200000
800000
400000
0
2% Glucose Yeast Peptone
12% Glucose Yeast Peptone
0
20
40
60
Hours After Culture Seeding
C
CFUs per 100uL/OD600
800000
600000
400000
200000
0
2% glucose sir2Δ
2% glucose wild-type
12% glucose sir2Δ
12% glucose wild-type
12% glucose sir2Δ (exp. #2)
12% glucose wild-type (exp. #2)
12% galactose sir2Δ
12% galactose wild-type
12% sucrose sir2Δ
12% sucrose wild-type
3% glycerol sir2Δ
3% glycerol wild-type
18% glycerol sir2Δ
18% glycerol wild-type
2% glucose YP sir2Δ
2% glucose YP wild-type
12% glucose YP sir2Δ
12% glucose YP wild-type

Figure 1.8. Initial viability yeast peptone cultures. (A) Initial stationary-phase viability of wild-type and *sir2Δ* cells grown in 2%- and 12%-glucose yeast peptone medium. Growth in 12%-glucose yeast peptone medium dramatically decreased initial viability of both wild-type and *sir2Δ* cells. Data shown is colony-forming units (CFUs) per 100 uL of culture at day 1 of chronological lifespan experiments, normalized to the cell density (OD_{600}) of the culture. (B) Viability of wild-type cells throughout log phase and early stationary phase in 2%- and 12%-glucose yeast peptone medium. Viability of 12%-glucose-grown cells dropped relative to 2%-glucose-grown cells early in log-phase growth. (C) Initial stationary-phase viability of wild-type (orange) and *sir2Δ* (blue) cells grown in a variety of media. No similar drop in viability is observed for other high-calorie media. Interestingly, *sir2Δ* increased initial viability in 12%-sucrose, 3%-glycerol, and 18%-glycerol media, despite having no impact in other media.

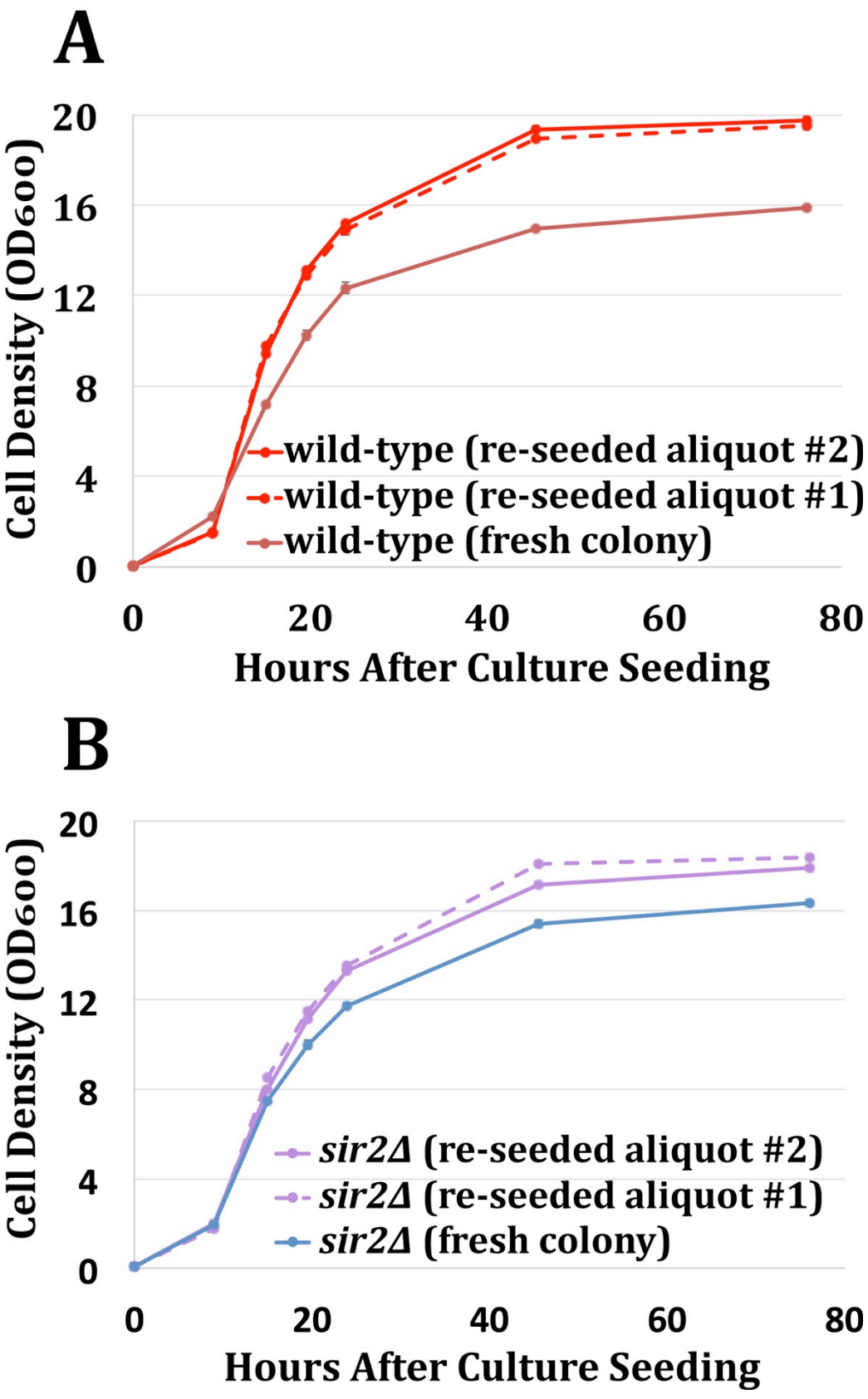

A
Cell Density (OD600)
20
16
12
8
4
0
0
20
40
60
80
Hours After Culture Seeding
wild-type (re-seeded aliquot #2)
wild-type (re-seeded aliquot #1)
wild-type (fresh colony)
B
Cell Density (OD600)
20
16
12
8
4
0
0
20
40
60
80
Hours After Culture Seeding
sir2Δ (re-seeded aliquot #2)
sir2Δ (re-seeded aliquot #1)
sir2Δ (fresh colony)

Figure 1.9. Growth of fresh cells and cells isolated from late-stage stationary-phase cultures in 12%-glucose yeast peptone medium. Aliquots of wild-type and *sir2Δ* late-stage stationary-phase 12% glucose yeast peptone cultures were used to seed fresh 12%-glucose medium. These cultures were grown alongside 12%-glucose cultures seeded with fresh colonies. Data for (A) wild-type and (B) *sir2Δ* are shown. The high-cell-density phenotype of late-stationary-phase cultures was partially heritable, as cultures seeded with late-stationary-phase aliquots reached a greater cell density than cultures seeded with fresh colonies. This occurred independent of *sir2Δ*.

Table 1.1. Genotypes of yeast strains used in this study

Strain:	Genotype:	Source
JRY4012 (W303-1a)	*MATa, his3, leu2, lys2, trp1, ura3, can1*	R. Rothstein/ Lab collection
JRY10779	*MATa his3 leu2 lys2 trp1 ura3 can1 sir2Δ::KAN^{MX}*	This Study

Chapter 2:

Nutritional control of chronological aging and heterochromatin in *Saccharomyces cerevisiae*

Introduction

Biological aging is a complex process, occurring in most (Rose, 1991) if not all (Gómez, 2010), organisms, that involves changes in physiology over time (Rose, *et al.* 2012). Late in life, especially once an organism has passed its peak in reproductive fitness, these physiological changes are often unfavorable for survival, eventually leading to death (Rose, *et al.* 2012). The budding yeast *Saccharomyces cerevisiae* has been useful in the study of cellular aging, with many genes important in mammalian aging having been first identified in studies of yeast aging (Longo, *et al.* 2012)

There have been two main approaches to the study of yeast lifespan (Longo, *et al.* 2012). The first focuses on replicative lifespan, defined as the number of progeny an individual yeast mother cell can produce through mitosis before it can no longer divide, entering senescence (Mortimer and Johnston, 1959). Replicative lifespan serves as a model of aging in actively dividing cell-types, such as germ line stem cells (Jazwinski, 1990). The second measure of yeast lifespan, chronological lifespan, is defined as the length of time that cells in a stationary phase culture remain viable and able to reenter the cell cycle upon introduction to fresh culture medium (Fabrizio and Longo, 2007). Chronological lifespan serves as a model of aging in post-mitotic cell-types, such as terminally differentiated cells (Longo, *et al.* 2012).

Calorie restriction, where calorie intake is reduced without a reduction in essential nutrients, extends lifespan and healthspan in organisms as diverse as yeast (Lin, *et al.* 2002), invertebrates (Klass, 1977), fish (Comfort, 1963), and mammals (McCay, 1935), through incompletely understood mechanism(s). Both replicative and chronological yeast lifespan is increased with calorie restriction (Kaeberlein, *et al.* 2004; Lin, *et al.* 2000; Smith, *et al.* 2007). Nutrient sensing and signaling pathways such as Insulin/IGF, Tor and AMP Kinase pathways have been implicated as effectors in calorie-restriction-mediated longevity in various organisms (Anderson and Weindruch, 2010), although exactly how they mediate the beneficial aging effects of calorie restriction requires further investigation. Changes in mitochondrial function (Anderson and Weindruch, 2007; Zahn, *et al.* 2007), fat usage and storage (Zhu, *et al.* 2004; Zhu, *et al.* 2007), and insulin signaling (Chiba, *et al.* 2007; Mair and Dillin, 2008) are thought to play downstream roles in some organisms.

In addition to the nutrient sensing pathways listed above, a class of NAD^+-dependent protein deacetylases (Imai *et al.,* 2000; Landry *et al.,* 2000a; Smith *et al.,* 2000) known as Sirtuins has been implicated in calorie restriction-mediated longevity (Guarente and Picard, 2005). Sirtuins are named after Sir2, a protein found in the budding yeast *Saccharomyces cerevisiae* whose primary role is the removal of acetyl groups from the N-terminal tails of histones H3 and H4 and some metabolic enzymes. The lysine at H4 position 16 is Sir2's primary target for its role in gene silencing at *HML* and *HMR*, as well as at telomeres and rDNA (Rusche, *et al.* 2003).

The work connecting Sirtuins to life extension via calorie restriction originally came from replicative aging studies of *S. cerevisiae*. Sir2 regulates lifespan, with deletion of *SIR2* shortening lifespan, and overexpression of *SIR2* extending it (Kaeberlein, *et al.* 1999). *S. cerevisiae* grown on 0.5% glucose, considered by some as a calorie-restricted diet, have significantly longer replicative lifespans than cells grown on 2% glucose, typically considered a calorically unrestricted diet. The longevity of 0.5% glucose-grown cells was initially shown to be dependent on Sir2: *sir2Δ* cells experienced no lifespan extension with calorie restriction (Lin, *et al.* 2002). The authors argued that calorie content of the growth medium could influence NAD^+ levels by affecting the redox balance of the cell. Since Sir2 depends on NAD^+ for its enzymatic function, changing NAD^+ levels could activate or inhibit Sir2, leading to downstream changes in aging and lifespan. In addition to being activated by NAD^+, Sir2 is inhibited by nicotinamide (NAM), a compound produced when Sir2 consumes a molecule of NAD^+ as part of the deacetylation reaction (Bitterman, *et al.* 2002). A network of enzymes recycles NAM back to NAD^+, to prevent NAM-induced inactivation of Sir2 (Sandmeier, *et al.* 2002). Several of these enzymes are influenced by the levels of a variety of nutrients, including nitrogen (Medvedik, *et al.* 2007), phosphorus (Lu, *et al.* 2011), and carbon (Gasch, *et al.* 2000), providing an alternate mechanism for nutrient sensing by Sir2.

Although observations linking Sir2 and calorie restriction were later supported by studies in other organisms (Tissenbaum and Guarente, 2001; Rogina and Helfand, 2004; Bordone, *et al.* 2007), the original yeast conclusions (Kaeberlein, *et al.* 2004), as well as related work in worms and flies (Burnett, *et al.* 2011) has since been questioned. Additionally, studies of yeast chronological lifespan have revealed no role for Sir2 in the calorie-restriction aging response (Smith, *et al.* 2007; Kaeberlein, *et al.* 2006) despite Sir2's ability to regulate chronological lifespan under some conditions (Fabrizio, *et al*. 2005). The discrepancies in the literature, particularly with respect to replicative aging, have been attributed to differences in strain background and media composition (Couzin-Frankel, 2011), leaving the role of Sir2 in calorie restriction, particularly in yeast, uncertain.

The mechanism(s) of calorie restriction-mediated longevity points to evolutionarily conserved nutrient sensing and signaling pathways like Insulin/IGF1 (Gesing, *et al.* 2014), AMPK (Greer, *et al.* 2007), RAS/PKA (Wei, *et al.* 2008), Tor/Sch9 (Kaeberlein, 2005), and possibly Sir2 (Guarente and Picard, 2005; Kaeberlein and Powers, 2007). The activities of these pathways are modified not just by sugar concentration, but also by the levels of many other nutrients. For instance, the levels of amino acids impact chronological aging (Maruyama, *et al*. 2016) and could, in principle, alter the response to calorie restriction.

Yeast chronological aging is studied almost exclusively on synthetic complete minimal medium (SC), which has high ammonium sulfate levels, and is weakly buffered against changes in pH compared to natural yeast substrates (Oliva, *et al.* 2011; Garde-Cerdán, *et al.* 2011; Sanchez, 2008; Coghe, *et al.* 2005) and standard yeast peptone medium (YP) (Weinberger, *et al.* 2010). SC medium is used in chronological aging studies because yeast grown to saturation in this medium arrest efficiently in stationary phase, with most if not all cells remaining quiescent until

plated to fresh medium (Longo and Fabrizio, 2012). A molecular mechanism linked to pH in yeast has been proposed for chronological aging broadly and the calorie restriction response specifically (Burtner, *et al.* 2009), but it is unclear if this applies to cells grown in well-buffered environments.

It is important to note that there is no universally agreed upon calorie restriction protocol. The full-calorie, ad libitum, diet used is somewhat arbitrary, and varies from organism to organism (Koubova and Guarente, 2003; Taormina and Mirisola, 2014; Piper and Bartke, 2008). The arbitrary nature of calorie restriction protocols is evident in replicative and chronological aging studies with *S. cerevisiae.* Both protocols use 2% glucose as the ad libitum, high calorie diet[4]. But in nature, *S. cerevisiae* seems particularly well-adapted to high-sugar environments, with many yeast substrates containing well over 10% sugar by weight. For reference, brewing wort typically ranges from 8-12% w/v sugar (Coghe, *et al.* 2005), tree saps contain as much as 16% sugar (Sanchez, 2008), and grapes can contain over 20% sugar (Oliva, *et al.* 2011; Garde-Cerdán, 2011). All of these substrates are favored environments of *S. cerevisiae*.

2% glucose has been the standard sugar concentration in the majority of *S. cerevisiae* laboratory research papers over the last 100 years. The choice of 2% glucose is practical, as the growth rate of yeast is fairly constant between 2% and 20% or more glucose (Slator, 1908; White, 1955). Rather than 2% glucose being calorically relevant, it instead seems to be a relic of laboratory economic history. It is possible the discrepancies in the literature over Sir2's role in calorie restriction-mediated longevity is due to the "full-calorie" diet itself being on the edge of calorie restriction for *S. cerevisiae*. If true, using a higher concentration of sugar for the full-calorie diet could expand the dynamic range of phenotypic measurement, allowing previously missed effects of Sir2 on lifespan to be revealed.

To better understand Sir2's role in lifespan extension via calorie restriction, I determined the chronological lifespan of wild-type and *sir2Δ* cultures using a newly developed genetic strategy to allow for investigation of longevity in previously unexplored media conditions. By using 2% glucose as a calorie-restricted environment and 12% glucose as a full-calorie diet, I identified a role for Sir2 in calorie restriction-mediated chronological longevity that was highly dependent on the growth conditions. I also discovered that these same environments alter Sir-based silencing at *HML* in wild-type cells.

Materials and Methods

Yeast strains and media

Genotypes of strains from this study are given in Table S1. JRY10779 was derived from W303 (JRY4012) using standard yeast methodology. JRY10782 came from the lab strain collection. UCC8650 was provided by Dr. Dan Gottschling. A PCR fragment containing p*SCW11-cre-EBD* and ~500bp of flanking sequence was generated using genomic DNA from UCC8650 as a template, and transformed into JRY10782 to generate strain JRY10786. JRY10759, JRY10762, JRY10765, and

JRY10768 were generated by mating JRY10776 to JRY4012, JRY527, JRY8822, or JRY9135, respectively, and selecting for diploids. In the case of liquid media, synthetic complete minimal medium (SC) was produced according to the standard protocol (Fabrizio and Longo, 2007), with minor changes as described. Media were prepared with either 2% w/v or 12% w/v glucose, with 10% w/v sorbitol added only to 2% media to control for osmolarity differences between 2%- and 12%-glucose cultures. Additionally, SC media were supplemented with four-fold excesses of leucine, lysine, tryptophan, histidine, and uracil as needed to complement strain auxotrophies, and pH-adjusted to 5.0 with NaOH. YP medium was produced according to the standard protocol, also with minor changes as described. Media was prepared with either 2% w/v or 12% w/v glucose, with 10% w/v sorbitol added only to 2% media as appropriate. Rather than autoclaving, which causes glucose to caramelize, media were filter-sterilized using 0.2 μm polyethersulfone filters. Solid complete minimal media were prepared using complete drop-out supplement mixture lacking tryptophan (CSM –Trp) (Sunrise Science Products). Solid yeast peptone media was prepared according to the standard protocol. All solid media included 0.5%, 2%, 6%, or 12% glucose, with or without sorbitol, as specified in figure legends.

Measurement of chronological lifespan

5 mL seed cultures of individual colonies (in either 2%- glucose SC or 2%-glucose YP media) were grown overnight, shaking at 200 RPM at 30°C. Flasks with 50 mL of appropriate media (both 2%- and 12%-glucose) were seeded to generate an initial cell concentration of 0.1 OD_{600} units, and incubated at 200 RPM at 30°C until growth ceased for a period of 24 hours as monitored by OD_{600} reading, usually on day 3 regardless of glucose concentration or type of medium. At this point, 100 μL aliquots of each culture were removed and the 50 mL cultures were left shaking at 200 RPM at 30°C. A 10-fold serial dilution series was created from the removed 100 μL aliquot, generating 1:10, 1:100, 1:1,000, and 1:10,000 dilutions. 100 μL of 1:10,000 dilution sample was then spread evenly over a fresh 2%-glucose YP plate and incubated at 30°C to determine the colony-forming units (CFU) score for each. At subsequent time-points, additional 100 μL aliquots were removed from the still-shaking 50 mL cultures, diluted, plated, and counted as before. The CFU score for each culture decreased as a function of time, generating a lifespan curve for each. CFU scores generated were typically based on counting between 50 and 500 colonies. All experiments were performed in biological triplicate. 250 mL Erlenmeyer flasks (Pyrex No. 4980 Stopper No. 6) with 38 mm silicone sponge closures (Chemglass Life Sciences CLS-1490-038) were used for all experiments. For the media-swap experiment (Figure S2), spent media was switched between wild-type and *sir2Δ* on day 3 following inoculation of cultures.

Genetic strategy for measurement of chronological lifespan

JRY10786 expresses cre, fused to the estradiol-binding domain of the murine estradiol receptor (cre-EBD), from daughter-cell-specific promoter p*SCW11*. Elsewhere in the genome, *loxP* sites flank *RFP*, upstream of a promoterless *GFP*. When cre-EBD is produced in a newly-forming daughter cell in the presence of estradiol, cells switch from transcribing *RFP* to transcribing *GFP*. 5 mL seed cultures of individual colonies (in either SC 2%- glucose or YP 2%-glucose media) were grown overnight and seeded to generate an initial cell concentration of 0.1 OD_{600} units and cultured as above until day 3. At this point, 100 µL of each culture was removed. 5 µL of 10 mM β-estradiol, dissolved in DMSO, was added to all 50 mL cultures to generate a final concentration of 1 µM, and the cultures were left shaking at 200 RPM at 30°C. A 10-fold serial dilution series was created from the removed 100 µL aliquot, generating 1:10, 1:100, 1:1,000, and 1:10,000 dilutions. 100 µL of 1:10,000 dilution sample was then spread evenly over a fresh 2%-glucose YP plate and incubated at 30°C. After 3 days, the plates were scanned face up using a Typhoon Trio (GE Healthcare Life Sciences, Buckinghamshire, England). The 488 nm laser and 520 nm emission filter were used to detect GFP fluorescence, and the 532 nm laser and 610 nm emission filter were used to detect RFP fluorescence. All colonies were counted, but only RFP-fluorescing colonies were used to generate a colony-forming units (CFU) score for each. At subsequent time-points, additional 100 µL aliquots were removed, serially diluted, plated, and counted as before. The CFU score for each culture decreased as a function of time, generating a lifespan curve for each, as described above. YP experiments were performed in biological triplicate. SC, no-cre, and no-estradiol control experiments were performed in duplicate. 250 mL Erlenmeyer flasks (Pyrex No. 4980 Stopper No. 6) with 38 mm silicone sponge closures (Chemglass Life Sciences CLS-1490-038) were used for all experiments.

Colony growth and imaging

Triplicate cultures were grown to log phase (0.4 OD_{600}) in 2%-glucose complete drop-out supplement mixture lacking tryptophan (CSM –Trp) (Sunrise Science Products) for data in Figure 7 or 2%-glucose YP for data in Figure 8. Tryptophan was excluded from the medium because its intrinsic fluorescence interferes with colony imaging. CSM medium is very similar to SC medium, especially with regard to pH buffering strength and total nitrogen, differing only in the specific proportions of amino acids, adenine, and uracil. Cultures were diluted 1:20,000 and plated on appropriate solid medium (CSM-Trp or YP) containing 0.5%, 2%, 6%, or 12% glucose, with or without sorbitol as specified. This resulted in 10-20 colonies per plate. CSM-Trp colonies were imaged on day 5 of growth, whereas YP colonies were imaged on day 4. All colonies were imaged using a Zeiss Axio Zoom.V16 microscope and ZEN software, with a Zeiss AxioCam MRm camera and PlanApo Z 0.5× objective.

Stability of silencing in liquid YP culture

5 mL seed cultures of individual colonies in 2%-glucose YP media were grown overnight, shaking at 200 RPM at 30°C. 50 mL of appropriate media (both 2%- and 12%-glucose) was seeded to generate an initial cell concentration of 0.1 OD_{600} units. 50 mL cultures shook at 200 RPM at 30°C. Aliquots were removed at regular time intervals during log-phase growth and continuing throughout stationary phase. Aliquots were diluted and plated to give ~50-500 cells per plate. After 3 days, the plates were scanned face up using a Typhoon Trio as above. The number of all-green colonies was divided by the total number of colonies to determine silencing stability within a culture at that time point.

Data availability

Strains are available upon request. **Table S2.1** contains descriptions of all strain genotypes.

Results

Calorie restriction extended yeast chronological lifespan over a broad range of sugar concentrations in complete minimal medium

While calorie restriction extends yeast chronological lifespan when starting glucose concentration in complete minimal medium is dropped below 2%, chronological lifespan has rarely been studied at higher glucose concentrations comparable to many natural niches of yeast (Smith *et al.* 2007; Longo, *et al*. 2012). I measured the chronological lifespan of a wild-type strain (JRY4012) grown in either 2% or 12% glucose complete minimal medium. Sorbitol was added to 2%-glucose medium to control for osmotic pressure differences between 2%- and 12%-glucose media. Growth at 2% glucose resulted in a greater mean and maximal lifespan as compared to growth at 12% glucose **(Figure 2.1)**. Higher osmotic pressure of 12%-glucose cultures did not cause the shortened lifespan of these cultures or influence the effect of *sir2Δ* on lifespan, as adding sorbitol to 2%-glucose cultures did not shorten lifespan and actually extended lifespan of 2%-glucose-grown cells independent of Sir2 **(Figure S2.1)**. Thus calorie restriction extended *S. cerevisiae* chronological lifespan across a wide range of glucose concentrations, not just from 2% and below. Therefore, these glucose concentrations defined a new and physiologically relevant context for studying calorie-level-mediated impacts on yeast chronological lifespan.

sir2Δ dramatically extended chronological lifespan in 12%-glucose complete minimal cultures and had little effect in 2%-glucose cultures

Previous studies have found that calorie restriction extends chronological lifespan independently of Sir2 in cultures grown in complete minimal 2%-glucose

conditions (Smith, *et al.* 2007)**,** which I confirmed **(Figure 2.2A)**. However, deletion of *SIR2* dramatically increases maximum chronological lifespan of cultures when media is replaced with water, an extreme calorie restriction state (Fabrizio, *et al.* 2005). To determine whether Sir2 is involved in calorie restriction-mediated longevity under our new protocol, I measured chronological lifespan of wild-type and *sir2Δ* cultures in complete minimal medium with 2% or 12% glucose **(Figure 2.2)**. Surprisingly, deletion of *SIR2* dramatically extended both mean and maximum chronological lifespan in 12% glucose-grown cultures **(Figure 2.2B)**. Therefore, Sir2's impact on chronological lifespan varied dramatically depending on the initial calorie content of growth medium. In this experimental context, Sir2 acted to decrease lifespan as glucose was consumed from a starting level of 12%. Sir2's effect on aging in 12% glucose seems to have both a cell-intrinsic and a cell extrinsic component, as swapping of spent media between wild-type and *sir2Δ* cultures at the start of stationary phase resulted in a similar intermediate longevity phenotype for both genotypes **(Figure S2.2)**. I discuss these two components more extensively below.

sir2Δ shortened chronological lifespan in 2%-sugar yeast peptone cultures while having little effect in 12%-sugar cultures

To determine how Sir2 regulates aging in cells grown in other media, I had to get around a previously documented phenomena in which a subpopulation of cells in a stationary-phase culture continue to divide, even as most cells in a culture remain quiescent (Allen, *et al.* 2006) or die. Complex media like yeast peptone support larger nonquiescent populations in stationary-phase cultures than does complete minimal medium, which is one reason why complete minimal medium is used in chronological aging experiments (Fabrizio and Longo, 2007). If a stationary-phase culture has a subpopulation of cells that continue to divide, that culture is now a mixture of both chronologically old cells and young cells. A culture that appears to retain viability for a longer period of time could reflect actual increased longevity of individual cells. Alternatively, it could result from higher rates of stationary-phase cell division producing new cells. Quantitatively rigorous studies of aging at the population level are nearly impossible under these conditions. Experiments using 12%- and 2%-glucose YP revealed extensive cell division, especially in stationary-phase 12%-glucose-grown cultures, complicating interpretation of aging dynamics **(Figure 2.3A)**. This phenomenon, where stationary-phase cultures rapidly lose viability and a surviving subset re-enter the cell cycle, appears to be an example of adaptive regrowth, which been documented previously (Fabrizio, *et al*. 2004).

To circumvent this dilemma, I developed a genetic strategy, based in part on the mother enrichment program (Lindstrom and Gottschling, 2009), to differentiate between old cells (those present at the very beginning of stationary phase) and young cells (those born during stationary phase) **(Figure 2.3B)**. Expression of the cre recombinase (Abremski and Hoess, 1984) is driven by the promoter for *SCW11*, a gene encoding a cell wall protein that is expressed only in newly forming daughter

cells and never in old mother cells (Doolin, *et al.* 2001; Colman-Lerner, *et al.* 2001). Cre is also fused to the estradiol-binding domain of the murine estradiol receptor (cre-EBD). The cre-EBD hybrid protein remains in the cytoplasm until β-estradiol is added to the growth medium, when it binds to the estradiol-binding domain and allows cre-EBD to be shuttled into the nucleus (Lindstrom and Gottschling, 2009). Elsewhere in the genome, an *RFP* gene, flanked by *loxP* sites, lies downstream of a constitutive promoter, and upstream of a promoterless *GFP* gene. In cultures of this strain lacking β-estradiol grown to stationary phase, cre-EBD protein is produced in all newly forming daughter cells, but remains in the cytoplasm, unable to act on *loxP* sites flanking *RFP.* Once cultures reach stationary phase, β-estradiol is spiked into the culture medium to a final concentration of 1 μM. Now, if a non-quiescent cell divides, the newly forming daughter cell will produce cre-EBD protein, now in the presence of β-estradiol, cre-EBD is shuttled into the nucleus where it can act on the *lox-P* sites, excising *RFP* and bringing *GFP* under the control of the constitutive promoter (Cheng, *et al.* 2000). Rather than expressing *RFP* like their aging mothers, newly formed daughter cells express *GFP.* When diluted aliquots of the culture are plated to fresh medium over time, colonies forming on the plate will express either *RFP* or *GFP*, depending on whether they descended from an old mother cell or a young daughter cell, respectively **(Figure 2.3C)**. By counting only *RFP*-expressing colonies, the resulting lifespan curves represent the aging dynamics of old mother cells present at the start of stationary phase.

I first measured chronological lifespan of wild type and *sir2Δ* isolates of this strain in 2%- and 12%-glucose complete minimal media. Most if not all cells remained quiescent in stationary phase, with no increase in the proportion of *GFP*-expressing colonies beyond a low background level **(Figure 2.4A and B)**. Aging characteristics of wild-type and *sir2Δ* cultures, both 2%- and 12%-glucose, mirrored those observed without the use of this genetic strategy **(Figure 2.4C and D)**. There was also no significant change in aging dynamics in strains lacking cre-EBD or in strains grown in medium lacking β-estradiol, as expected.

I then measured chronological lifespan of wild-type and *sir2Δ* isolates of this strain in 2%- and 12%-glucose YP media. As previously reported, 2%-glucose YP cultures had a significant number of daughter cells born in stationary phase, with these cultures eventually being composed of roughly 20% *GFP*-expressing cells **(Figure 2.5A)**. 12%-glucose cultures, on the other hand, were quickly heavily represented by newborn *GFP*-expressing cells **(Figure 2.5B)**. By ignoring *GFP*-expressing colonies, lifespan curves for 2%- and 12%-glucose YP media represented only age-matched mother cells. Surprisingly, loss of Sir2 had no effect in 12%-glucose YP cultures **(Figure 2.5D)**. In contrast, loss of Sir2 in 12%-glucose complete minimal cultures dramatically extended mean and maximal chronological lifespan under those conditions **(Figure 2.2B)**. Also surprisingly, loss of Sir2 significantly shortened mean and maximal chronological lifespan in 2%-glucose YP cultures **(Figure 2.5C)**. This again contrasted with loss of Sir2 on 2%-glucose complete minimal cultures, which had little if any effect on chronological lifespan under those conditions **(Figure 2.2A)**.

Sir2's impact on chronological lifespan varied dramatically depending on aspects of the medium beyond sugar content. In YP, *sir2Δ* decreased lifespan in low glucose and had no effect in high glucose. Therefore, for wild-type cells growing in YP, Sir2 *increased* lifespan as starting calorie content *decreased* **(Figure 2.5C and D)**. In complete minimal medium, on the other hand, *sir2Δ* had no effect in low glucose and increased lifespan in high glucose. Therefore, for wild-type cells growing in minimal medium, Sir2 facilitates a *decrease* in lifespan as starting calorie content *increased* **(Figure 2.2A and B)**. These phenotypes provided an expanded view of the role for Sir2 in calorie restriction-mediated chronological longevity.

Increasing glucose concentration strengthened Sir-based silencing at *HML* in complete minimal medium

Sir2's primary function is in transcriptional silencing through the deacetylation of histone tails, resulting in heterochromatin formation at discrete loci within the genome. Therefore I explored whether this range of culture media also affected the strength of Sir2-based transcriptional silencing. The Sir2/3/4 complex is necessary for silencing *HML*, and loss of Sir function results in constitutive transcription of the *α1* and *α2* genes contained within (Rusche, *et al.* 2003). I employed a recently developed method from our lab that marks cells that have experienced transient losses of silencing at the *HML* locus (Dodson and Rine, 2015) **(Figure 2.6)**. In this method, known as the CRASH assay for Cre-Reported Altered States of Heterochromatin (Liu, *et al.* 2016), the coding sequence of *α2* at *HML* has been replaced with the coding sequence of *cre*, and *cre* is expressed only if Sir-based silencing at *HML* is disrupted. If cre protein is produced, it acts on *loxP* sites flanking *RFP*, upstream of *GFP*. Cells that have lost silencing, even transiently, switch from red to green fluorescence **(Figure 2.6A)**. This switch is permanent and heritable. When cultures are diluted, plated and grown into colonies, green sectors form in an otherwise red colony **(Figure 2.6B)**. Each of these green sectors represents a loss-of-silencing event in the cell at the apex of the sector. The green sectoring rate of a strain can be assessed, either qualitatively or quantitatively (Dodson and Rine, 2015; Liu, *et al.* 2016), to determine the stability of Sir-protein based silencing at *HML* relative to wild type.

I plated the wild-type CRASH strain on solid drop-out minimal medium on a range of glucose concentrations, 0.5%, 2%, 6% and 12%. Interestingly, increasing glucose concentration stabilized silencing at *HML*, with fewer green sectors seen in 12% glucose colonies as compared to 0.5% glucose colonies **(Figure 2.7)**. Colonies grown on 2% and 6% glucose (not shown) fit this general trend. Supplementing lower-glucose media with sorbitol to achieve similar osmotic pressures in each case had no effect on silencing phenotypes (not shown).

Increasing glucose concentration weakened Sir-based silencing at *HML* in yeast peptone medium

Because of the surprising differences in the effect of glucose concentrations on aging in the two media types, I explored the impact of increasing glucose concentration on silencing at *HML* in YP medium. Colonies from wild-type CRASH cells were imaged following growth on solid YP media containing 0.5%, 2%, 6% or 12% glucose. Quite surprisingly, increasing glucose levels caused a marked destabilization of silencing in a unique spatio-temporal pattern **(Figure 2.8)**. All previously studied interventions that destabilized silencing in the CRASH assay resulted in loss-of-silencing events relatively early in colony growth and continued throughout the growth of the colony, forming a visible green sectors of sizes proportional to the timing of the events (Dodson and Rine, 2015; Liu, *et al.* 2016). Here, however, loss-of-silencing events, particularly in 6% and 12% glucose, occurred late in colony development, preventing their outgrowth into a visible green sector. Instead, red cells and green cells were next to one another, giving a yellow appearance when the two fluorescence channels were merged. This appearance was not due to inappropriate expression of both fluorophores in a single cell, as streaking these colonies onto fresh solid medium to isolate single colonies revealed close to half of the cells in 6% and 12% glucose had switched from red to green (not shown). Strikingly, 0.5%-and 2%-glucose-grown colonies completely lacked this phenotype, and appeared quite similar to one another. Hence, while glucose concentrations previously used to study calorie restriction showed no change in Sir-based silencing, higher glucose concentration had a dramatic effect on heterochromatin stability.

Stationary-phase cells in 12%-glucose liquid cultures lost silencing at high rates compared to 2%-glucose-grown cultures

Since cells losing silencing in high-glucose-grown colonies weren't dividing much, if at all, at the time they were imaged, I wanted to see if stationary-phase cells in particular were more likely to lose silencing at *HML*, or whether the high glucose conditions caused elevated loss of silencing rates continuously during growth. I inoculated liquid YP medium containing either 2% or 12% glucose with the CRASH strain and grew cultures to stationary phase. At time points throughout log-phase growth and during stationary phase, aliquots were plated to fresh solid medium and the proportion of all-green colonies was quantified. For all-green colonies, the founding cell had to have lost silencing in liquid culture, before its plating. Cells grown in 12% glucose lost silencing at a rate similar to 2%-glucose-grown cells during log-phase growth. In stationary phase, however, 12%-glucose-grown cultures exhibited high rates of silencing loss, eventually plateauing with 35% of cells having lost silencing **(Figure 2.9)**. Given that, under standard experimental conditions, wild-type cells lose silencing at *HML* only once every 1,000 cell-divisions (Dodson and Rine, 2015), this rate represents a massive destabilization of Sir-based silencing based upon changes in physiology and not genotype. The period of

silencing instability **(Figure 2.9B)** preceded the period of stationary-phase regrowth **(Figure 2.9A)**.

Glucose control of heterochromatin was robust to genetic background

To determine whether the effect of glucose levels on heterochromatin stability was specific to the genetic background of our strains, I mated the haploid W303 CRASH strain to *S. cerevisiae* haploid strains of either W303 or s288c backgrounds. Additionally, I mated the CRASH strain to *S. paradoxus* and *S. bayanus* haploid strains. I plated all four of the resulting diploids on solid YP media with 0.5%, 2%, 6%, or 12% glucose, and imaged the resulting colonies as before. As with the W303 haploid strain, all of these diploid strains lost silencing at the tops of colonies grown on the higher glucose media **(Figure 2.10)**.

Discussion

This work demonstrated that calorie restriction extended chronological lifespan across a wider range of sugar concentrations, not just below 2% **(Figure 2.1)**. There is evidence that Sir2 does not mediate the extension of chronological lifespan in response to calorie restriction, at least in any previously used protocols (Smith, *et al.* 2007). Even so, *sir2Δ* does extend lifespan of cells experiencing extreme nutrient restriction in water, while having little effect in media with 2% glucose (Fabrizio, *et al.* 2005). In the case of extreme nutrient restriction, Sir2 acts to oppose the beneficial effects on lifespan. However, because all nutrients are limiting in water, determining which nutrient(s) are involved is not possible. Under our new protocol, Sir2 has a clear role in reducing lifespan as glucose levels increase in complete minimal medium **(Figure 2.2)**. Classically, calorie restriction-mediated longevity is thought of as a beneficial effect on lifespan of decreasing calorie content, rather than a detrimental effect on lifespan of increasing calorie content. However, these two views are logically equivalent ways of describing the same phenomenon. What is clear, however, is that Sir2 is not sufficient for calorie restriction-mediated longevity in this context, as 12%-glucose *sir2Δ* cultures did not phenocopy 2%-glucose *sir2Δ* cultures **(Figure 2.2)**.

Sir2's effect on aging in 12% glucose seems to have both a cell-intrinsic and a cell-extrinsic component. Swapping wild-type and *sir2Δ* 12%-glucose spent media at the start of stationary phase results in a similar, intermediate longevity phenotype for both genotypes **(Figure S2.2)**. Therefore, the composition of stationary-phase media isn't sufficient to determine lifespan. At least part of Sir2's contribution came before stationary phase and irreversibly altered aging dynamics. Acidification of culture medium has been proposed as the primary mechanism for yeast chronological aging in unbuffered complete minimal media (Burtner, *et al.* 2009). Sir2's removal of acetyl groups from histones and other proteins could affect the acidity of the culture, possibly explaining Sir2's negative role in aging in high glucose complete minimal cultures. Additionally, Sir2 modulates the activity of Pck1, an enzyme involved in gluconeogenesis (Lin, *et al.* 2009). Sir2's deacetylation

of Pck1 may mediate the Sir-dependent effects on chronological lifespan (Orlandi, *et al.* 2016). Our data are consistent with Sir2 altering the activity of Pck1 to affect culture acidification and ultimately lifespan. However, the intermediate longevity observed in the media-swap experiment implies that Sir2 must exert an additional effect, either through Pck1 or through another target, during log-phase growth. Addition of nicotinamide in stationary phase phenocopied deletion of *SIR2* with respect to chronological aging in 2% glucose and in extreme dietary restriction. Therefore Sir2's aging role in these contexts is restricted to its enzymatic function alone (Orlandi, *et al.* 2016). If Pck1 mediates the Sir-dependent reduction in lifespan in 12%-glucose cultures, Pck1 function must be altered before stationary phase in this condition. Alternatively, a different Sir2 target could be responsible for the cell-intrinsic effects on lifespan seen following growth in 12% glucose.

Under some growth conditions, a fraction of stationary-phase cells regrow as others lyse (Fabrizio and Longo, 2007; Fabrizio, *et al.* 2004). This regrowth phenomenon was observed to such a high degree in 2%- and 12%-glucose YP cultures that it initially prevented study of chronological aging in these conditions **(Figure 2.3A)**. However, by deploying our newly developed genetic strategy to differentiate aging mother cells from newborn progeny **(Figure 2.3B)**, it is clear that calorie restriction extends the lifespan of individual cells, even as the cultures themselves have lower total viability at many time points **(comparing 12%-glucose data from Figure 2.3A to Figure 2.5D)**. In contrast to cultures grown in complete minimal medium, in YP medium *sir2Δ* had no effect on the lifespan of 12%-grown cells **(Figure 2.5D)**, while significantly shortening the mean and maximal lifespan of 2%-grown cells **(Figure 2.5C)**. This phenotype was consistent with a partial role for Sir2 in calorie restriction-mediated longevity in YP medium in which Sir2 was necessary for the complete lifespan extension via calorie restriction. It is important to note that in YP medium *sir2Δ* 2% cultures didn't phenocopy 12% cultures, demonstrating that Sir2 was not sufficient for calorie restriction-mediated longevity in this medium, just as it was not sufficient in complete minimal medium.

Sir2's impact on calorie restriction-mediated longevity varied dramatically depending on type of growth medium. In YP, Sir2 *extends* lifespan as glucose is *decreased*. Conversely, in complete minimal medium, Sir2 *shortens* lifespan as glucose is *increased*. In both cases, Sir2 is responding to changes in glucose to alter aging dynamics in a way that makes 2% glucose cultures live longer than 12% glucose cultures. In both cases, the exact mechanism through which Sir2-mediated, glucose-dependent, lifespan divergence occurs is unknown. It is also not clear whether a common downstream target, presumably a protein that is deacetylated by Sir2, mediates all of these effects, or whether different targets of Sir2 contribute to calorie restriction-mediated longevity in different growth media.

Interestingly, Sir-based silencing at *HML* was *stabilized* as glucose increases in minimal medium (CSM), while silencing is *destabilized* as glucose increases in YP medium **(compare figures 2.7 and 2.8)**. This change in directionality is reminiscent of the change in directionality of *sir2Δ* aging phenotypes when switching from complete minimal medium to YP medium. It will be interesting to see if the different effects of media act directly through Sir2, perhaps through NAD+

levels or phosphorylation (Kang, *et al.* 2015), to alter Sir-based silencing at *HML*, or indirectly through other targets. Perhaps a common downstream target of glucose, and possibly Sir2, mediates the opposite effects on heterochromatic silencing seen in complete minimal and YP media as glucose levels increase.

The marked loss of silencing in 12% glucose YP cultures during stationary phase points to the possibility that subtelomeric genes normally silenced by Sir2 (Aparicio, *et al.* 1991) are expressed under these conditions, providing some advantage to cells. Interestingly, subtelomeric regions are enriched for genes with a role in metabolism (Ai, *et al.* 2002), although few subtelomeric genes significantly increase in expression over wild-type levels in a *sir2Δ* strain during log-phase growth in 2% glucose (Ellahi, *et al.* 2015). However, it is possible that expression levels of important metabolic genes do change in a Sir2-dependent manner at higher glucose concentrations and/or during stationary phase.

Previously, the study of *S. cerevisiae* chronological aging was mostly confined to complete minimal media in which stationary-phase cells almost exclusively enter a quiescent, non-dividing state, ensuring that the population of cells being studied is as age-matched as possible. Complete minimal medium efficiently arrests stationary-phase cells because the pH of the medium drops significantly, below a level that allows for growth (Longo and Fabrizio, 2012). Media like pH-buffered complete minimal, YP, and many natural yeast substrates do not reach such low pHs, allowing for varying levels of regrowth. It is difficult, if not impossible, to interpret population-level aging data in a mixed-age population, especially when the relative distribution of individual ages is unknown. As a result, despite their potential physiological relevance, media allowing for stationary-phase growth have been avoided. With our new genetic strategy, however, yeast chronological aging can now be studied in any medium, regardless of its potential for stationary-phase growth. This is especially relevant to experiments in high-calorie and pH-buffered media, which support high levels of stationary-phase regrowth **(Figure 2.3; unpublished data)**. While data supports acidification of growth media via acetate production as the molecular mechanism driving yeast chronological aging (Burtner, *et al.* 2009), it is unclear whether this mechanism is relevant in an environmental context where pH remains more stable. Given that the first gene studied using this strategy, *SIR2*, is shown to have dramatically different aging roles in different environmental contexts, it seems especially important to study aging across these contexts.

Taken together, a picture emerges of Sir2 as an important regulator of yeast aging that responds to nutrient cues including, but not limited to, glucose. It is especially intriguing that Sir2 can either extend or shorten chronological lifespan in response to changes in nutrients. Many genes have either a positive (e.g. *SOD1* (Longo, *et al.* 1996)) or a negative (e.g. *SCH9* (Longo, 2003)) impact on chronological lifespan, often independent of the limited number of environments tested. The variety of inputs that lead to a variety of outputs positions Sir2 as a central regulator, responding to nutritional cues to either extend or shorten lifespan. In times of nutrient scarcity, it makes sense for yeast to prioritize cell-cycle arrest and longevity over reproduction, as reproduction is energy-expensive and their

offspring would be born into an environment unlikely to support survival. By remaining viable and conserving scarce resources, the chances increase that a yeast cell might encounter an energy-rich substrate where it can begin growing again. In times of plenty, when yeast are dividing rapidly and often in competition with other microorganisms with even faster division-rates, it makes sense to prioritize fast growth, even if accompanied by the high costs of genome instability and other forms of cellular damage that are thought to drive aging. Additionally, an apoptosis-like cell death program exists in yeast that is induced by chronological aging (Fabrizio and Longo, 2008). Under certain conditions, this programmed cell death enhances the maximal chronological longevity of a culture by killing off most of the cells, releasing nutrients and allowing for the regrowth of a robust, adapted sub-population of cells (Fabrizio, *et al.* 2004). It makes sense that, within a yeast colony or liquid culture that is essentially clonal, group selection (Leigh, 2010; Frank, 2013) could play a role in their evolution. Group selection could drive the development of an altruistic aging program as posited for *S. cerevisiae* (Fabrizio, *et al.* 2004), one that benefits the culture as a whole at the expense of individual cells.

Acknowledgements

I thank Dr. Dan Gottschling for providing us with the Mother Enrichment Program parent strain (UCC8650), from which I obtained the p*SCW11*-cre-EBD PCR fragment for use in our new genetic strategy. I also thank Dr. Anne Dodson, who provided JRY9628, JRY10776, and JRY10782. I also thank members of our lab, past and present, for helpful discussions that shaped this work. This work was supported by an NIH predoctoral fellowship (5 F31 AG047795-03) to DFM, as well as a grant from the National Institutes of Health to JR (GM31105).

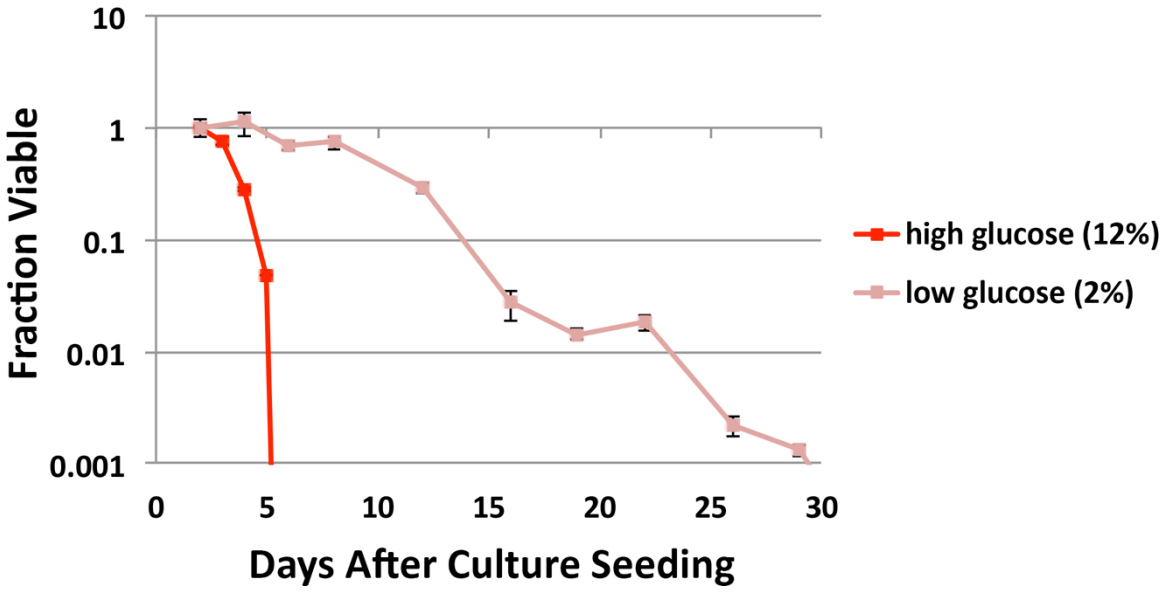


Figure 2.1. Chronological lifespan in high- and low- glucose complete minimal medium. A wild-type strain was grown to stationary phase in either 2% (low) or 12% (high) glucose and aliquots were removed, diluted, and plated over time. Colonies that grew were counted and the daily total was normalized to the total number of colonies viable at the first timepoint to give the fraction viable. Y-axis is cut off at 0.001 to zoom in on most relevant viability window.

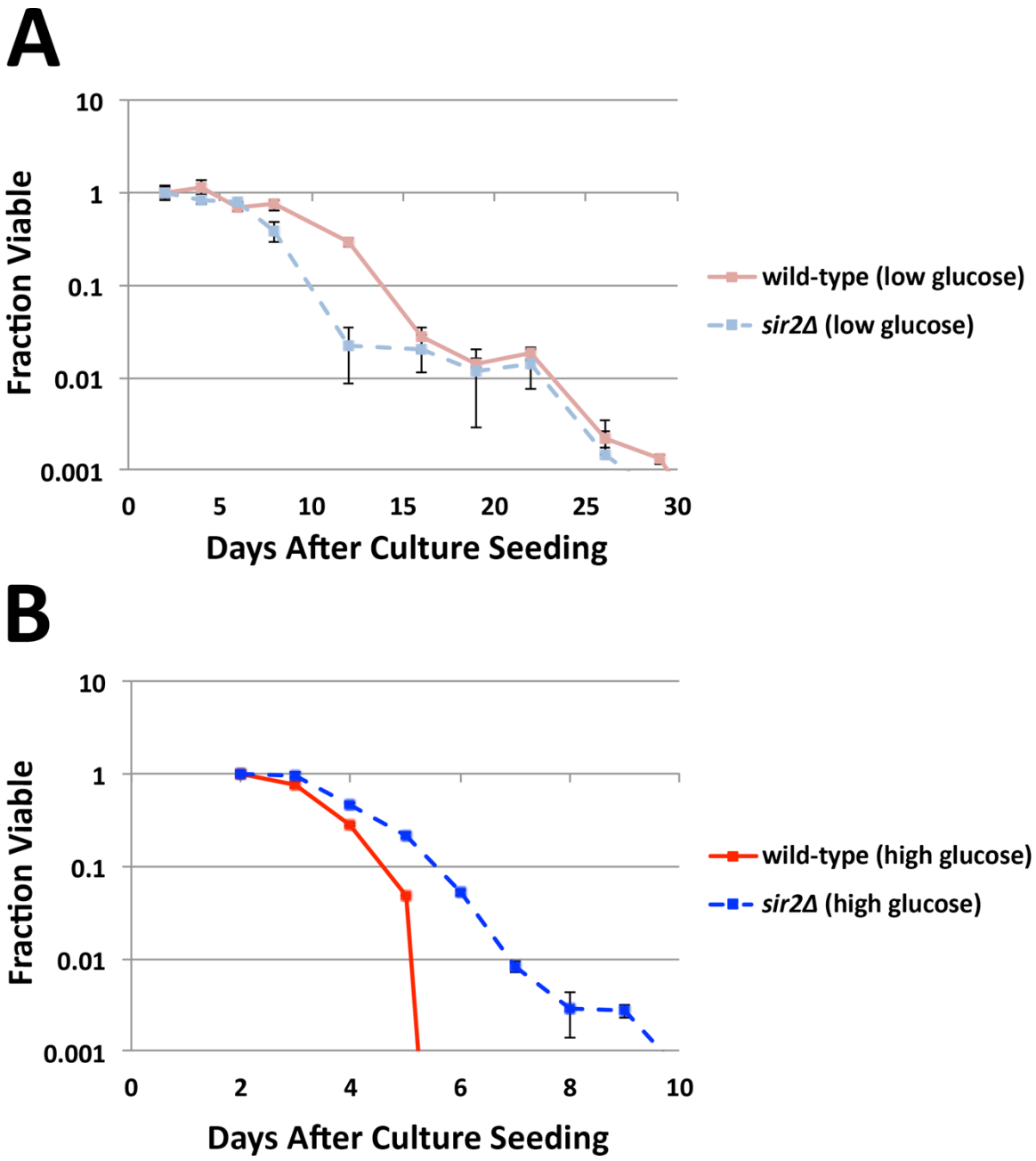


Figure 2.2. Effect of *sir2Δ* on chronological lifespan in high- and low- glucose complete minimal medium. Wild-type and *sir2Δ* strains were grown to stationary phase in either 2% (A) or 12% (B) glucose and aliquots were removed, diluted, and plated over time. Colonies that grew were counted and the daily total was normalized to the total number of colonies viable at the first time point to give the fraction viable. *sir2Δ* had no effect on lifespan in 2% glucose (A), while it significantly extended lifespan in 12% glucose (B). Y-axis is cut off at 0.001 to zoom in on most relevant viability window.

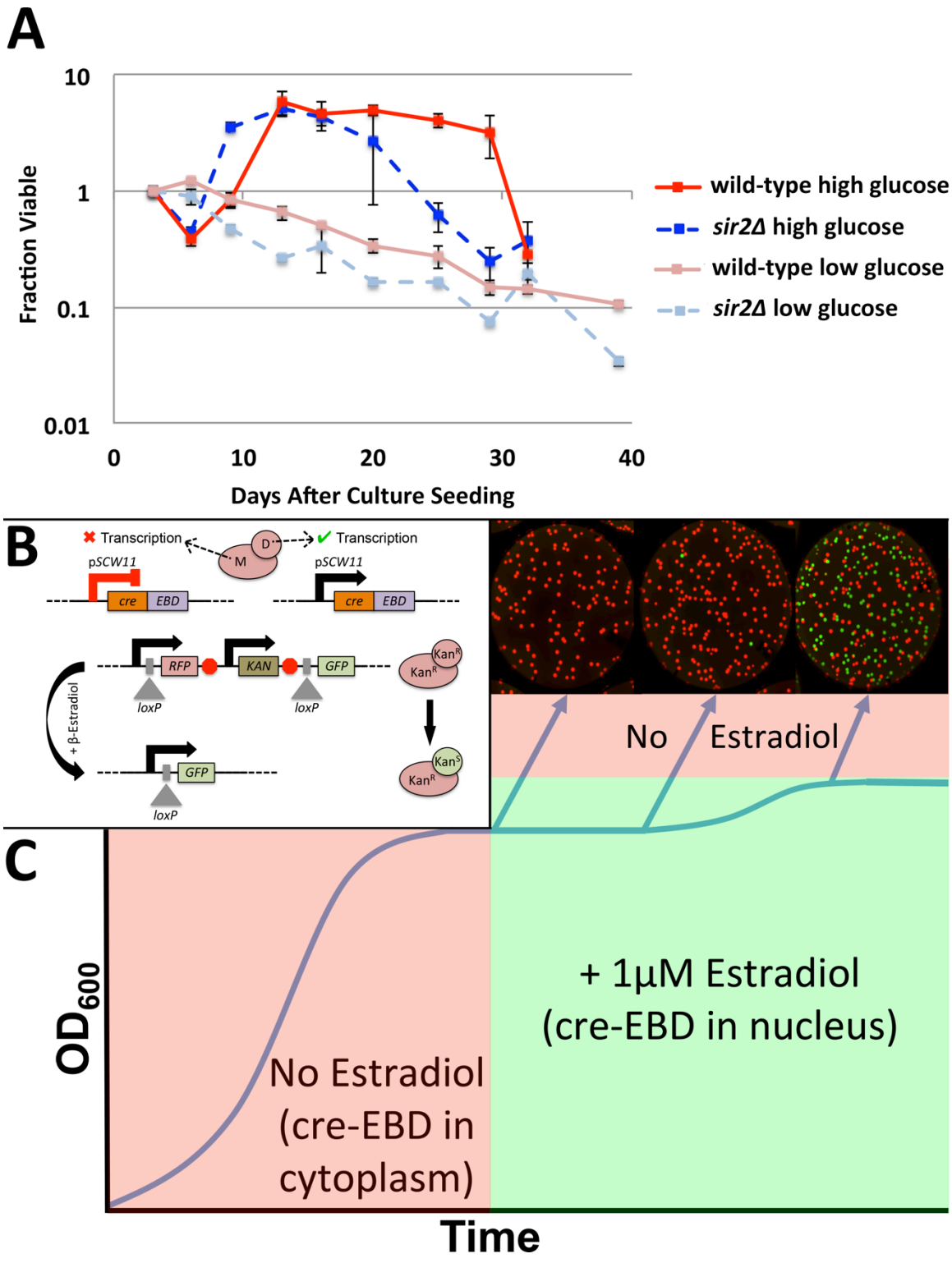


Figure 2.3. Genetic strategy for studying chronological aging and regrowth in any medium. (A) High and low glucose YP media allow for significant levels of stationary-phase regrowth, complicating interpretation of aging results. (B) Diagram of genetic components. Cre protein is produced only in newly-forming

daughter cells, and is only present in the nucleus in the presence of estradiol. If cre is in the nucleus, it acts on *loxP* sites flanking *RFP* and upstream of *GFP*, changing cells from red to green. (C) Diagram of modified chronological lifespan assay. Estradiol added to culture following log-phase growth period. Colonies formed from cells born after estradiol addition will fluoresce green and should be ignored when assaying chronological lifespan.

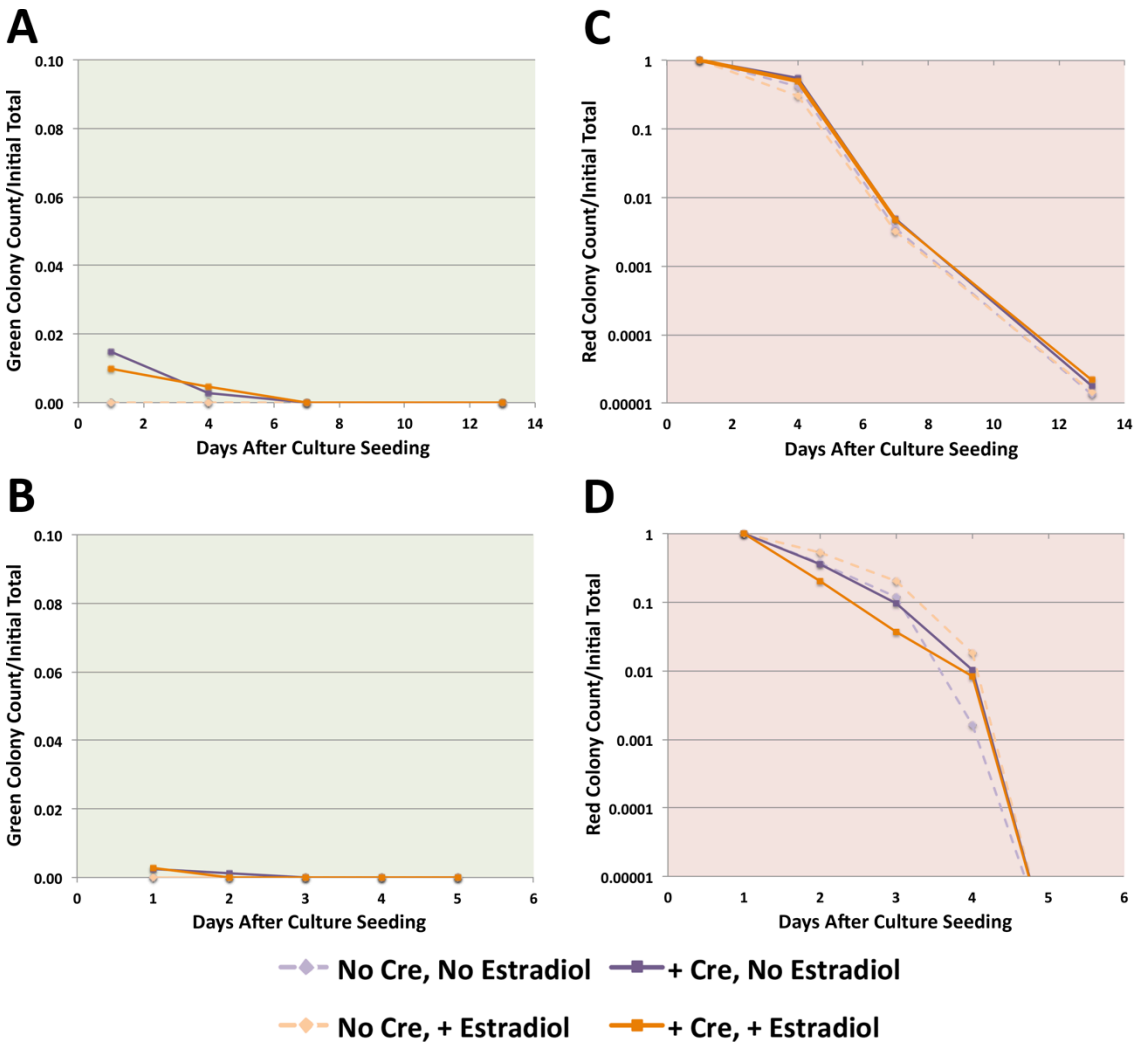


Figure 2.4. Chronological lifespan and stationary-phase regrowth in high- and low-glucose complete minimal medium. Green (A and B) or red (C and D) colonies were counted and normalized to the total number of colonies viable at the first time point. (A) and (C) represent 2%-glucose cultures, while (B) and (D) represent 12%-glucose cultures. Control experiments lacking cre and/or estradiol were included. Switching was never observed in experiments lacking cre, and no switching above background was observed without addition of estradiol. Complete minimal media did not support stationary-phase regrowth.

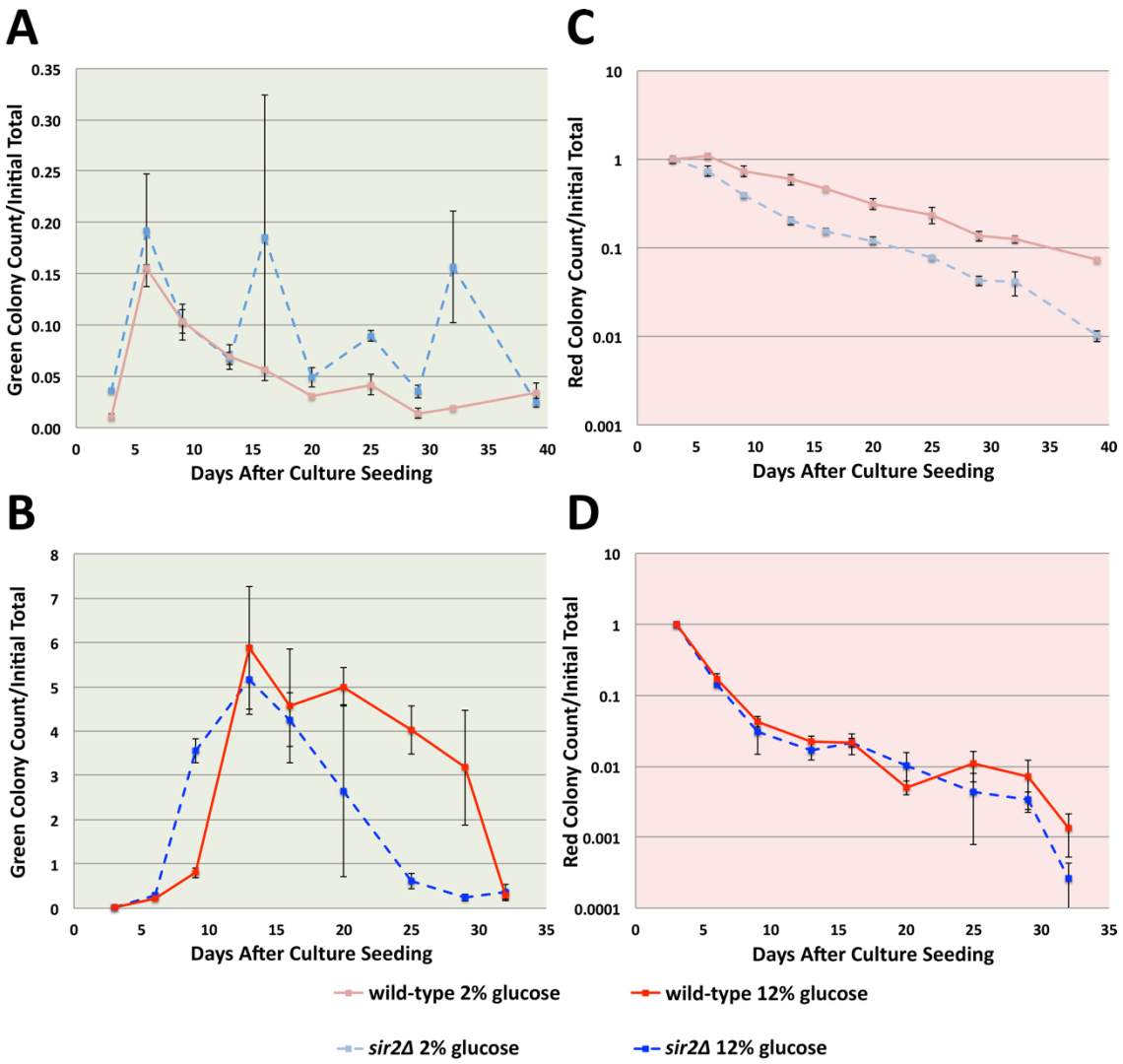


Figure 2.5. Effect of *sir2Δ* on chronological lifespan and stationary-phase regrowth in high- and low- glucose yeast peptone medium. Green (A and B) or red (C and D) colonies were counted and normalized to the total number of colonies viable at the first time point. (A) and (C) represent 2%-glucose cultures, while (B) and (D) represent 12%-glucose cultures. Both glucose concentrations allowed for stationary-phase regrowth (A and B), although regrowth was significantly increased in 12% glucose (B). Considering only red colonies, *sir2Δ* significantly decreased lifespan of 2%-glucose cultures (C), a phenotype that would have otherwise been obscured by stationary-phase regrowth of these *sir2Δ* cultures (A). In 12%-glucose cultures, however, *sir2Δ* had no significant effect on lifespan (D).

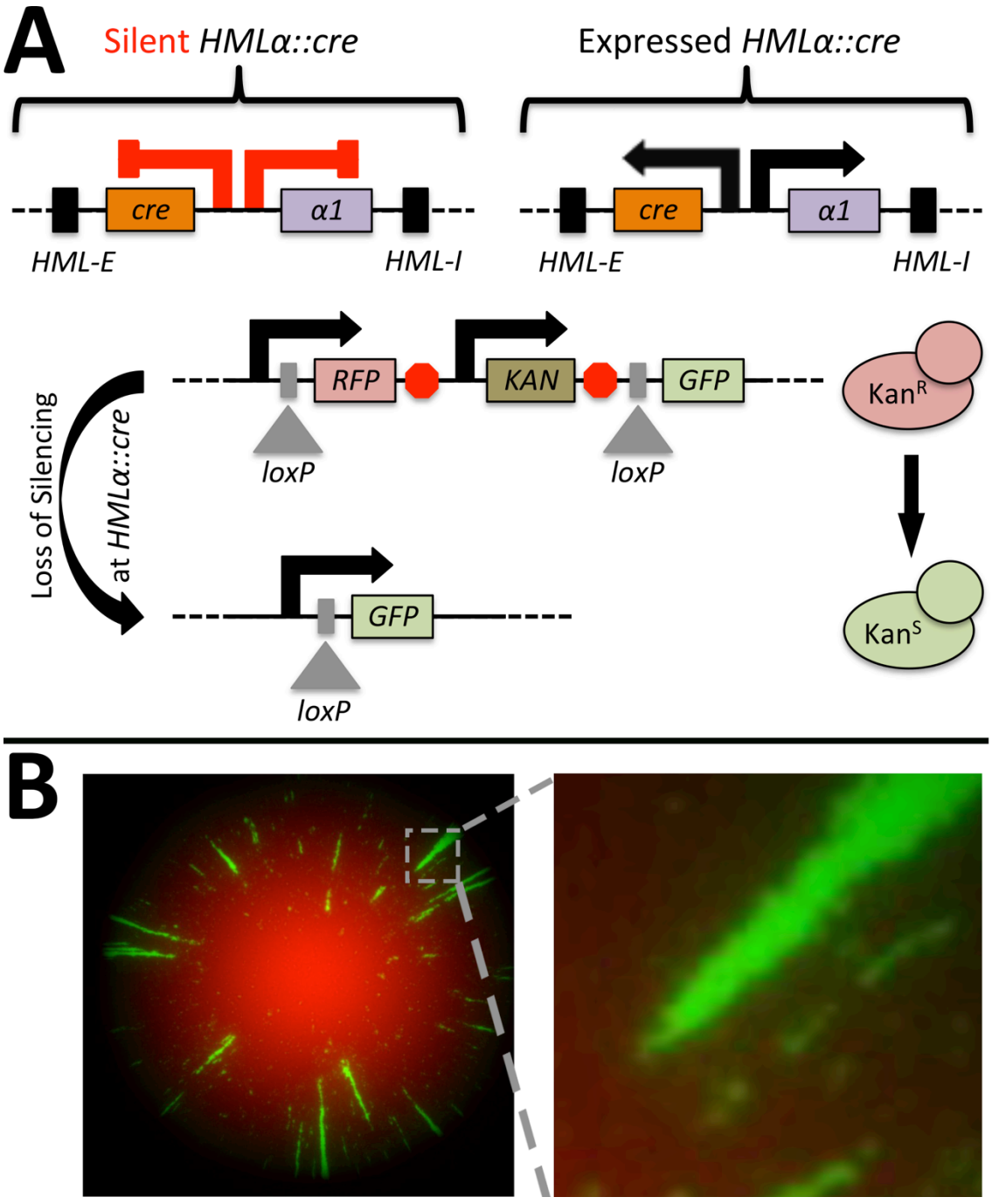


Figure 2.6. CRASH assay design. (A) Diagram of genetic components of the CRASH assay. *cre* replaces the *α2* gene at *HML*, and is only expressed if Sir-based heterochromatic silencing is lost at *HML*. If it is expressed, it acts on *loxP* sites flanking *RFP* and upstream of *GFP*, changing the cell from red to green. Descendants of these cells also express *GFP* rather than *RFP*. When colonies are grown, loss-of-silencing events result in visible green sectors (B), and the rate of green sector formation represents the rate of loss-of-silencing for a particular genetic background or environmental condition.

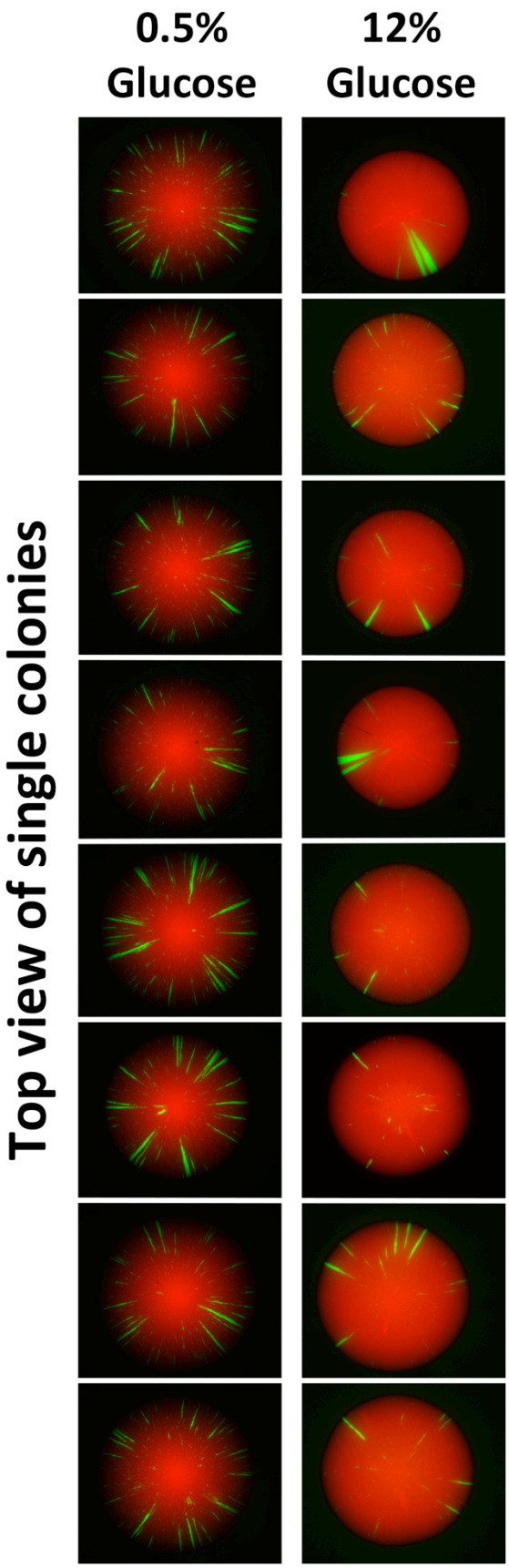

0.5%
Glucose
12%
Glucose
Top view of single colonies

Figure 2.7. Effect of glucose on stability of Sir-based silencing during growth on complete minimal medium. The CRASH strain was plated on solid medium with 0.5%, 2%, 6%, or 12% glucose and resulting colonies were imaged. 0.5% and 12% colony images are shown side-by-side for greater contrast. Growth in lower glucose resulted in a higher loss-of-silencing rate, as evidenced by the higher rate of green sector formation. This trend holds with 2% and 6% glucose-grown colonies as well (not shown).

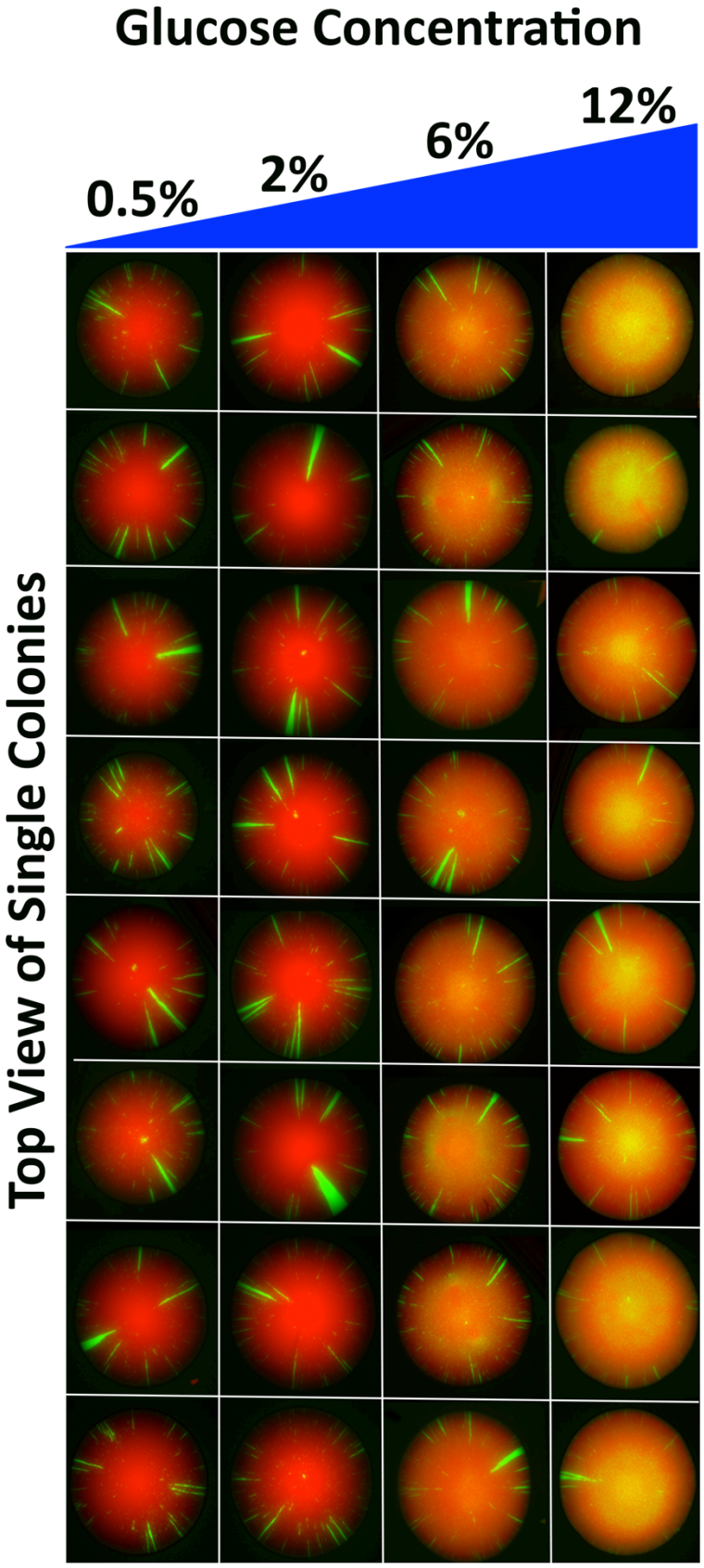

Glucose Concentration
0.5%
2%
6%
12%
Top View of Single Colonies

Figure 2.8. Effect of glucose on stability of Sir-based silencing during growth on yeast peptone medium. The CRASH strain was plated on solid medium with 0.5%, 2%, 6%, or 12% glucose and resulting colonies were imaged. Growth in 6% and 12% glucose resulted in a high loss-of-silencing rate during late cell divisions, as evidenced by yellowing of the tops of colonies when red and green fluorescence channels are merged. Since silencing is being lost in cells that don't undergo many more cell divisions, large green sectors aren't forming.

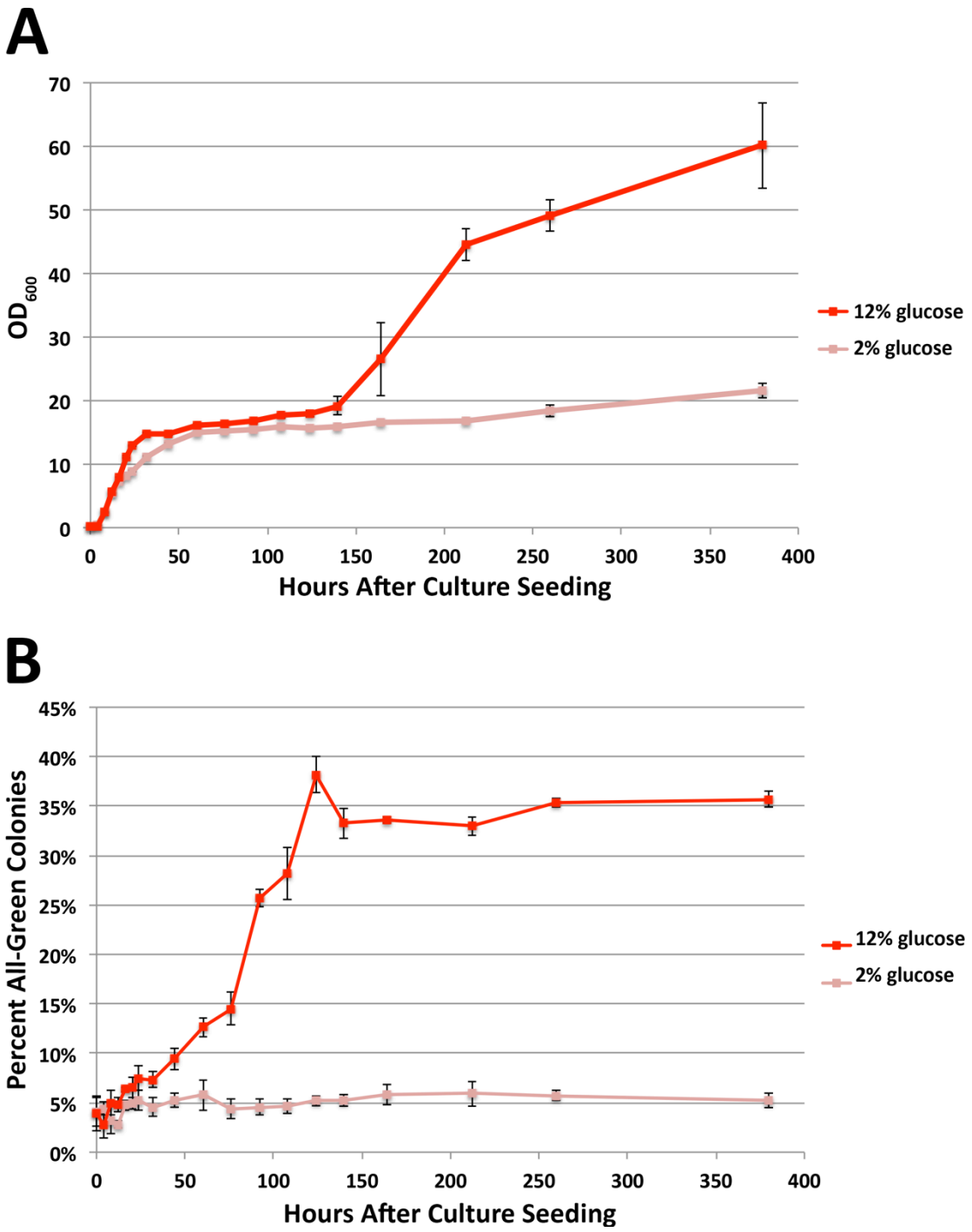


Figure 2.9. Loss-of-silencing in high- and low-glucose stationary-phase liquid yeast peptone cultures. The CRASH strain was grown to stationary phase in 2%- and 12%-glucose liquid YP media. Cell density (OD_{600}) was monitored throughout (A). Aliquots were also removed, diluted, and plated, and all-green colonies that grew were quantified as a percentage of total colonies (B). 12%-glucose cultures had high loss-of-silencing rates following log-phase growth, but preceding the period of culture regrowth (compare A to B).

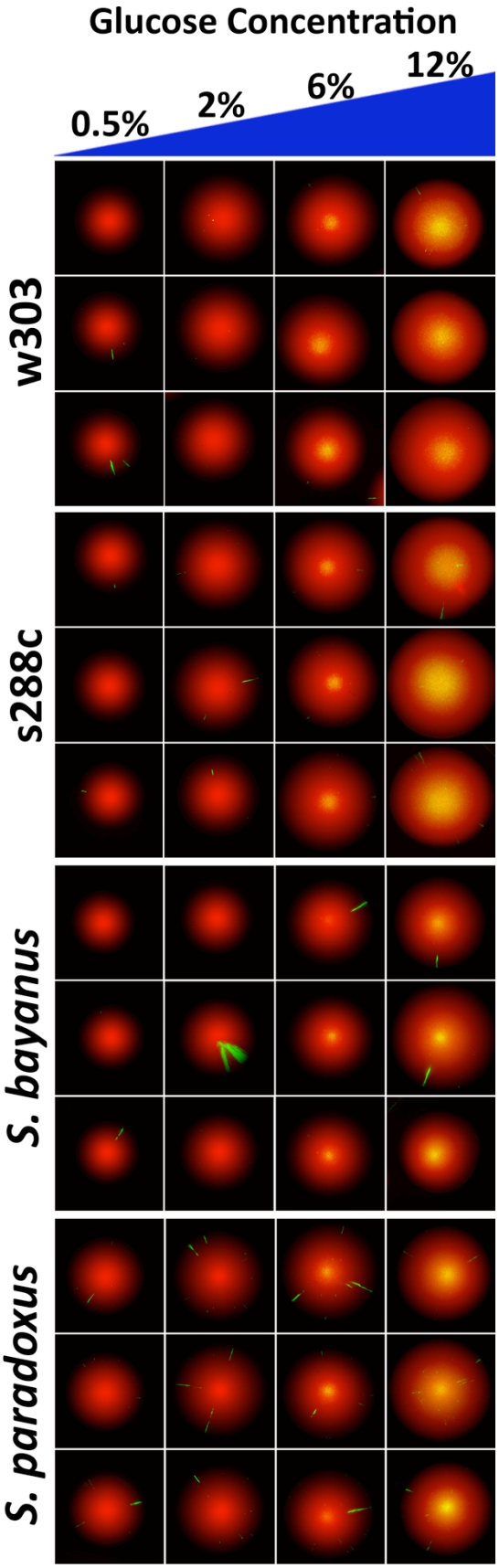

Glucose Concentration
0.5%
2%
6%
12%
w303
s288c
S. bayanus
S. paradoxus

Figure 2.10. Glucose control of heterochromatin was robust to genetic background. The CRASH strain (w303) was mated to haploid isolates of *S. cerevisiae* (w303 and s288c), *S. bayanus*, and *S. paradoxus* genetic backgrounds. The resulting diploids were plated on solid YP media with 0.5%, 2%, 6% or 12% glucose and imaged after 4 days of growth. The previously observed loss-of-silencing phenotype **(Figure 2.8)** is apparent in all of these additional genetic backgrounds.

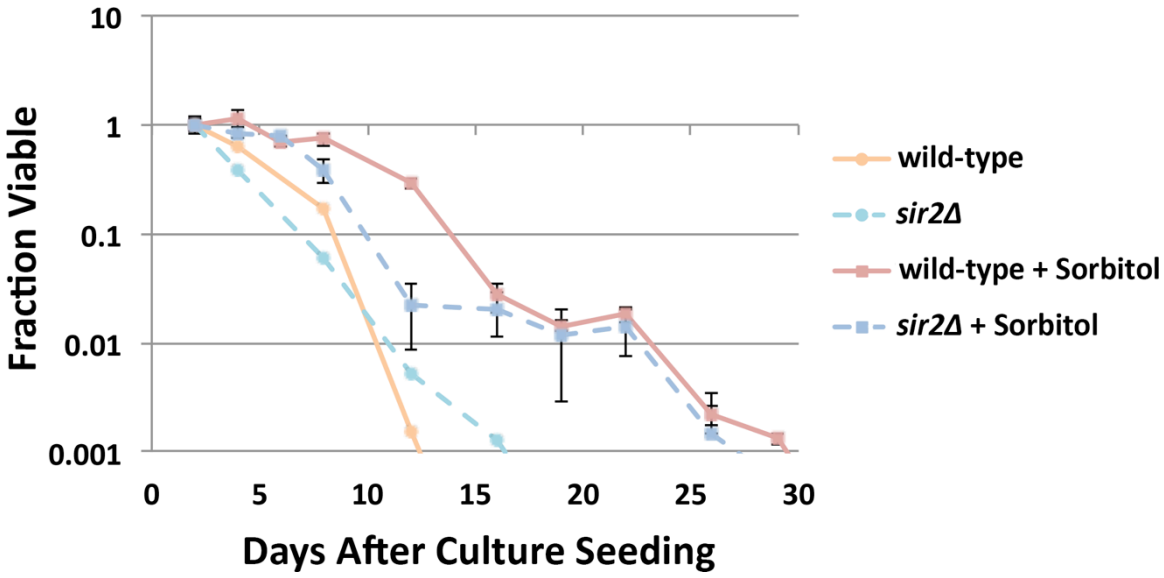


Figure S2.1. Increasing osmotic pressure of 2%-glucose cultures increases chronological lifespan. Adding sorbitol to increase the osmotic pressure of 2%-glucose cultures to that of 12%-glucose cultures does not decrease lifespan, and instead increases it. The change in lifespan between 2%- and 12%-glucose cultures is therefore not explained by differences in the osmotic pressure of the culture media. Inclusion or exclusion of sorbitol did not significantly affect any other observations made in this study (data not shown). Y-axis is cut off at 0.001 to zoom in on most relevant viability window.

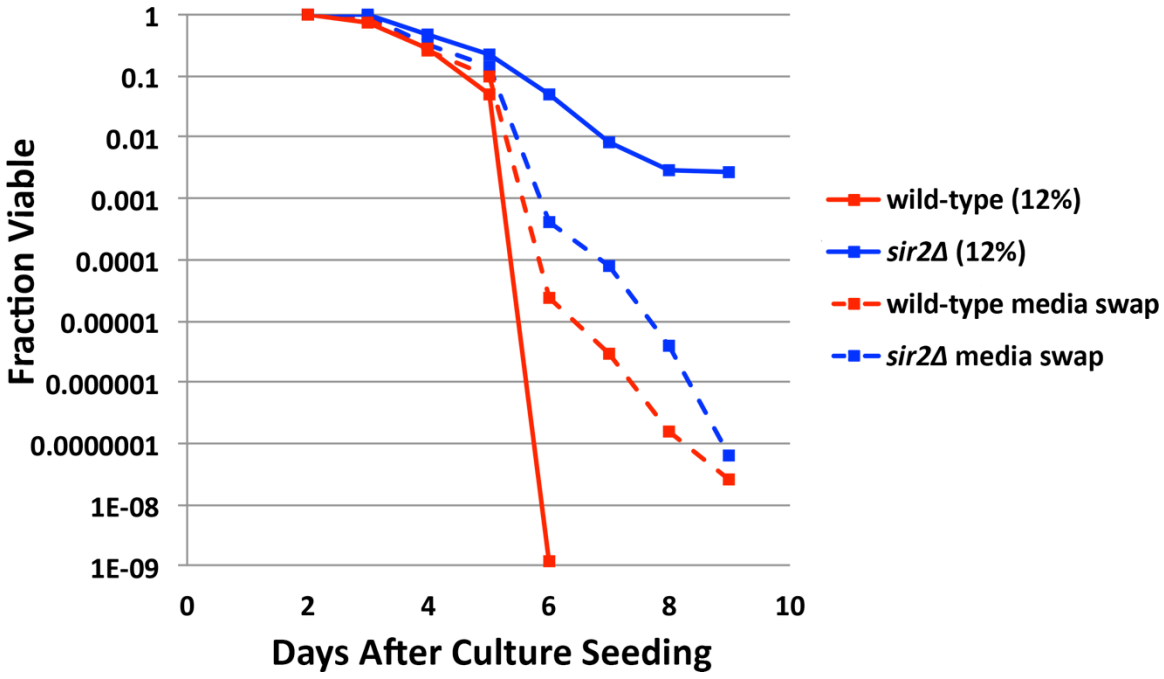


Figure S2.2. Cell-intrinsic and cell-extrinsic effects of Sir2 on chronological lifespan in high-glucose complete minimal medium. Wild-type and *sir2Δ* cultures were grown to stationary phase, and spent media from half of these cultures was swapped between genotypes. Swapping of spent media resulted in an intermediate phenotype for each genotype, demonstrating that Sir2-dependent cell-extrinsic changes to media composition aren't sufficient to explain the entire *sir2Δ* phenotype.

Table S2.1. Genotypes of yeast strains used in this study

Strain:	Genotype:	Source
UCC8650	*MATa, his3Δ1, leu2Δ0, lys2Δ0, ura3Δ0, hoΔ::PSCW11-cre-EBD78-NATMX*	D. Gottschling
JRY527 (s288c)	*MATa, ade2-101, lys2, ura3-52, his3Δ200, met2*	Lab collection
JRY4012 (W303-1a)	*MATa, his3, leu2, lys2, trp1, ura3, can1*	R. Rothstein/ Lab collection
JRY8822 (*S. bayanus)*	*MATa, lys2Δ, ura3Δ, hoΔ::NAT^{MX}*	Lab collection
JRY9135 (*S. paradoxus*)	*MATa, lys2Δ, ura3Δ, hoΔ::NAT^{MX}*	Lab collection
JRY9628	*ADE2, lys2, TRP1, hmlα2Δ::CRE, matΔ::NatMX, ura3Δ::pGPD:loxP:yEmRFP;tCYC1:KanMX:loxP:yEGFP :tADH1*	Lab collection
JRY10759 (W303 x W303)	*ADE2, lys2, trp1-1/TRP1, HML/hmlα2Δ::CRE, ura3-1/ura3Δ::pGPD:loxP:yEmRFP;tCYC1:KanMX:loxP:yEGFP:tADH1*	This Study
JRY10762 (W303 x s288c)	*ade2-101/ADE2, lys2, TRP1, HML/hmlα2Δ::CRE, ura3-52/ura3Δ::pGPD:loxP:yEmRFP;tCYC1:KanMX:loxP:yEGFP:tADH1, his3Δ200/HIS3, met2/MET2*	This Study
JRY10765 (*S. cerevisiae x S. bayanus*)	*ADE2, lys2, TRP1, HML/hmlα2Δ::CRE, ura3Δ/ura3Δ::pGPD:loxP:yEmRFP;tCYC1:KanMX:loxP :yEGFP:tADH1, hoΔ::NAT^{MX}/ho*	This Study
JRY10768 (*S. cerevisiae x S. paradoxus*)	*ADE2, lys2, TRP1, HML/hmlα2Δ::CRE, ura3Δ/ura3Δ::pGPD:loxP:yEmRFP;tCYC1:KanMX:loxP :yEGFP:tADH1, hoΔ::NAT^{MX}/ho*	This Study
JRY10776	*MATα ADE2, lys2, TRP1, hmlα2Δ::CRE, ura3Δ::pGPD:loxP:yEmRFP;tCYC1:KanMX:loxP:yEGFP :tADH1*	This Study
JRY10779	*MATa his3 leu2 lys2 trp1 ura3 can1 sir2Δ::KAN^{MX}*	This Study
JRY10782	*MATα ADE2, lys2, TRP1, ura3Δ::pGPD:loxP:yEmRFP;tCYC1:Kan^{MX}:loxP:yEGFP: tADH1*	This Study
JRY10786	*MATα ADE2, lys2, TRP1, ura3Δ::pGPD:loxP:yEmRFP;tCYC1:Kan^{MX}:loxP:yEGFP: tADH1 hoΔ::PSCW11-cre-EBD78-NATMX*	This Study
JRY10787	*MATα ADE2, lys2, TRP1, ura3Δ::pGPD:loxP:yEmRFP;tCYC1:Kan^{MX}:loxP:yEGFP: tADH1 hoΔ::PSCW11-cre-EBD78-NATMX sir2Δ::NAT^{MX}*	This Study

Chapter 3:

Sir-dependent metabolism of quinolone derivatives during growth on a non-fermentable carbon source

Introduction

Sir2 requires NAD^+ to deacetylate proteins. When an acetyl group is removed from a substrate protein by Sir2, NAD^+ is broken into nicotinamide (NAM) and 2-oxyacetyl-ADP-ribose (2-oAADPR). In addition to being activated by NAD^+, Sir2 is inhibited by NAM (Bitterman, *et al.* 2002). A network of enzymes recycles NAM back to NAD^+, preventing inactivation of Sir2 by a rising NAM concentration (Sandmeier, *et al.* 2002). Additionally, NAD^+ is synthesized by yeast from tryptophan via the *de novo* kynurenine pathway (Murata, *et al*. 2013). One of the intermediate compounds in this pathway, quinolinic acid, can also be imported into the cell from the external growth medium via the Tna1 transporter (Murata, *et al*. 2013).

In addition to its in vivo modification via the kynurenine pathway, tryptophan is also extensively oxidized upon exposure to UV (Perdivara, *et al*. 2010). UV-oxidation of tryptophan explains the yellowing of proteinaceous materials like wool that are left in sunlight for long periods (Leaver and Lennox, 1965). Known UV-oxidation products of tryptophan include kynurenine, hydroxytryptophan, dihydroxytryptophan, and N-formylkynurenine, among others (Perdivara, *et al*. 2010). Other alkaloid compounds, including quinoline and its derivatives, are biosynthesized from tryptophan in a variety of species (da Silva, *et al*. 2007).

While performing chronological aging experiments in synthetic complete medium with 3% glycerol **(Figure 1.6C)**, I observed a yellow-brown color change in stationary-phase *sir2Δ* cultures but not in wild-type cultures **(Figure 3.1)**. To identify small molecules responsible for this color change, I performed gas chromatography and mass spectroscopy on small molecules isolated from chronologically aging wild-type and *sir2Δ* cultures.

Materials and Methods

Yeast strains and media

Genotypes of strains from this study are given in **Table 3.1**. JRY10779 was derived from W303 (JRY4012) using standard yeast methodology. Synthetic complete minimal medium was produced according to the standard protocol (Fabrizio and Longo, 2007), with minor changes as described. Media were prepared with 3% glycerol as a carbon source. Additionally, synthetic complete media were supplemented with four-fold excesses of leucine, lysine, tryptophan, histidine, and uracil as needed to complement strain auxotrophies, and pH-adjusted to 5.0 with NaOH. Rather than autoclaving, which causes glucose to caramelize, all media were filter-sterilized using 0.2 μm polyethersulfone filters.

Gas Chromatography and Mass Spectroscopy

Wild-type and *sir2Δ* colonies were used to seed 5 mL of synthetic complete medium with 3% glycerol. Cultures were grown to stationary phase until yellow-brown color emerges. A PDMS Twister stir bar (Gerstel, 011222-001-00) was submerged in a sample vial with 5 mL of appropriate liquid culture (0.2 μm-filtered to remove cells) for one hour at room temperature, spinning on a magnetic stir plate. The stir bar was then dried with a Kimwipe and put into a Gerstel thermal desorption sample tube. Transport adapters were put on sample tubes which were then loaded into the sampling tray. For the analysis of samples, an Agilent 7890A/5975C GC-MS and HP-5MS column (0.25 μm film thickness, 30m × 0.25mm) was used. Automated sampling was performed with the Gerstel MPS system and analysis was performed using MAESTRO integrated into Chemstation software. The Gerstel Thermal Desorption Unit (TDU) was used to thermally desorb samples before injecting into the column via a Gerstel CIS-4 Cooled Injection System. The temperature program for desorption was 30°C for 24 seconds, followed by an increase of 60°C per minute up to 250°C, followed by a 5-minute hold. The transfer line temperature was set to 275°C. The injection was cooled with liquid nitrogen to −100°C with a 36 second hold time. The injector inlet was operated in solvent vent mode, with vent pressure of 9.1473 psi, vent flow of 30 mL per minute; purge flow of 6 mL per minute. The gas chromatography temperature program was 40°C for 2 minutes, temperature was increased 4°C per minute until 140°C, followed by a temperature increase of 15°C per minute until 195°C. The carrier gas head pressure was 9.1473 psi for a flow rate of 1.2 mL per minute. The gas chromatography instrument was operated in constant flow mode. The time-of-flight mass spectroscopy instrument was operated in electron ionization mode with the electron voltage set to autotune values. The detector scanned from 30 to 300amu at a threshold of 150 with 3 samples for a scanning rate of 2.69 scans each second. The MSD transfer line temperature was set to 280°C. The ion source temperature was set to 230°C and the quadrupole temperature was set to 150°C. Data files were inspected visually using Chemstation. Peaks were identified using the NIST 08 database.

Results

A yellow-brown color emerged in the medium of stationary-phase *sir2Δ* cells grown on 3% glycerol synthetic complete medium

I had previously performed chronological lifespan experiments using wild-type and *sir2Δ* strains grown on synthetic complete medium with 3% glycerol as a carbon source **(Figure 1.6C)**. During the course of these experiments, I observed the formation of a yellow-brown color in the external medium of *sir2Δ* cultures but not in wild-type cultures **(Figure 3.1)**. This color change was similar to the color change that is seen when tryptophan within a solution is oxidized (Leaver and Lennox, 1965; Perdivara, *et al*., 2010).

Quinoline and its derivatives were enriched in the medium of stationary-phase *sir2Δ* cultures

To identify the small molecule(s) responsible for the yellow-brown color of stationary-phase *sir2Δ* cultures, I performed gas chromatography and time-of-flight mass spectroscopy on small molecules isolated from stationary-phase wild-type and *sir2Δ* cultures. I used the Gerstel Twister PDMS stir bar system to isolate small molecules from filtered, stationary-phase media, and determined the identity of these small molecules using an Agilent 7890A/5975C GC-MS and HP-5MS column **(Figure 3.2)**. Several small molecules differed significantly in abundance between wild-type and *sir2Δ* cultures. Quinoline and several related derivatives were highly enriched in *sir2Δ* cultures relative to wild-type, and were among the most significant Sir2-dependent differences observed **(Figure 3.3)**.

Quinoline and its derivatives were found in fresh 3%-glycerol synthetic complete medium and *sir2Δ* inhibits their removal

Since quinoline and its derivatives were enriched in *sir2Δ* cultures relative to wild-type, I wanted to know whether these compounds were being produced *de novo* in a *sir2Δ*-dependent fashion or whether they were present in fresh medium and were instead removed in a Sir2-dependent fashion. I performed GC-MS analysis on three independent cultures of both wild-type and *sir2Δ*, as well as on fresh medium that hadn't been seeded with either genotype. Interestingly, quinoline and its derivatives were present in fresh medium, as well as in *sir2Δ* cultures. These compounds were also seen in wild-type cultures, but at lower levels **(Figure 3.4)**. Thus, Sir2 was functioning to remove these compounds from the culture medium.

Discussion

These experiments showed that Sir2 was involved in a process that removed quinoline and related compounds from fresh 3% glycerol synthetic complete medium during growth. Chronological aging experiments in this medium revealed a color-change in *sir2Δ* cultures during stationary phase, resulting in a yellow-brown coloration **(Figure 3.1)**. I utilized the Gerstel PDMS Twister stir bar system to isolate and concentrate quinoline and related compounds responsible for this change, and identified them using GC-MS **(Figure 3.2)**. Deleting *SIR2* resulted in more of these compounds being present in stationary-phase culture medium **(Figure 3.3)**. GC-MS analysis of fresh culture medium revealed the presence of these compounds, indicating that Sir2 was involved in their removal, rather than their production **(Figure 3.4)**.

Quinoline is closely related to known UV-degradation products of tryptophan (Perdivara, *et al*. 2010). Since these quinoline compounds were mysteriously present in fresh media and seemed to increase over time in stationary-phase cultures exposed to light, these compounds likely formed as a result of UV-degradation of tryptophan. It is possible known UV-degradation products of

tryptophan were modified *in vivo* (da Silva, *et al*. 2007) or upon exposure to high temperatures during GC-MS analysis (Proctor, 1983) to produce the compounds I identified. It is also possible these known degradation products were enriched in *sir2Δ* cultures but failed to be detected by my GC-MS protocol (Lawrence, 1987). Many of these known degradation products are more polar than the compounds we identified, and polar compounds are notoriously difficult to identify by GC-MS as they are more difficult to vaporize and more likely to decompose when heated at high temperatures during GC-MS analysis (Proctor, 1983). I was unable to determine which of these compounds were responsible for the color change, although it is likely they all contributed. I was also unable to quantify their exact concentrations in the medium.

Wild-type cells were able to remove these compounds from the culture medium at a greater rate than *sir2Δ* cells **(Figure 3.3 and 3.4)**. While quinoline and other identified compounds aren't known to be metabolized by *S. cerevisiae*, quinolinic acid, the oxidized form of quinoline, is imported into yeast cells by the Tna1 transporter and can be used to produce NAD^+ via the kynurenine pathway (Murata, *et al*. 2013). While a large number of processes reduce NAD^+ to NADH and others drive the reverse reaction, sirtuins, including Sir2, are the only enzymes that consume NAD^+ in *S. cerevisiae* (Kato and Lin, 2014). Deleting another yeast sirtuin, *HST1*, raises intracellular levels of NAD^+ (Bedalov, *et al*. 2003), and it is possible that deleting *SIR2* has a similar effect. Consistent with this possibility, *SIR2* increases release of nicotinamide riboside, a molecule that cells can utilize to replenish their NAD^+ pools (Lu, *et al*. 2009). Taken together, it is possible that *sir2Δ* cells have less kynurenine pathway activity while growing in glycerol, resulting in more tryptophan and quinolinic acid in the culture medium. An alternate explanation for my observations could be that the growth of *sir2Δ* cells was decreased relative to wild-type in 3% glycerol synthetic complete medium **(Figure 1.6A)**. Decreased growth could also have led to increased levels of tryptophan and quinolinic acid in the culture medium, which could have been broken down or converted into the quinoline compounds I detected. Additional experiments will be required to determine the validity of these and other possible explanations.

Acknowledgements

I thank Dr. Michael Eisen and Dr. Kelly Schiabor for allowing me access to the GC-MS setup used in these experiments. I give special thanks to Dr. Schiabor for developing the experimental method used and giving training and assistance with use of the instrument.

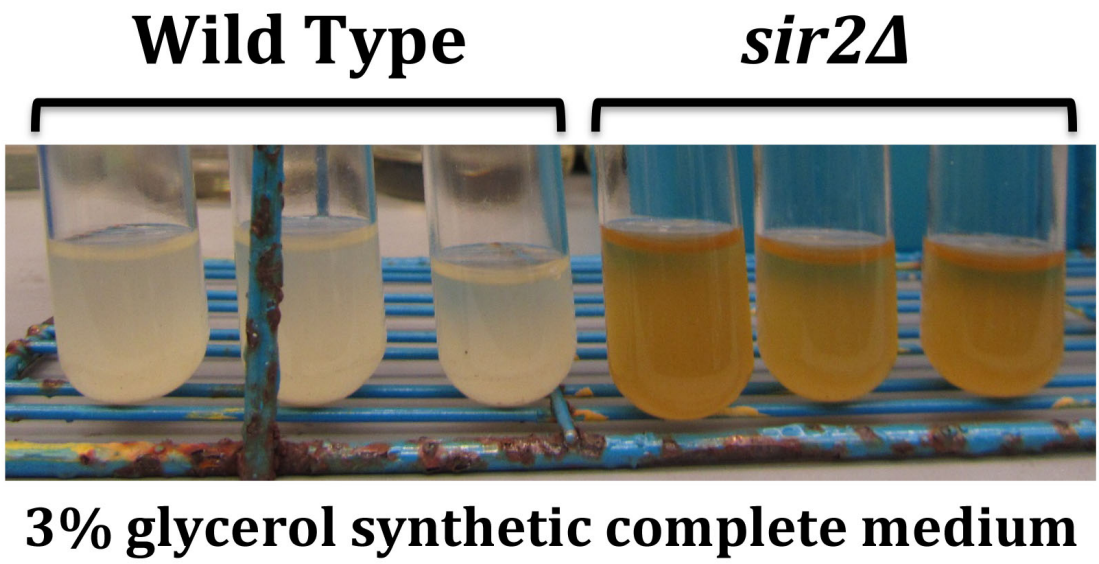


Figure 3.1. Color of glycerol-grown, stationary-phase cultures. Wild-type and *sir2Δ* cells were grown to stationary phase in 3% glycerol synthetic complete medium. After several days in stationary phase, a yellow-brown color emerged in *sir2Δ* cultures. Wild-type cultures remained white in color.

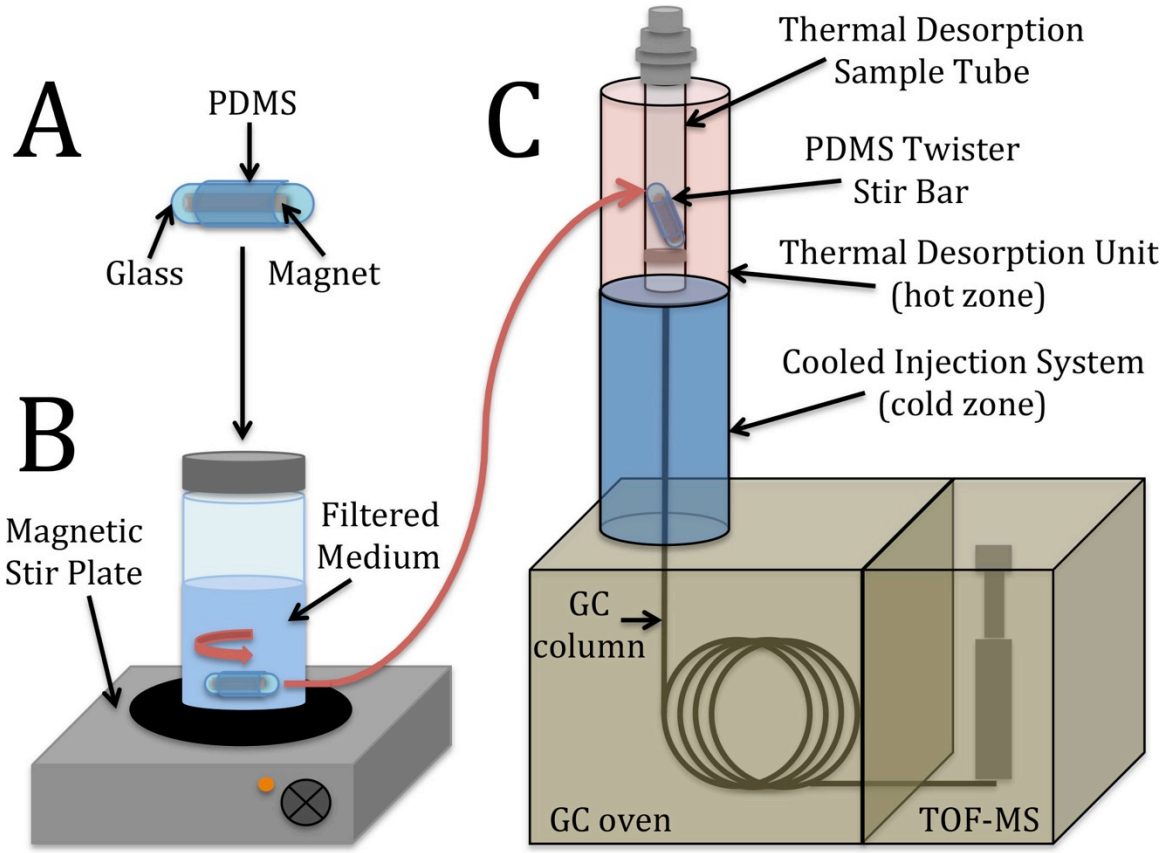


Figure 3.2. Overview of gas chromatography and mass spectroscopy experimental setup. (A) Diagram of Gerstel PDMS stir bar. A magnet was encased in glass and coated with polydimethylsiloxane (PDMS), an inert polymeric compound that traps and enriches a wide variety of small molecules. (B) A PDMS stir bar was submerged in filtered medium from wild-type or *sir2Δ* cultures, or in fresh medium. The stir bar was spun for one hour at room temperature using a magnetic stir plate. (C) The PDMS stir bar was transferred to a thermal desorption sample tube and heated in the thermal desorption unit to release small molecules trapped in the PDMS. These small molecules were cooled and condensed before entering the GC column, where they were separated and identified by measuring their time-of-flight before encountering the detector in the mass spectrometer.

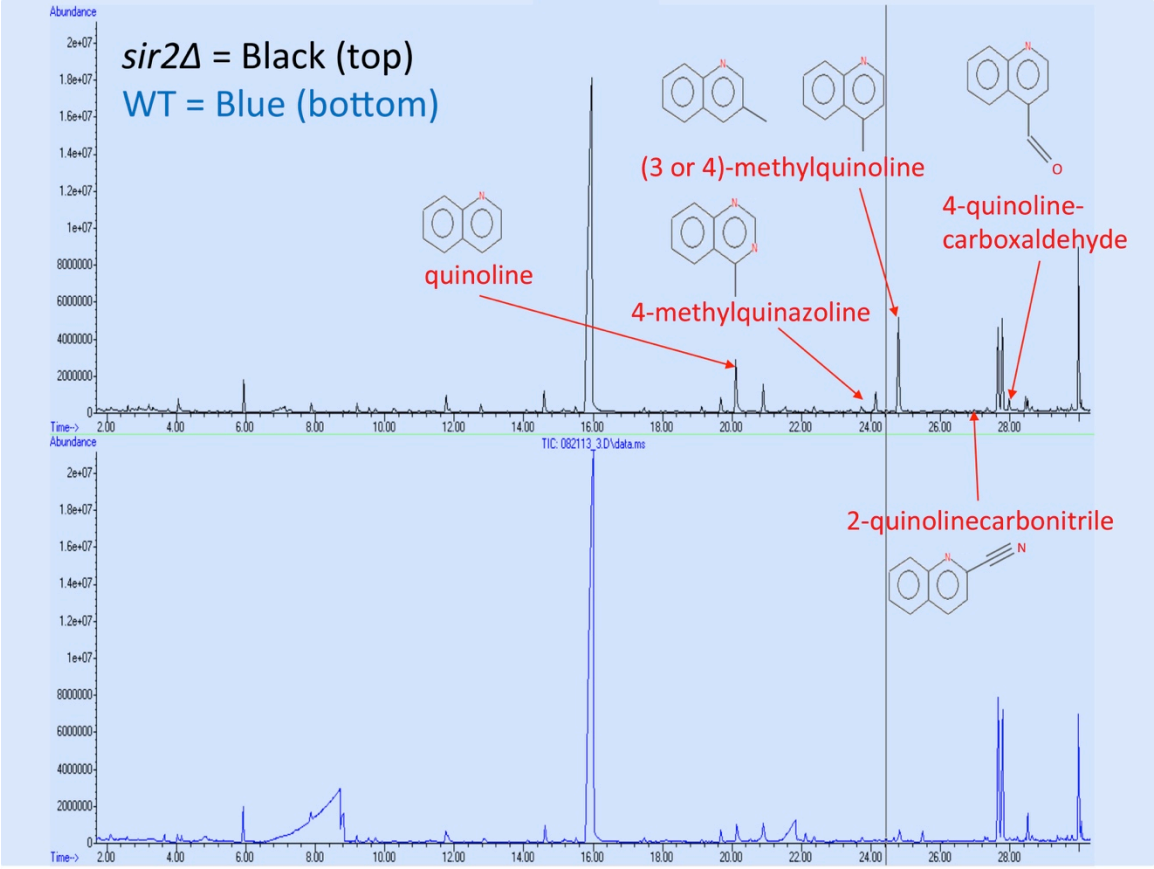


Figure 3.3. GC-MS data for wild-type and *sir2Δ* filtered media. Time-in-column (TIC) data for small molecules isolated from *sir2Δ* (top) and wild-type (bottom) stationary-phase media. Quinoline compounds enriched in *sir2Δ* medium were identified using the Chemstation-integrated NIST 08 database and labeled with red arrows and chemical structures.

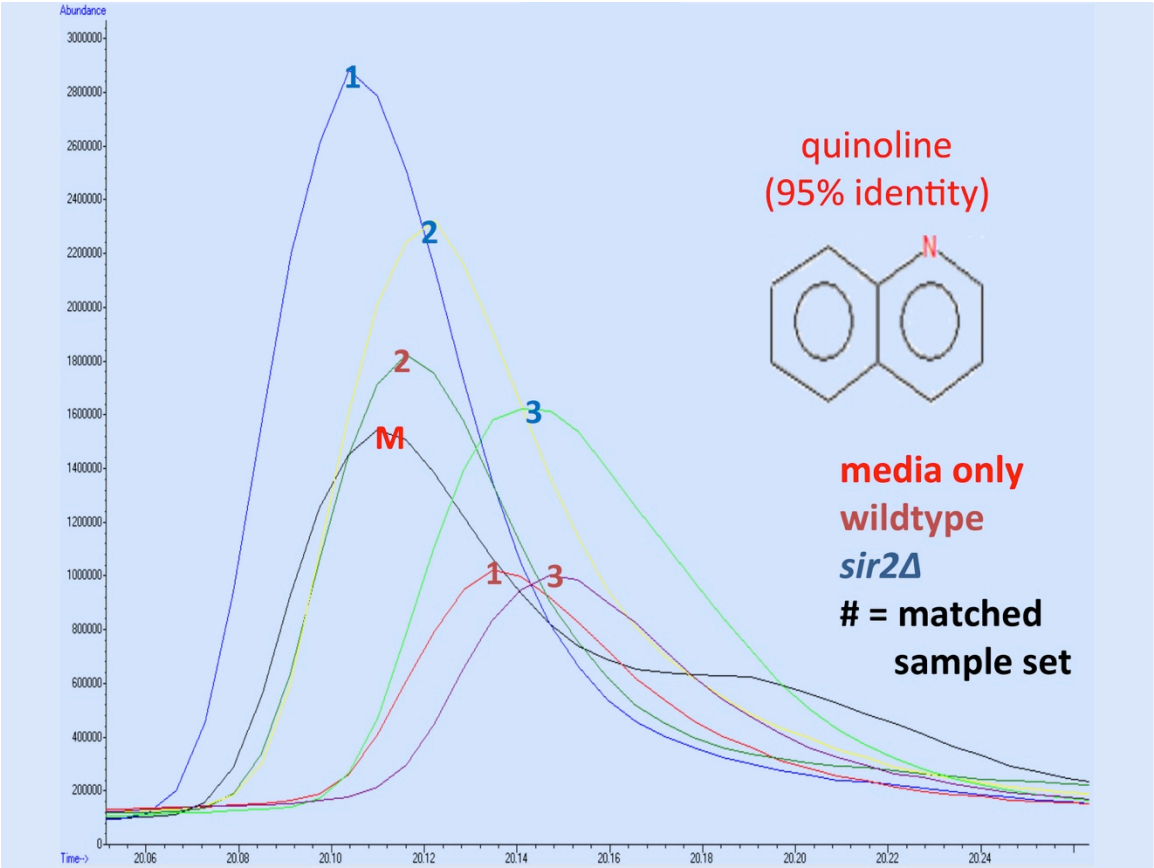


Figure 3.4. Close-up view of quinoline TIC peak. Data from seven independent samples shown here: three wild-type samples, three matched *sir2Δ* samples, and one sample of fresh medium. Quinoline is present in fresh media that was never seeded with cells. Quinoline is always more enriched in *sir2Δ* samples than in matched wild-type samples.

Table 3.1. Genotypes of yeast strains used in this study

Strain:	Genotype:	Source
JRY4012 (W303-1a)	*MATa, his3, leu2, lys2, trp1, ura3, can1*	R. Rothstein/ Lab collection
JRY10779	*MATa his3 leu2 lys2 trp1 ura3 can1 sir2Δ::KAN^{MX}*	This Study

Chapter 4:

Microfluidic analysis of yeast replicative lifespan during growth on high and low glucose media

Introduction

There have been two main approaches to the study of yeast lifespan (Longo, *et al.* 2012). The first measure of yeast lifespan, chronological lifespan, is defined as the length of time that cells in a stationary phase culture remain viable and able to reenter the cell cycle upon introduction to fresh culture medium (Fabrizio and Longo, 2007). Chronological lifespan serves as a model of aging in post-mitotic cell-types, such as terminally differentiated cells (Longo, *et al.* 2012). The second measure of yeast lifespan focuses on replicative lifespan, defined as the number of progeny an individual yeast mother cell can produce through mitosis before it can no longer divide, entering senescence (Mortimer and Johnston, 1959). Replicative lifespan serves as a model of aging in actively dividing cell-types, such as germ line stem cells (Jazwinski, 1990). Yeast replicative aging is generally studied on yeast peptone medium (YP), while yeast chronological aging is studied almost exclusively on synthetic complete minimal medium (SC) (Longo, *et al*., 2012). Sir2 regulates aging in both of these yeast-aging paradigms. For chronological aging, deletion of *SIR2* dramatically extends lifespan under conditions of extreme nutrient depletion (Fabrizio, *et al*., 2005). For replicative aging, deletion of *SIR2* shortens lifespan, and overexpression of *SIR2* extends it (Kaeberlein, *et al.* 1999). Sir2 deacetylates histone tails as part of the RENT complex with Net1 and Cdc14 to repress PolII transcription and recombination in the rDNA (Gottlieb and Esposito, 1989; Smith and Boeke, 1997; Shou, *et al*., 1999; Straight, *et al.*, 1999). Repression of recombination between rDNA repeats by the RENT complex is thought to extend replicative lifespan by suppressing the formation of extra-ribosomal circles (ERCs), formed when rDNA repeats loop out of the genome (Guarente and Picard, 2005).

Both chronological and replicative yeast lifespan is increased with calorie restriction, whereby calorie intake is reduced without a reduction in essential nutrients (Kaeberlein, *et al.* 2004; Lin, *et al.* 2000; Smith, *et al.* 2007). Sirtuins have been implicated in the extension of replicative lifespan via calorie restriction (Guarente and Picard, 2005). *S. cerevisiae* grown on 0.5% glucose, considered by some as a calorie-restricted diet, have significantly longer replicative lifespans than cells grown on 2% glucose, typically considered a calorically unrestricted diet. The longevity of 0.5% glucose-grown cells was initially shown to be dependent on Sir2: *sir2Δ* cells experienced no lifespan extension with calorie restriction (Lin, *et al.* 2002).

Although observations linking Sir2 and calorie restriction were later supported by studies in other organisms (Tissenbaum and Guarente, 2001; Rogina and Helfand, 2004; Bordone, *et al.* 2007), the original yeast conclusions (Kaeberlein, *et al.* 2004), as well as related work in worms and flies (Burnett, *et al.* 2011) has since been questioned. Additionally, studies of yeast chronological lifespan have revealed no role for Sir2 in the calorie-restriction aging response (Smith, *et al.* 2007; Kaeberlein, *et al.* 2006) despite Sir2's ability to regulate chronological lifespan under some conditions (Fabrizio, *et al*. 2005). The discrepancies in the literature, particularly with respect to replicative aging, have been attributed to differences in

strain background and media composition (Couzin-Frankel, 2011), leaving the role of Sir2 in calorie restriction, particularly in yeast, uncertain.

Yeast calorie restriction protocols use 2% glucose as the ad libitum, high calorie diet (Longo, *et al*. 2012). However, in nature, *S. cerevisiae* seems particularly well-adapted to high-sugar environments, with many yeast substrates containing well over 10% sugar by weight (Coghe, *et al.* 2005; Sanchez, 2008; Oliva, *et al.* 2011; Garde-Cerdán, 2011). It is possible the discrepancies in the literature over Sir2's role in extending replicative lifespan via calorie restriction is due to the "full-calorie" diet itself being on the edge of calorie restriction for *S. cerevisiae*. If true, using a higher concentration of sugar for the full-calorie diet could expand the dynamic range of phenotypic measurement, allowing previously missed effects of Sir2 on lifespan to be revealed, as was the case in my investigations into yeast chronological lifespan.

To determine whether using a wider range of glucose concentrations would clarify Sir2's role in calorie restriction and replicative aging, I used a microfluidics strategy to film individual trapped cells as their progeny were washed away. By watching movies of individual positions and counting progeny, the replicative lifespan for multiple cells could be determined in a single experiment. Surprisingly, there was no statistical difference between high- and low-glucose replicative lifespan of wild-type cells, casting doubt on the relevance of this microfluidics strategy for studying the impact of calorie restriction on replicative lifespan.

Materials and Methods

Yeast strains and media

A wild-type W303 strain (JRY4012) was the only strain used in this study. YP medium was produced according to the standard protocol, with minor changes as described. Media was prepared with either 2% w/v or 12% w/v glucose, with 10% w/v sorbitol added only to 2% media. Rather than autoclaving, which causes glucose to caramelize, all media were filter-sterilized using 0.2 μm polyethersulfone filters.

Microfluidic analysis of yeast replicative lifespan

I seeded 5 mL portions of 2%- and 12%-glucose yeast peptone medium with fresh wild-type colonies and shook overnight at 30°C**.** I then diluted seed cultures to a cell density of 0.1 OD_{600} in the same medium and grew shaking at 30°C to 0.7 OD_{600}. Cells were spun down gently, washed with water, and concentrated to 5 OD_{600} units. A temperature-controlled, camera-equipped Nikon Eclipse Ti-E inverted research microscope (Nikon Instruments; Melville, NY) was used for imaging of microfluidic chips. A PDMS chip (Zhang, *et al*. 2012) was attached to the stage insert with double-sided tape. The syringe attachment was removed from 21-guage blunt tip needles (0.20 x 0.5, Nordson Efd., 7918233) and needles were inserted into the ends of segments of 75% ethanol-washed 0.75 mm PTFE tubing

(Microsolv Technology, 49210-30). Tubing was inserted needle-end first into inlet and outlet holes on the chip. A 5 mL syringe was used to pump 75% ethanol through the channels of the chip to wash, repeated twice. The chip was then washed once with water using a BS-series Programmable Syringe Pump (Braintree Scientific, BS-8000 120V) set to 750 µL per hour flow-rate for 20 minutes or until all air-bubbles were removed from the tubing and chip. Inlet tubes were removed from the chip, placed in the tubes containing log-phase cells, and the pump directionality was reversed to suck up the cells into approximately 10 inches of the tubing. Inlets were placed back into the chip and cells were pumped into the chip at 400 µL per hour. Once cells were visually confirmed to have been loaded onto the chip, inlet tubes were removed and attached to 60 mL syringes filled with appropriate fresh media. Inlet lines were cleared with fresh media, removing all air bubbles, and inlet lines were placed back into the chip. Flow-rate was set to 400 µL per hour. NIS-Elements imaging software, included with the Nikon Eclipse Ti-E, was used to control the motorized stage movement and image capture. The following parameters were used: 4 gain; 60 ms exposure; blank emission wheel; zero excitation wheel; 40x0.75 objective; engaged auto-shutter; automatic contrast; Z dimension off; 15 minute image capture interval time; 30°C incubator temperature. Multi-dimensional image acquisition was used and positions on the chip containing trapped cells were selected manually. Experiment duration was 72 hours. Once completed, images for each unique position on the chip were separated into unique photos, appropriately cropped, and compiled into animated .GIF files. Animations were watched and the number of cell divisions for a given mother cell were quantified.

Results

Calorie restriction failed to extend lifespan of wild-type cells in a microfluidics chip with fresh medium flowing through it

I obtained microfluidics chips designed for the study of yeast replicative lifespan from Dr. Hao Li **(Figure 4.1B)**. These chips contain platforms that trap large mother cells at specific positions within the chip while allowing smaller daughter cells to flow through the chip **(Figure 4.1C)**. An inverted microscope with a camera and a motorized stage **(Figure 4.1A)** was used to take images of each position on the chip **(Figure 4.2)** at 15-minute intervals, and these images were sorted into unique folders for each chip position. Images were cropped and compiled into animations for each position that could be scored for the number of cell divisions **(Figure 4.3)**. This gave a replicative lifespan for each cell at each position. I analyzed the data in three different ways **(Figure 4.4)**. For the first analysis, I included data from every cell in the chip, regardless of how quickly it died or whether it was washed away from the chip during analysis **(Figure 4.4A).** For the second analysis, I included data from cells where I was able to observe their complete lifespan, but that had completed at least 15 cell divisions **(Figure 4.4B)**. For the final analysis, I included data from cells where I was able to observe their

complete lifespan, from birth to senescence and death **(Figure 4.4C)**. Surprisingly, there was no statistical difference between the replicative lifespans of wild-type cells growing in either 2%- or 12%-glucose yeast peptone medium, regardless of the method of analysis **(Figure 4.4)**.

Discussion

At least in the context of my experimental setup, calorie restriction did not extend the replicative lifespan of wild-type cells **(Figure 4.4)**. At first glance, these results contradicted published literature on calorie restriction and yeast replicative lifespan (Lin, *et al.* 2000; Kaeberlein, *et al.* 2004). However, there are important differences between the experimental setup I used and the experimental setup used in these earlier studies. In my setup, replicatively-aging mother cells are constantly exposed to fresh medium in the microfluidics chip **(Figure 4.1)**. In past studies, micromanipulation was utilized to move daughter cells away from a mother cell that remained stationary on solid media (Lin, *et al.* 2000; Kaeberlein, *et al.* 2004). As a result, these mother cells experience a dynamic growth environment; one that is gradually depleted for essential nutrients and that gradually accumulates metabolic waste products like acetate and ethanol. Mother cells in the microfluidics chip experienced a static growth environment; one where essential nutrients were replenished and metabolic waste products were eliminated. It is entirely possible that the beneficial effects of calorie restriction on replicative aging require a dynamic growth environment. Growth on media with higher glucose would produce higher levels of metabolic waste products like ethanol and acetate, and these products could accelerate replicative aging. These waste products would fail to accumulate in both high- and low-glucose conditions in the microfluidics chip, masking any beneficial effect of calorie restriction on replicative lifespan. Alternatively, the ability of a cell to sense decreasing levels of essential nutrients might be necessary for the benefits of calorie restriction on replicative lifespan. In the microfluidics chip, essential nutrients never decrease from their starting levels.

A recent study of yeast replicative lifespan found that the benefits of calorie restriction were lost when calorie-restricted mother cells were transferred to fresh medium (Mei and Brenner, 2015), supporting the hypothesis that a dynamic growth environment is essential for replicative lifespan extension via calorie restriction. In that study, replicative lifespan was determined using the classical protocol, with one modification. Daughter buds were removed from mother cells dividing on solid medium via micromanipulation as is typical. After 15 generations, however, mother cells were moved to fresh medium. When calorie-restricted cells were moved to fresh calorie-restricted medium, they no longer had their lifespans extended as compared to calorie-restricted cells that were never moved to fresh medium. Cells given the "fully-fed" diet, which in this case was 2% glucose, did not see a change in lifespan when they were moved to fresh medium. The authors determined that lifespan extension was dependent on an unidentified, dialyzable longevity factor released by calorie-restricted mother cells during earlier stages of growth that was utilized during later stages. If these results are accurate and also apply to calorie

restriction above 2% glucose, my experimental setup would have precluded the build-up of this longevity factor, masking the benefits of calorie restriction.

Additional support for the hypothesis that a dynamic growth environment is essential comes from an in-depth meta-analysis of studies of the effect of calorie restriction on yeast replicative lifespan (Huberts, *et al*. 2014). The authors analyzed data from 40 different replicative lifespan studies and found enormous amounts of variation, with only a mild, although statistically significant, difference in lifespan between calorie-restricted (0.5% glucose) and fully-fed (2% glucose) cells. Additionally, the authors performed experiments using a microfluidics setup similar to mine and found no difference between the replicative lifespans of calorie-restricted or fully-fed cells. After controlling for other variables, the authors concluded that growth on solid medium or micromanipulation itself was the basis for the incongruent results of micromanipulation and microfluidics experiments. If a diffusible longevity factor is necessary for lifespan extension via calorie restriction, that would explain this discrepancy between the two methods. Additionally, this could explain the wide variation seen in micromanipulation experiments. As daughter buds are removed from mother cells during the course of analysis, it is very likely that mother cells would also be displaced, to varying degrees, from their initial position on the plate. It is not even clear whether all of the authors of papers included in the meta-analysis even attempted to keep mother cells at their exact initial positions, allowing the diffusible longevity factor to accumulate for later utilization.

Two relevant experiments would help determine if the existence of a diffusible longevity factor underlies the incongruous results described above. The first experiment would be to measure replicative lifespan of 2%- and 12%-glucose-grown cells using the classical micromanipulation protocol, taking care not to move mother cells from their initial positions on plates. At the same time, mother cells growing on separate 2%- and 12%-glucose plates would be moved to a new position on the plate after each generation. If a diffusible longevity factor extends lifespan, I would expect to see replicative lifespan of immobilized, 2%-glucose-grown mother cells increase relative to the replicative lifespan of mother cells growing in all other experimental conditions. A second relevant experiment would be to measure replicative lifespan using a microfluidics chip as I have done, except with two separate programmable pumps connected to the inlet of each lane on the chip. One pump would contain fresh medium, while the other pump would contain filtered, conditioned medium from stationary-phase cultures. At the beginning of the experiment, the relative flow-rate of the fresh-medium pump would be set to 100%, while the relative flow-rate of the conditioned-medium pump would be set to 0%. Over the course of the experiment, the relative flow-rate of the fresh-medium pump would gradually decrease at the same rate as the flow-rate of the conditioned-medium pump increased, until the end of the experiment when the fresh-medium pump would be contributing 0% to the flow-rate and the conditioned-medium pump would be contributing 100% to the flow-rate. This would create a dynamic growth environment, one that should lead to a build-up of any diffusible longevity factor. Under this experimental setup, I would expect to see the replicative lifespan

of 2%-glucose-grown cells increase relative to 12%-glucose-grown cells, at which point I could determine the contribution of Sir2 to this phenotype.

Acknowledgements

Thanks to Dr. Georjana Barnes and Dr. David Drubin for letting me use their Nikon Eclipse Ti-E microscope. Thanks to Dr. Eric Lewellyn for training and assistance with the use of the microscope. Finally, thanks to Dr. Hao Li and Dr. Ke Zou for providing the microfluidics chips I used for experiments and for training me on their use.

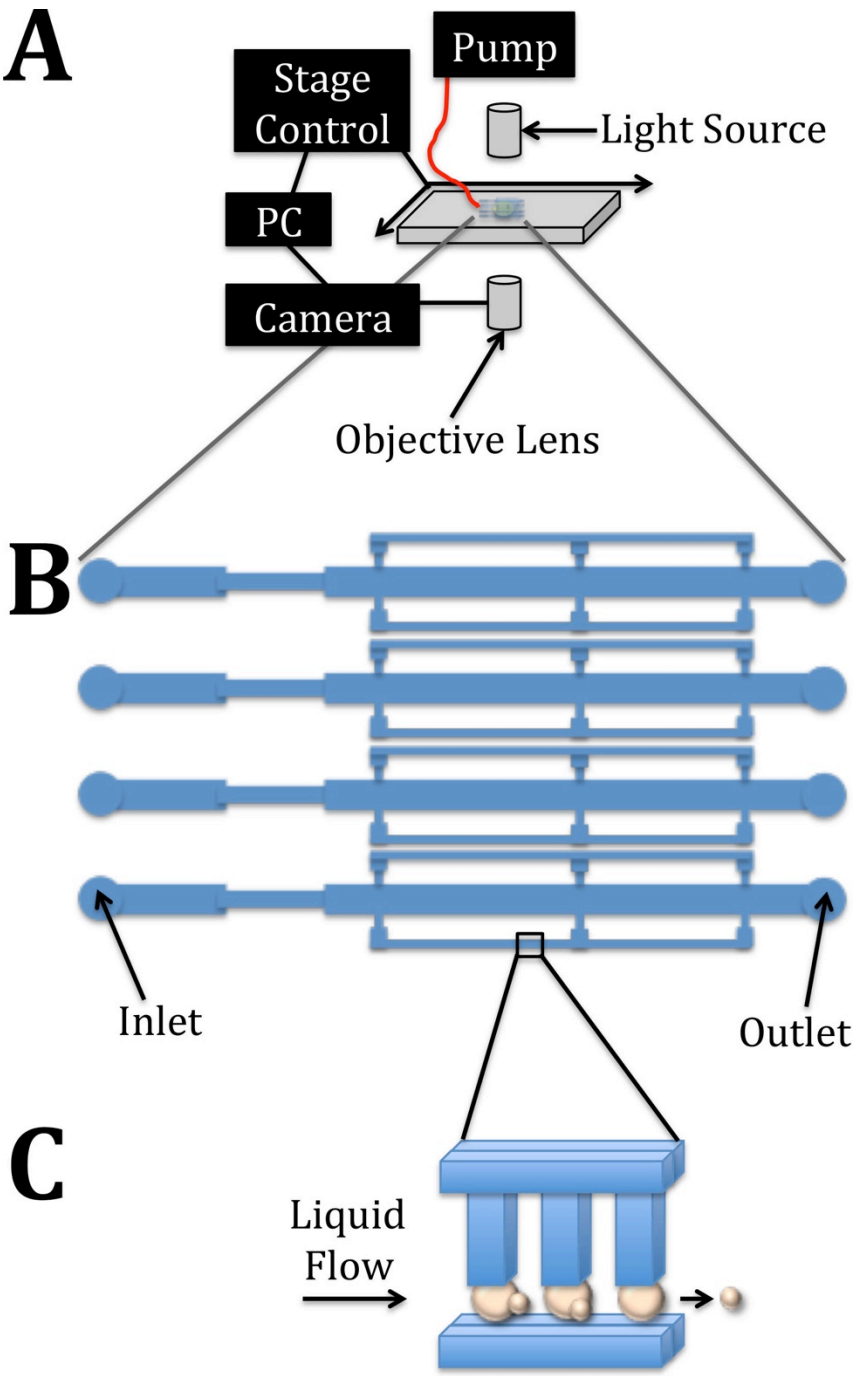


Figure 4.1. Overview of replicative lifespan microfluidics setup. (A) Diagram of microscope setup, with motorized stage control and camera both controlled by the same computer. An automatic pump loads cells into the chip, and then pumps fresh media through the chip. (B) Diagram of microfluidics chip, with four independent channels, each with two side channels connecting to the main channel at three points. (C) Pillars descend from the roof of these side channels and trap mother cells for imaging, allowing smaller daughter cells to be swept away by media flow.

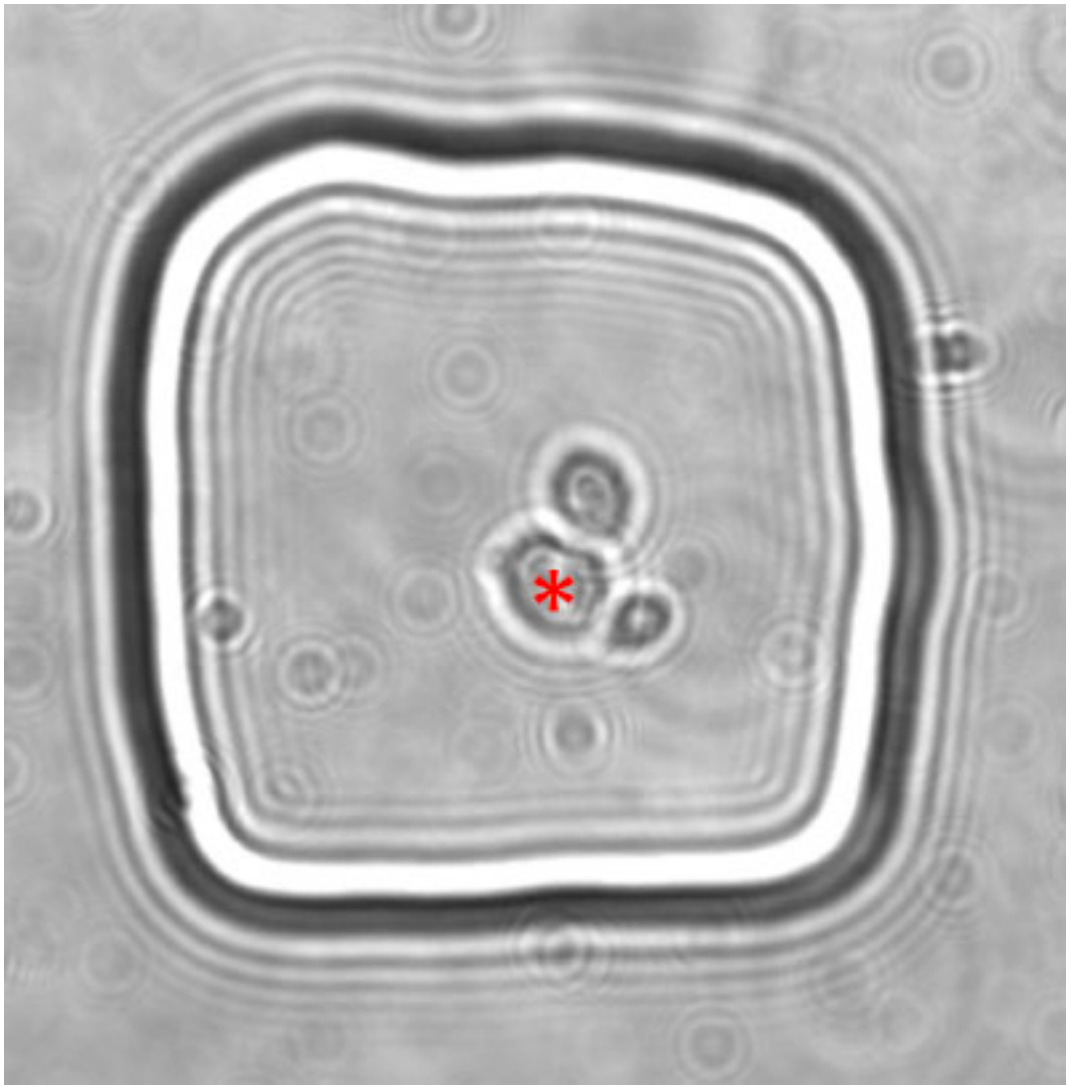


Figure 4.2. Still image of a single position on the microfluidics chip. Immobilized, dividing mother cell is identified with a red asterisk (*). The number of daughter buds given off by this mother cell before it senesces and dies represents its replicative lifespan.

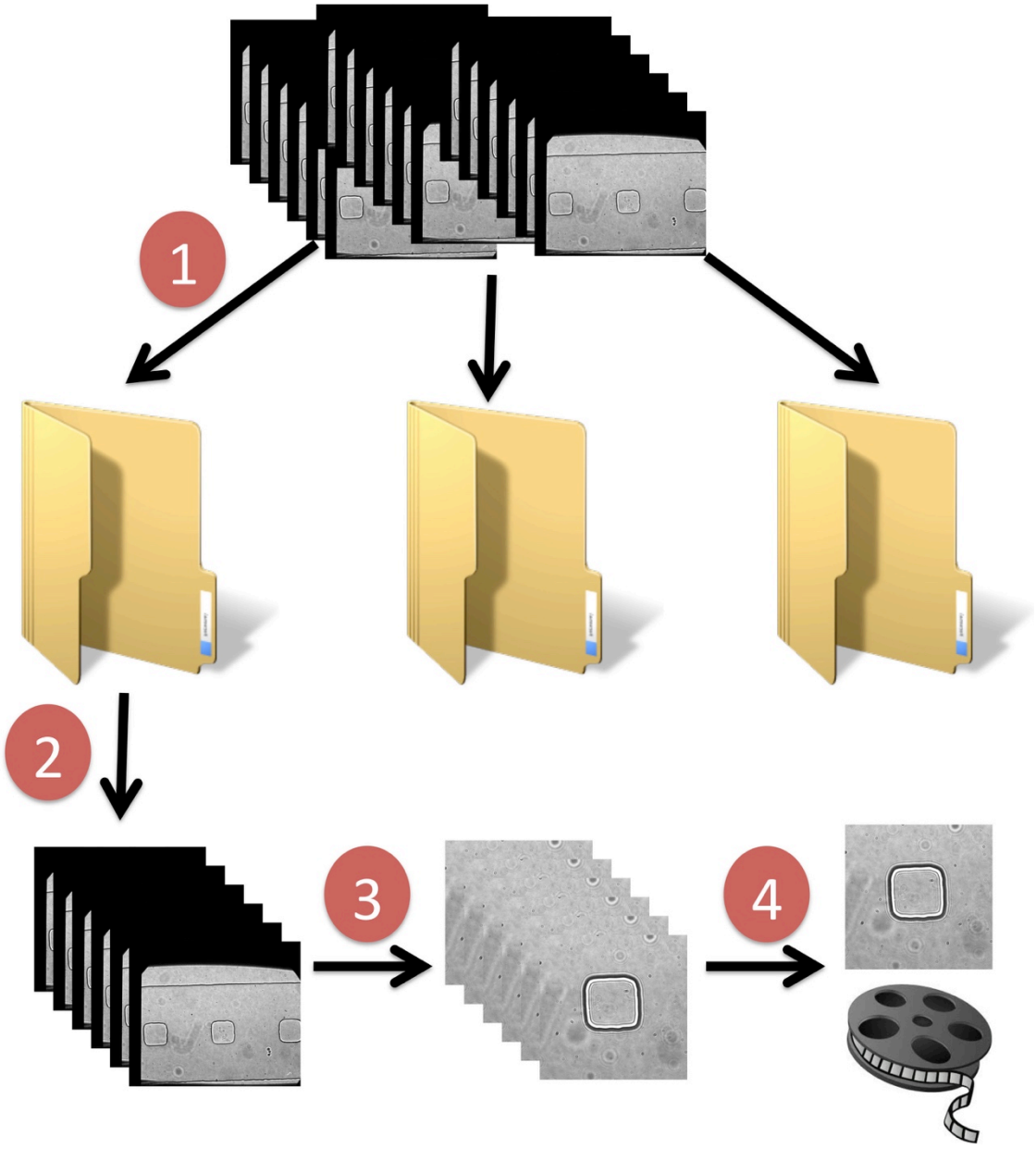


Figure 4.3. Overview of pipeline for data analysis. 1) Images from each position on the chip were sorted into a unique folder. 2) Images from each position were put into sequential order. 3) Images were cropped so that a single chip position was visible and was centered in the images. 4) Sequential cropped images were compiled into a .GIF animation for viewing and analysis.

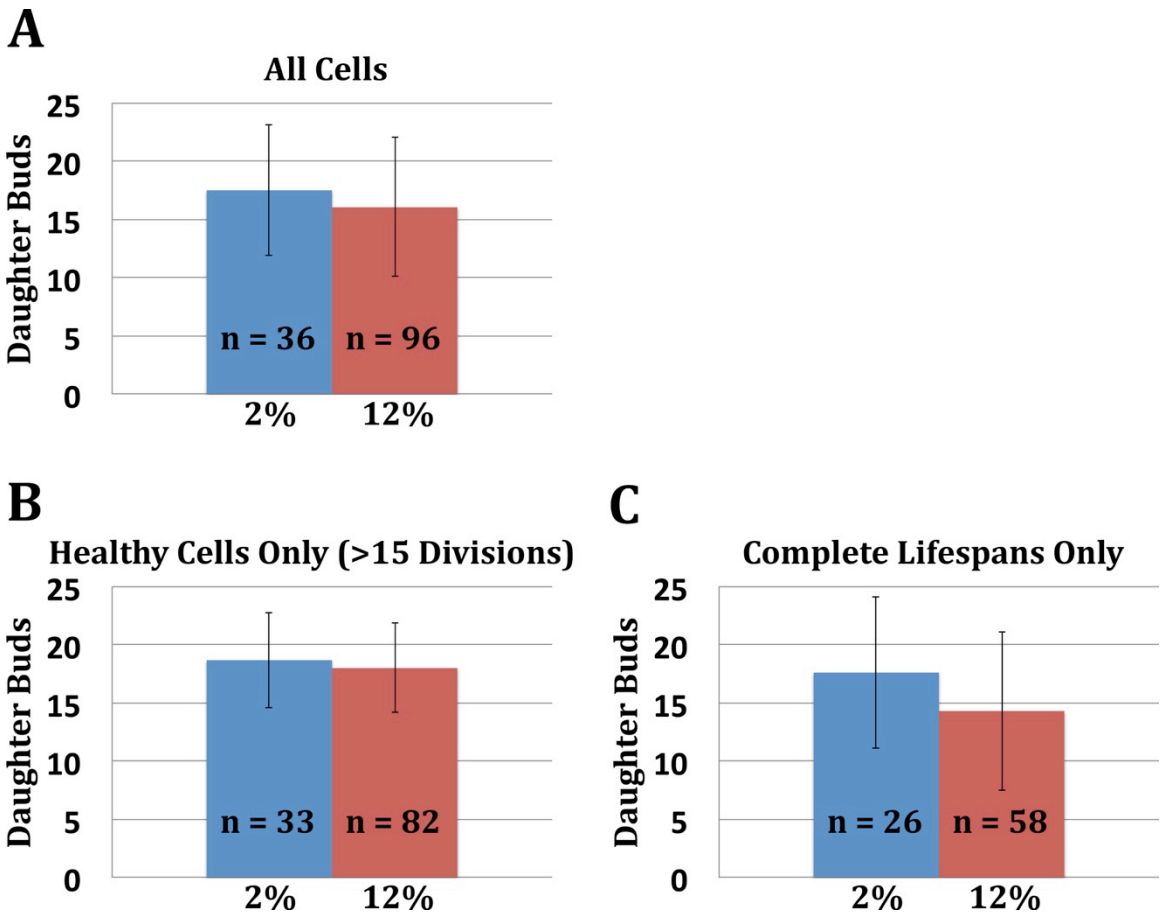


Figure 4.4. Replicative lifespan data for wild-type cells exposed to high- and low-glucose medium. Wild-type cells were loaded onto two lanes of a microfluidics chip with either fresh 2%- or 12%-glucose yeast peptone medium continuously flowing through the lanes. (A) represents replicative lifespans of all trapped cells, including those that washed away before senescence and death were observed. (B) represents replicative lifespans of only those trapped cells that were deemed healthy, meaning they gave off at least 15 daughter buds. This data also included cells that washed away before senescence and death were observed. (C) represents replicative lifespans of only those trapped cells where a complete lifespan was observed. This means the birth of a mother cell was observed, as well as every subsequent budding event until senescence and death of that mother cell. The number of mother cells (n) represented in each bar is given. There was no statistically significant difference between 2%- and 12%-glucose-grown cells regardless of how data was analyzed.

Part II:

Sir silencing and mating-type control of DNA damage repair

Chapter 5:

Sir protein-independent repair of dicentric chromosomes in *Saccharomyces cerevisiae*

Introduction

Sir proteins are necessary for the establishment and maintenance of heterochromatic gene silencing in the budding yeast *Saccharomyces cerevisiae* (reviewed in Rusche *et al.,* 2003; Kueng *et al.,* 2013). Sir2 is an NAD+-dependent protein deacetylase that primarily removes acetyl modifications from N-terminal tails of histones H3 and H4 (Landry *et al.,* 2000a; Smith *et al.,* 2000; Imai *et al.,* 2000). These deacetylated histone tails serve as high-affinity binding surfaces for Sir3 and Sir4 at telomeres and the silent mating loci (Hecht *et al.,* 1995). Sir-mediated heterochromatin formation represses transcription and recombination through the occlusion of factors necessary for these processes (Loo and Rine, 1994; Singh and Klar, 1992; Gottschling, 1992; Steakley and Rine, 2015). In many organisms, heterochromatin forms near and at the centromere where it contributes to the fidelity of chromosome segregation (reviewed in Allshire and Karpen, 2008; and Allshire and Ekwall, 2015).

The *SIR2*, *SIR3* and *SIR4* genes encode proteins that assemble into a complex (Moazed *et al.,* 1997), that is essential for the proper regulation of cell type. Haploid yeast express a single mating-type locus allele, designated either *MATa* or *MATα*. Yeast also have additional copies of *MATa* and *MATα* genes at the *HMRa* and *HMLα* loci, respectively, which are transcriptionally silenced by the Sir proteins (Rine *et al.,* 1979; Klar *et al*., 1981; Rine and Herskowitz, 1987). Yeast strains with the *HO* allele can switch their mating-type by undergoing a double-stranded DNA break at the *MAT* locus followed by gene conversion, with *MAT* being the recipient of genetic information from one of these silenced donor loci. *MATa* and *MATα* haploid cells can mate, producing an a/α diploid. Two proteins encoded by the *MAT* alleles, a1 and α2, form a heterodimer that represses haploid-specific genes including some of those responsible for non-homologous end joining, which is relevant to this study (Aström *et al*., 1999, reviewed in Haber, 2012).

Unlike in *S. pombe* and most other eukaryotes, *Saccharomyces'* centromeres have stood out as an exception due to their lack of heterochromatin. However, there is a report of a role for *S*. *cerevisiae* Sir2 in maintaining chromatin compaction when a chromosome is under artificial tension (Thrower and Bloom, 2001). This study used a strain with a second centromere, whose function was made conditional by being under the control of the *GAL1* promoter (hereafter *GALCEN3* after Thrower and Bloom), 45kb to the left of the endogenous centromere on chromosome III **(Figure 5.1A)**. In cells grown in medium containing glucose, the promoter is inactive and the conditional centromere is functional. In cells grown in medium containing galactose, the promoter is active, significantly inhibiting the function of this second centromere. The strain also contains a 10.1kb *lacO* array between the centromeres, and a *LacI-GFP* fusion gene to allow visualization of chromosome stretching during anaphase (Thrower and Bloom, 2001).

If microtubules emanating from opposite spindle poles attach to two functional centromeres on a single chromosome during mitosis, the chromosome will usually break (Brock and Bloom, 1994). Dramatic stretching of the chromosome is observed by microscopy in *sir2Δ* and *ku70Δ/80Δ* mutants before a

break occurs. The extent of stretching was reported as consistent with a near-complete loss of higher-order chromosome structure. In addition to stretching, *sir2Δ* and *ku70Δ/80Δ* mutants also suffered a significant drop in viability when the second centromere was active. Chromatin immunoprecipitation (ChIP) with anti-Sir2 sera using primers complementary to the *lacO* array revealed enrichment of Sir2, but only under conditions in which the second centromere was active. No ChIP signal was observed when the second centromere was inactive, implying that Sir2 bound *lacO* chromatin only when it was under tension (Thrower and Bloom, 2001). This result was potentially of great interest as it raised the possibility of condition-dependent assembly of Sir-protein based heterochromatin at repeated sequences and potentially at yeast centromeres when put under tension. While investigating this possibility further, we obtained results that offered a different explanation for key results from this study.

Yeast strains and media

Genotypes of strains used in this study are given in **Supplementary Table 5.1**. A conditionally dicentric strain KBY3615 was kindly provided by Professor K. Bloom (UNC Chapel Hill, Chapel Hill, NC). *sir2Δ::NAT^{MX}* (JRY10189), *sir3Δ::NAT^{MX}* (JRY10192), *sir4Δ::NAT^{MX}* (JRY10195), *ku70Δ::KAN^{MX}* (JRY10198) and *SIR2-13xMyc::KAN^{MX}* (JRY10207) strains were constructed in KBY3615 using standard yeast methodology. *sir3Δ::NAT^{MX}, hmlΔ::KAN^{MX}* (JRY10201) was constructed in JRY10192 using standard yeast methodology. Cultures were maintained at 30^{o}C in YP medium (2% peptone and 1% yeast extract) with 2% galactose (YPGal) to suppress function of conditional centromeres. Experiments compared YPGal-grown cultures to cultures with 2% glucose (YPD), where conditional centromeres were fully functional.

Quantitative viability of strains under dicentric conditions

Viability of dicentric strains was determined by plating equal numbers of galactose-grown cells (as measured by OD_{600} cell density) on both YPGal and YPD and counting colony forming units (CFUs) after 4 days of growth. CFU count on YPD was normalized to CFU count on YPGal for each strain to measure relative viability under dicentric conditions.

Chromatin immunoprecipitation and quantitative PCR

Cells for Chromatin Immunoprecipitation (ChIP) experiments were grown and treated as previously described (Thrower and Bloom, 2001) taking care to collect cells enriched for anaphase following release from 20μg/ml nocodazole. Anaphase enrichment was confirmed by microscopy, defined as >80% of cells with large buds and bilobed nuclei. The cells were fixed with 1% formaldehyde for 20 minutes and processed for ChIP analysis as previously described (Steakley and Rine, 2015), using EZview™ Red Anti-c-Myc Affinity Gel (Sigma E6654-1ML) for pull-

down of 13x-c-myc-Sir2. Cultures containing 5mM Nicotinamide were included as a negative control for Sir2 function (Landry, *et al.,* 2000b). For pull-down of kinetochore protein Mif2, chromatin was pre-cleared with 45µL of 50% v/v Protein A Sepharose™ CL-4B beads (GM Healthcare 17-0780-01) for one hour before being incubated overnight with polyclonal anti-Mif2 antibody (1:2000), generously provided by Arshad Desai (Akiyoshi *et al.* 2009). Chromatin was then incubated with 45µL of 50% v/v Protein A Sepharose™ CL-4B beads for three hours, before being washed and treated as previously described (Steakley and Rine, 2015). Quantitative PCR (qPCR) of input and immunoprecipitated (IP) DNA was performed using Thermo Scientific DyNAmo HS SYBR Green PCR Kits (Thermo Scientific F-410L) and a Stratagene Mx3000P qPCR system. Primers that detect *HMLα1* were used as a positive control for Sir2 binding. Primers that detect *KCC4*, *GALCEN3, CEN3*, and the *LEU2/lacO* junction were also used. Sequences of qPCR oligonucleotides are included in Table S2. IP enrichment values were normalized to input enrichment values, as well as to relative enrichment using primers that detect *ACT1*, where Sir2 has been shown to not bind [(IP(primer)/IN(primer)]/[IP(control)/IN(control)].

Results

Sir 2/3/4 complex was necessary for preserving viability of dicentric cells

In addition to its role in heterochromatin gene silencing, Sir2 has a role independent of the Sir3 and Sir4 in controlling the chromatin structure and recombination of rDNA. To determine whether Sir2 alone, or the entire Sir2/3/4 complex, was responsible for preserving viability of cells with dicentric chromosomes, we deleted *SIR3* and *SIR4* individually in a conditionally dicentric strain (KBY3615), and then measured the viability of these mutants alongside *sir2Δ* and *ku70Δ* mutants grown in both monocentric (galactose) and dicentric (glucose) conditions **(Figure 5.1B)**. The viability of *sir3Δ* and *sir4Δ* strains phenocopied that of the *sir2Δ and ku70Δ* mutants **(Figure 5.2)**. Therefore the entire Sir2/3/4 complex was necessary to preserve viability of cells with a dicentric chromosome.

Sir 2/3/4 complex preservation of dicentric viability was an indirect effect of mating type

There have been previous reports of Sir proteins having a role in DNA repair (e.g. Tsukamoto *et al.,* 1997) but to date these have proven to be indirect effects of mating type since *sir* mutants have the properties of a/a diploids in which non-homologous end joining is repressed (Aström *et al*., 1999; Lee *et al*., 1999). To test whether the vulnerability of dicentric chromosomes in *sir* mutants was also an indirect effect of mating-type, we deleted *HML* in the *MATa sir3Δ* dicentric strain. This strain, despite being Sir-, expressed only a-specific cell-type genes. This deletion restored viability to wild-type levels **(Figures 5.2 and 5.3)**. Sir2/3/4

repression of transcription at *HML* was therefore sufficient to prevent a loss of viability in *MATa* cells with a dicentric chromosome.

Sir2 did not occupy chromatin between centromeres of a dicentric chromosome

We re-evaluated the previously reported Sir2 enrichment at the *lacO* array during growth in glucose medium, when the dicentric chromosome would have the potential to create tension on the operator array, taking advantage of the enhanced sensitivity of quantitative PCR over the endpoint-PCR analyses used previously (Thrower and Bloom, 2001). We fused a c-terminal 13x-myc tag to *SIR2* in the dicentric strain, and used an anti-myc monoclonal antibody (Evans *et al.,* 1985), which we have used in multiple different studies to detect Sir2 with specificity and sensitivity, and in the context of the Sir2, Sir3, Sir4 complex which our results indicated was relevant to these observations (Thurtle and Rine, 2014; Ellahi *et al.,* 2015). In addition to the lacO array, we measured enrichment of Sir2 at multiple other genomic positions that would experience tension in the dicentric state **(Figure 5.4A)**. As a positive control we observed 13x-myc-Sir2 enrichment at *HMLα1*, which was lost when cells were grown in 5mM nicotinamide, an inhibitor of Sir2 **(Figure 5.4B)**. While Sir2 enrichment was not expected for any experimental primer sets when cells were grown in galactose medium, enrichment would be expected in cells grown in glucose medium if Sir2 were recruited to chromatin under tension. Contrary to the results of the previous study, 13x-myc-Sir2 was not enriched at any of the regions tested in either galactose or glucose media, with or without nicotinamide **(Figure 5.4C-F).** We observed inner kinetochore protein Mif2 enrichment at both centromeres but not at *HML*, demonstrating that our inability to detect 13x-myc-Sir2 at centromeres did not stem from a general inability to detect bound proteins in these regions by ChIP. The binding of Mif2 was unaffected by NAM treatment, but increased upon activation of the conditional centromere (*GALCEN3*) by switching from galactose to dextrose media **(Supplementary Figure 5.1)**. The dependence of Mif2-binding at *GALCEN3* on growth in dextrose was consistent with data showing Mif2 is mostly evicted from a conditional centromere that has been inactivated by galactose-induced transcription (Collins *et al.,* 2005).

Discussion

Double-strand DNA breaks can be repaired either by homologous recombination with a sister chromatid, or by non-homologous end joining. Typically, homologous recombination is the preferred mechanism except for breaks that occur in haploids in G1, where there is no sister chromatid or homologous chromosome to guide repair (Aström *et al*., 1999; Lee *et al*., 1999). The repair of a dicentric chromosome broken by the forces of chromosome segregation is imperfectly amenable to homologous repair because the force that breaks a chromosome also moves the sister chromatid away form one of the two broken

fragments. In addition, at some frequency both of the sister dicentric chromatids would be broken in the same cell cycle. Hence, non-homologous end joining would be expected to play a significant role in the repair of double-stranded DNA breaks created by mis-segregation of dicentric chromosomes.

a/α diploid yeast and haploid Sir- mutants which express both *HMLα* and *HMRa* repress non-homologous end joining at least 20-fold (Aström *et al.,* 1999; Lee *et al.,* 1999), favoring repair via homologous recombination (Shrivastav *et al.,* 2008). As shown here and reported earlier (Thrower and Bloom, 2001) the viability of a strain with a dicentric chromosome was lost in cells lacking Sir protein function. However, rather than reflecting a role of Sir2 in controlling the probability that a chromosome would break under tension, our work established that preservation of viability by Sir protein function was mediated indirectly through the role of the Sir 2/3/4 complex in maintaining cell-type identity via repression of the mating-type genes at *HML* and *HMR*. This drop in viability was likely a result of repression of the non-homologous end joining repair pathway by the a1/α2 repressor in Sir- mutants. Restoration of haploid a-cell identity through deletion of *HMLα* restored viability in a Sir- dicentric strain. In addition loss of non-homologous end joining in the *ku70Δ* mutant phenocopied the reduced viability of a *sir2Δ*, *sir3Δ* or *sir4Δ* mutants. Taken together--the similarity of Sir- and Ku- phenotypes, the rescue of *sir3Δ* viability loss by deletion of *HML*, and the previously known repression of non-homologous end joining by the a1/α2 heterodimer (Frank-Vaillant and Marcand, 2001)--indicate that aberrant repression of non-homologous end joining in Sir- mutants was responsible for loss of viability.

The discrepancy between our finding that Sir2 could not be detected at regions of chromatin that were under tension and the earlier work was most likely due to methodological improvements over the intervening years. Our ChIP experiments used a more sensitive method than used previously, yet failed to reveal enrichment of Sir2 between the potentially tensioned pair of centromeres in anaphase-enriched cultures under any experimental condition tested. Moreover, we failed to detect Sir2 enrichment at additional regions under tension, as well as at the *lacO* array, yet did detect robust Sir2 enrichment at *HMLα*, as expected. We suggest that the repetitive nature of the *lacO* array was responsible for the artifactual signal of Sir2 enrichment. The earlier work used primers that flanked a *lacO* sequence that is repeated 32 times in the 10.1kb *lacO* array. Additionally, the primers used in the earlier study were insufficiently-specific, possibly as a result of the repetitive nature of the array. When we performed qPCR using these primers, the dissociation curve revealed their suboptimum performance, with multiple products of various sizes being amplified. While it is not clear how many PCR cycles were used in the previous study, the presence of 32 *lacO* 8mer repeats means that it might have been the equivalent of 5 cycles (2^5) too many.

In summary, the enhanced loss of viability of dicentric chromosomes in Sir- mutants can be attributed to an indirect effect on the repression of non-homologous end joining, and we found no evidence of recruitment of Sir2 to DNA under tension between two centromeres. As a final yet important point, we have no reason to doubt any of the microscopy data from the earlier work.

Acknowledgments

We thank Professor Kerry Bloom for providing the conditionally dicentric strain and for helpful discussions during the preparation of the manuscript. We thank Professor Arshad Desai for generously providing the anti-Mif2 antibody. We thank members of our lab for useful discussions during the course of this work. This work was supported by an NIH predoctoral fellowship (5 F31 AG047795-03) to DFM, an NSF predoctoral fellowship (DGE 1106400 to DLS), and a grant from the National Institutes of Health (GM31105 to JR).

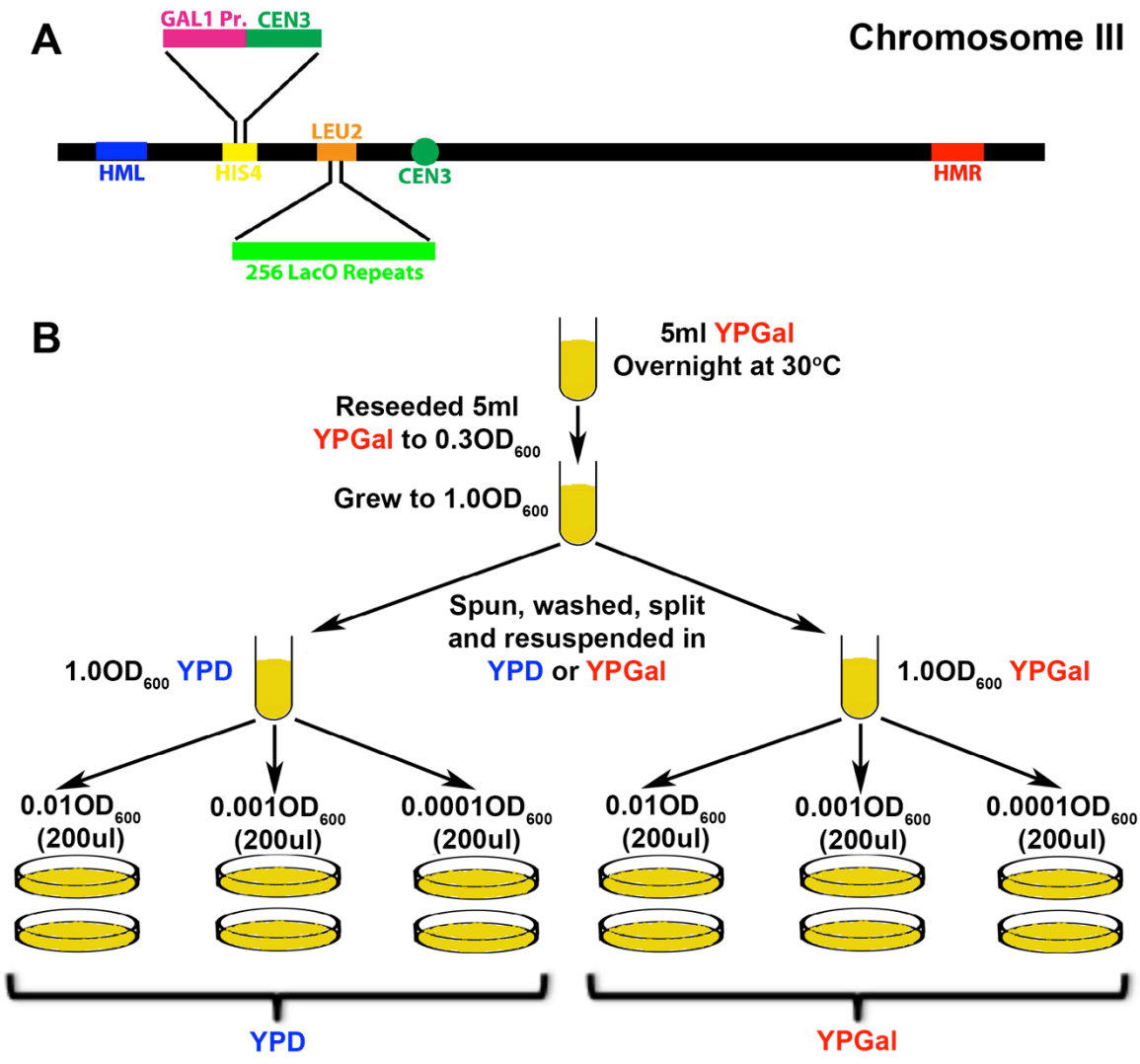


Figure 5.1. Experimental Design. **(**A) Diagram of modified chromosome III. Conditional centromere downstream from *pGAL1* is functional in glucose, mostly non-functional in galactose. (B) Diagram of viability assay. Cells grown to a density of 1.0 OD_{600} in galactose medium (YPGal). Cultures are split, washed, and resuspended in either glucose media (YPD) or YPGal. Serial dilutions of cultures were then plated on either YPGal or YPD media. Counting colony-forming units (CFUs) gives a measure of viability on each media.

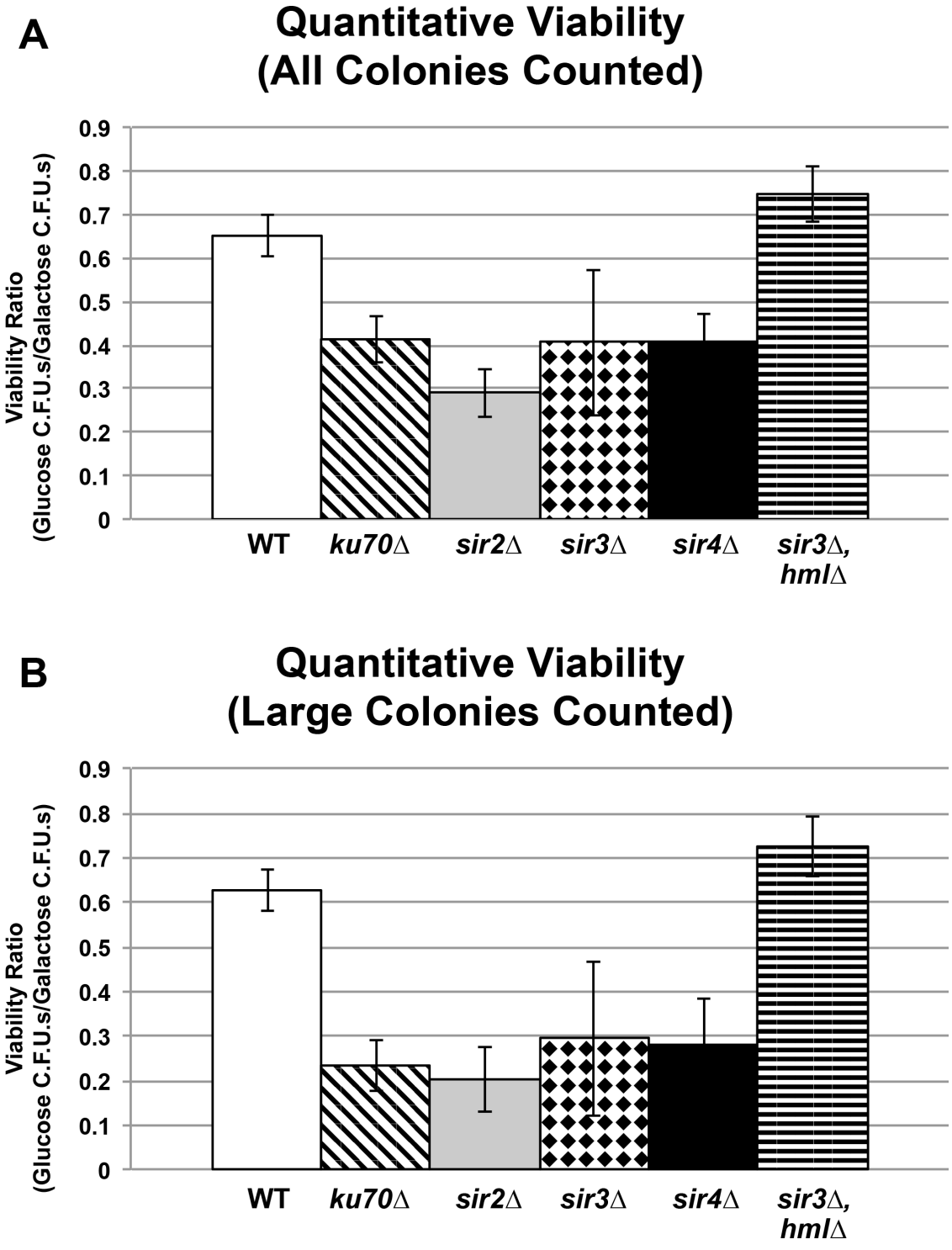


Figure 5.2. Quantitative viability decrease in Sir- mutants rescued by deletion of *HMLα.* Data represents colony-forming units (CFUs) in glucose where second centromere is functional, normalized to CFUs in galactose, where second centromere is mostly non-functional. (A) All colonies, regardless of size, are counted. (B) Only large colonies are counted.

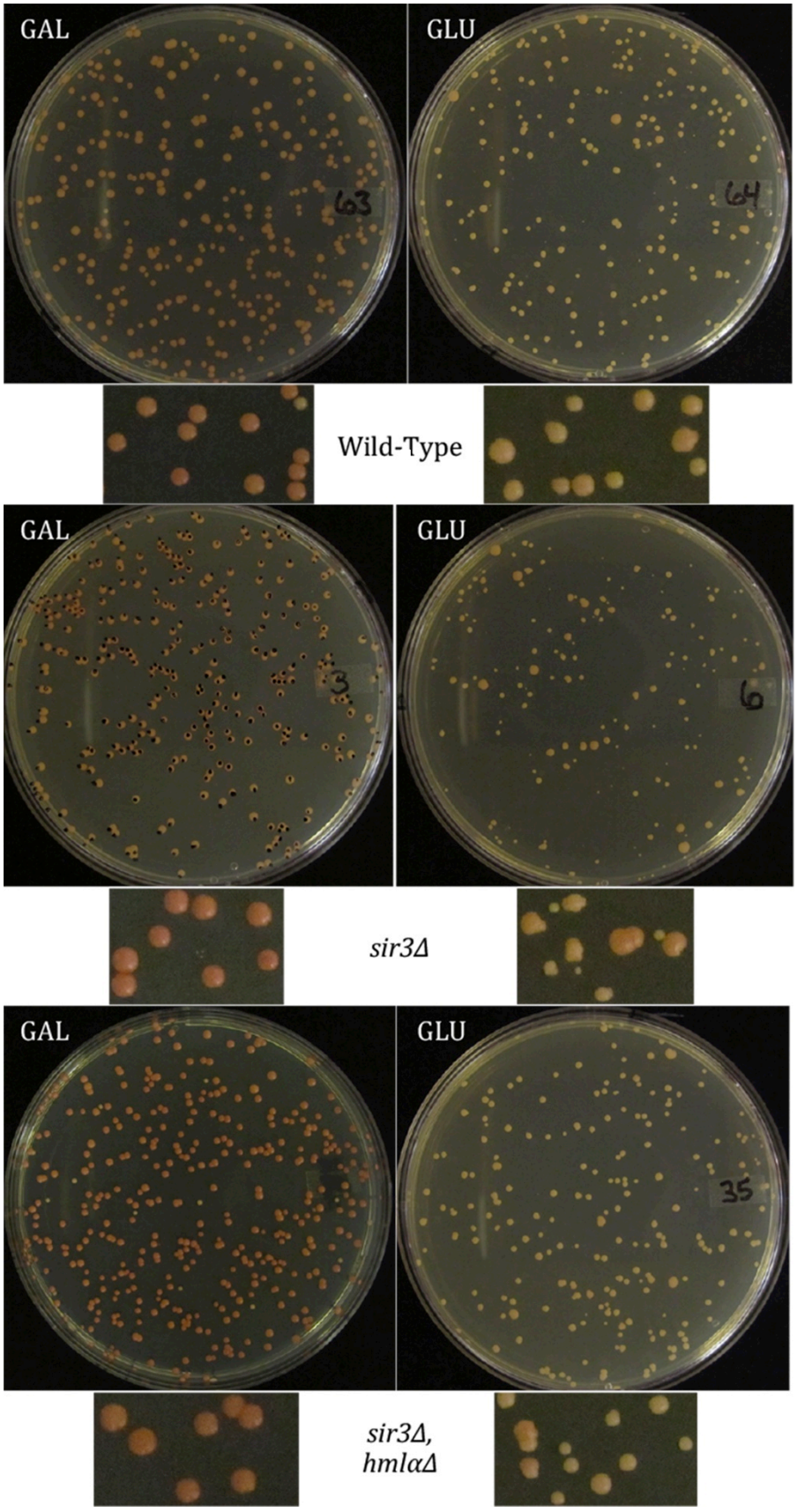

GAL
GLU
63
64
Wild-Type
GAL
GLU
3
6
sir3Δ
GAL
GLU
35
sir3Δ,
hmlαΔ

Figure 5.3. Loss of viability and colony phenotypes in Sir- mutants rescued by deletion of *HMLα.* Left column shows strains grown on galactose, where second centromere should be mostly inactive. Right column shows strains grown on glucose, where second centromere should be active. *sir3Δ* strain (middle panel) is less viable than wild-type (top panel) and colony size and shape changes when grown on glucose, consistent with increased DNA damage. Deletion of *HMLα* in a *sir3Δ* background (bottom panel) restores these phenotypes to wild type. Close-up view of representative colonies shown below each plate.

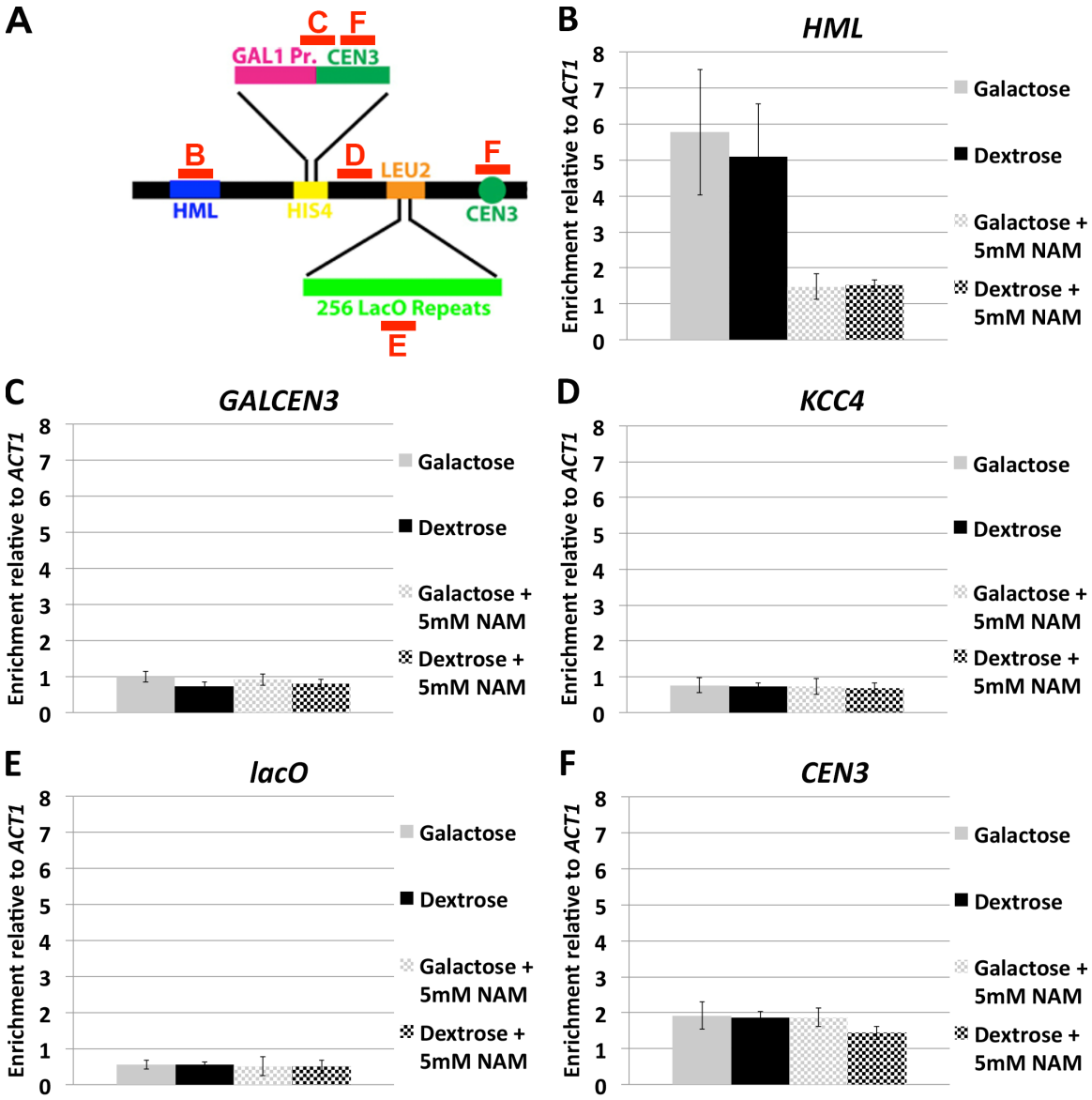


Figure 5.4. Sir2 did not occupy chromatin between centromeres of a dicentric chromosome. (A) Regions of Chromosome III homologous to qPCR primers used in this figure. (B-F) 13x-myc-Sir2 enrichment using primer sets diagrammed in (A), was performed in glucose (2nd centromere functional) and galactose (2nd centromere non-functional), with or without 5mM NAM. All enrichment values normalized to *ACT1* primer set enrichment. Sir2 enrichment is not observed anywhere, regardless of status of the conditional centromere. The appearance of an approximate 2-fold 13x-myc-Sir2 enrichment at *CEN3* in all samples is due to the *CEN3* primers amplifying both centromeres on Chromosome III, not due to Sir2 occupancy.

Table S5.1. Yeast strains used in this study

Strain:	Genotype:	Source
KBY3615 (JRY10186-JRY10188)	*MATa ade2-1 can1-100 his3-11,15::GFP-LacI-HIS3 his4::URA3-GALCEN3 leu2-3,112::lacO-LEU2 trp1-1 ura3-1 SPC29-CFP::HYG^{MX}*	Thrower and Bloom, 2001
JRY10189-JRY10191	*MATa ade2-1 can1-100 his3-11,15::GFP-LacI-HIS3 his4::URA3-GALCEN3 leu2-3,112::lacO-LEU2 trp1-1 ura3-1 SPC29-CFP::HYG^{MX} sir2Δ::NAT^{MX}*	This Study
JRY10192-JRY10194	*MATa ade2-1 can1-100 his3-11,15::GFP-LacI-HIS3 his4::URA3-GALCEN3 leu2-3,112::lacO-LEU2 trp1-1 ura3-1 SPC29-CFP::HYG^{MX} sir3Δ::NAT^{MX}*	This Study
JRY10195-JRY10197	*MATa ade2-1 can1-100 his3-11,15::GFP-LacI-HIS3 his4::URA3-GALCEN3 leu2-3,112::lacO-LEU2 trp1-1 ura3-1 SPC29-CFP::HYG^{MX} sir4Δ::NAT^{MX}*	This Study
JRY10198-JRY10200	*MATa ade2-1 can1-100 his3-11,15::GFP-LacI-HIS3 his4::URA3-GALCEN3 leu2-3,112::lacO-LEU2 trp1-1 ura3-1 SPC29-CFP::HYG^{MX} ku70Δ::KAN^{MX}*	This Study
JRY10201-JRY10203	*MATa ade2-1 can1-100 his3-11,15::GFP-LacI-HIS3 his4::URA3-GALCEN3 leu2-3,112::lacO-LEU2 trp1-1 ura3-1 SPC29-CFP::HYG^{MX} sir3Δ::NAT^{MX} hmlΔ::KAN^{MX}*	This Study
JRY10207-JRY10209	*MATa ade2-1 can1-100 his3-11,15::GFP-LacI-HIS3 his4::URA3-GALCEN3 leu2-3,112::lacO-LEU2 trp1-1 ura3-1 SPC29-CFP::HYG^{MX} SIR2-13xMyc::KAN^{MX}*	This Study

Table S5.2. qPCR Oligonucleotides used in this study

Name:	**Sequence (5'-3'):**
ACT1 Forward	TGT CCT TGT ACT CTT CCG GT
ACT1 Reverse	CCG GCC AAA TCG ATT CTC AA
CEN3 Forward	CGC CAA ACA ATA TGG AAA ATC C
CEN3 Reverse	CCA CCA GTA AAC GTT TCA TAT ATC C
HMLα1 Forward	GCC CAC TTC TAA GCT GAT TTC AAT CTC TCC
HMLα1 Reverse	GGC TTC GAA GTA AAC ATA TTG TGA ATG TCG
GALCEN3 Forward	GAA GAG GAA AAA TTG GCA GTA ACC
GALCEN3 Reverse	CGC TGA TTA ATT ACC CCA GAA ATA AGG
KCC4 Forward	AAA TCA GAG ACA TCC TTA GTC ATC C
KCC4 Reverse	GAG TCA GCC AGT GGA TAT AGA TAG G
lacO-LEU2 Forward	TAC ATA CCT AAT ATT ATT GCC TTA T
lacO-LEU2 Reverse	AAT TGT TAT CCG CTC ACA ATT CCA
lacO 8mer Forward	AGG CGC CGA ATT CCA CA
lacO 8mer Reverse	AGA ATT CGT CGA GGA ATT C

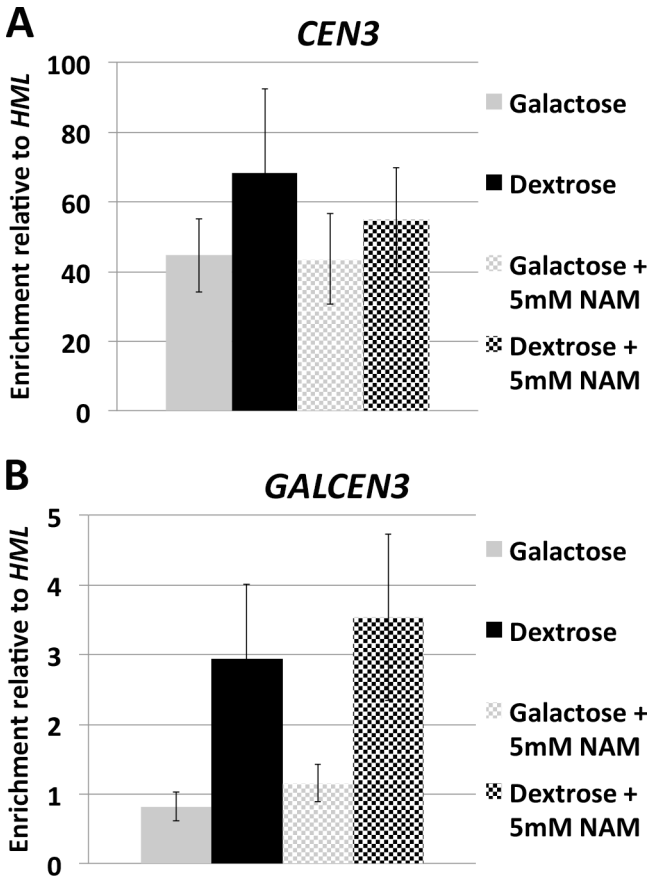


Figure S5.1. Inner kinetochore protein Mif2 binds centromeric chromatin as expected. (A) Mif2 is enriched at *CEN3* regardless of NAM treatment, and signal increases upon switching from galactose to dextrose media due to activation of the second centromere, which is also amplified by the *CEN3* primer set. (B) Primer set specific to the conditional, second centromere (*GALCEN3*) shows enrichment of Mif2 only when grown in dextrose as expected. All enrichment values normalized to *HMLα1* primer set enrichment.

References

Abremski, K., and R. Hoess, (1984). Bacteriophage P1 site-specific recombination. Purification and properties of the Cre recombinase protein. J. Biol. Chem. 259: 1509-1514.

Ai, W., P. G. Bertram, C. K. Tsang, T. F. Chan, and X. F. Zheng, (2002). Regulation of subtelomeric silencing during stress response. Mol. Cell. 10: 1295-1305.

Akiyoshi, B., C. R. Nelson, J. A. Ranish, and S. Biggins, (2009). Quantitative proteomic analysis of purified yeast kinetochores identifies a PP1 regulatory subunit. Genes Dev. 23: 2887–2899.

Allen, C., S. Büttner, A. D. Aragon, J. A. Thomas, and O. Meirelles, *et al.*, (2006). Isolation of quiescent and nonquiescent cells from yeast stationary-phase cultures. J. Cell Biol. 174: 89-100.

Allshire, R. C., and G. H. Karpen, (2008). Epigenetic regulation of centromeric chromatin: old dogs, new tricks? Nat. Rev. Genet. 9: 923-937.

Allshire, R. C., and K. Ekwall, (2015). Epigenetic Regulation of Chromatin States in *Schizosaccharomyces pombe*. Cold Spring Harb. Perspect. Biol. 7: a018770.

Anderson, R. M., and R. Weindruch, (2007). Metabolic reprogramming in dietary restriction. Interdiscip. Top. Gerontol. 35: 18-38.

Anderson, R. M., and R. Weindruch, (2010). Metabolic reprogramming, caloric restriction and aging. Trends Endocrinol. Metab. 21: 134-141.

Aparicio, O. M., B. L. Billington, and D. E. Gottschling, (1991). Modifiers of position effect are shared between telomeric and silent mating-type loci in *S. cerevisiae*. Cell. 66: 1279-1287.

Aström, S. U., S. M. Okamura, and J. Rine, (1999). Yeast cell-type regulation of DNA repair. Nature. 397: 310.

Bedalov, A., M. Hirao, J. Posakony, M. Nelson, and J. A. Simon, (2003). NAD+-dependent deacetylase Hst1p controls biosynthesis and cellular NAD+ levels in *Saccharomyces cerevisiae*. Mol. Cell. Biol. 23: 7044-7054.

Bitterman, K. J., R. M. Anderson, H. Y. Cohen, M. Latorre-Esteves, and D. A. Sinclair, (2002). Inhibition of silencing and accelerated aging by nicotinamide, a putative negative regulator of yeast Sir2 and human SIRT1. J. Biol. Chem. 277: 45099-45107.

Bordone, L., D. Cohen, A. Robinson, M. C. Motta, E. van Veen, *et al.*, (2007). SIRT1 transgenic mice show phenotypes resembling calorie restriction. Aging Cell. 6: 759-767.

Brachmann, C. B., J. M. Sherman, S. E. Devine, E. E. Cameron, L. Pillus, *et al.*, (1995). The *SIR2* gene family, conserved from bacteria to humans, functions in silencing, cell cycle progression, and chromosome stability. Genes Dev. 9: 2888-2902.

Brock, J. A., and K. Bloom, (1994). A chromosome breakage assay to monitor mitotic forces in budding yeast. J. Cell Sci. 107: 891-902.

Burnett, C., S. Valentini, F. Cabreiro, M. Goss, M. Somogyvári, *et al.*, (2011). Absence of effects of Sir2 overexpression on lifespan in *C. elegans* and *Drosophila*. Nature. 477: 482-485.

Burtner, C. R., C. J. Murakami, B. K. Kennedy, and M. Kaeberlein, (2009). A molecular mechanism of chronological aging in yeast. Cell Cycle. 8: 1256-1270.

Byrne, K. P., and K. H. Wolfe, (2005). The Yeast Gene Order Browser: combining curated homology and syntenic context reveals gene fate in polyploid species. Genome Res. 15: 1456-1461.

Cheng, T. H., C. R. Chang, P. Joy, S. Yablok, and M. R. Gartenberg, (2000). Controlling gene expression in yeast by inducible site-specific recombination. Nucleic Acids Res. 28: E108.

Chiba, T., H. Yamaza, and I. Shimokawa, (2007). Role of insulin and growth hormone/insulin-like growth factor-I signaling in lifespan extension: rodent longevity models for studying aging and calorie restriction. Curr. Genomics. 8: 423-428.

Coghe, S., H. D'Hollander, H. Verachtert, and F. R. Delvaux, (2005). Impact of Dark Specialty Malts on Extract Composition and Wort Fermentation. Journal of the Institute of Brewing. 111: 51-60.

Collins, K. A., A. R. Castillo, S. Y. Tatsutani, and S. Biggins, (2005). De Novo Kinetochore Assembly Requires the Centromeric Histone H3 Variant. Mol. Biol. Cell. 16: 5649-5660.

Colman-Lerner, A., T. E. Chin, and R. Brent, (2001). Yeast Cbk1 and Mob2 activate daughter-specific genetic programs to induce asymmetric cell fates. Cell. 107: 739-750.

Comfort, A., (1963). Effect of delayed and resumed growth on the longevity of a fish (*Lebistes reticulatus*, Peters) in captivity. Gerontologia. 49: 150-155.

Conant, G. C., and K. H. Wolfe, (2007). Increased glycolytic flux as an outcome of whole-genome duplication in yeast. Mol. Syst. Biol. 3: 129.

Couzin-Frankel J., (2011). Genetics. Aging genes: the sirtuin story unravels. Science. 334: 1194-1198.

da Silva, M. F., M. S. Soares, J.B. Fernandes, and P.C. Vieria, (2007). Alkyl, aryl, alkylarylquinoline, and related alkaloids. Alkaloids Chem. Biol. 64:139-214.

Dodson, A. E., and J. Rine, (2015). Heritable capture of heterochromatin dynamics in *Saccharomyces cerevisiae*. eLife. 4: e05007.

Doolin, M. T., A. L. Johnson, L. H. Johnston, and G. Butler, (2001). Overlapping and distinct roles of the duplicated yeast transcription factors Ace2p and Swi5p. Mol. Microbiol. 40: 422-432.

Ellahi, A., D. M. Thurtle, and J. Rine, (2015). The Chromatin and Transcriptional Landscape of Native *Saccharomyces cerevisiae* Telomeres and Subtelomeric Domains. Genetics. 200: 505-521.

Evan, G. I., G. K. Lewis, G. Ramsay, and J. M. Bishop, (1985). Isolation of monoclonal antibodies specific for human c-myc proto-oncogene product. Mol. Cell. Biol. 5: 3610-3616.

Fabrizio, P., C. Gattazzo, L. Battistella, M. Wei, C. Cheng, *et al.*, (2005). Sir2 blocks extreme life-span extension. Cell. 123: 655-667.

Fabrizio, P., L. Battistella, R. Vardavas, C. Gattazzo, L. L. Liou, *et al.*, (2004). Superoxide is a mediator of an altruistic aging program in *Saccharomyces cerevisiae*. J. Cell Biol. 166: 1055-1067.

Fabrizio, P., and V. D. Longo, (2007). The chronological life span of *Saccharomyces cerevisiae*. Methods Mol. Biol. 371: 89-95.

Fabrizio, P., and V. D. Longo, (2008). Chronological aging-induced apoptosis in yeast. Biochem. Biophys. Acta. 1783: 1280-1285.

Frank, S. A., (2013). Natural selection. VII. History and interpretation of kin selection theory. J. Evol. Biol. 26: 1151-1184.

Frank-Vaillant, M., and S. Marcand, (2001). NHEJ regulation by mating type is exercised through a novel protein, Lif2p, essential to the ligase IV pathway. Genes Dev. 15: 3005-3012.

Froyd, C. A., and L. N. Rusche, (2011). The duplicated deacetylases Sir2 and Hst1 subfunctionalized by acquiring complementary inactivating mutations. Mol. Cell. Biol. 31: 3351-3365.

Garde-Cerdán, T., C. Lorenzo, A. M. Martínez-Gil, J. F. Lara, F. Pardo, *et al.*, (2011). Evolution of Nitrogen Compounds During Grape Ripening from Organic and Non-Organic Monastrell – Nitrogen Consumption and Volatile Formation in Alcoholic Fermentation, p. 123-138 in *Research in Organic Farming*, edited by R. Nokkoul. InTech, Croatia.

Gasch, A. P., P. T. Spellman, C. M. Kao, O. Carmel-Harel, M. B. Eisen, *et al.*, (2000). Genomic expression programs in the response of yeast cells to environmental changes. Mol. Biol. Cell. 11: 4241-4257.

Gesing, A., K. A. Al-Regaiey, A. Bartke, and M. M. Masternak, (2014). Growth hormone abolishes beneficial effects of calorie restriction in long-lived Ames dwarf mice. Exp. Gerontol. 58: 219-229.

Gómez, J. M., (2010). Aging in bacteria, immortality or not-a critical review. Curr. Aging Sci. 3: 198-218.

Gottlieb, S., and R. E. Esposito, (1989). A new role for a yeast transcriptional silencer gene, *SIR2*, in regulation of recombination in ribosomal DNA. Cell. 56: 771-776.

Gottschling, D.E., (1992). Telomere-proximal DNA in *Saccharomyces cerevisiae* is refractory to methyltransferase activity in vivo. Proc. Natl. Acad. Sci. U S A. 89: 4062-4065.

Greer, E. L., D. Dowlatshahi, M.R. Banko, J. Villen, K. Hoang, *et al.*, (2007). An AMPK-FOXO pathway mediates longevity induced by a novel method of dietary restriction in *C. elegans*. Curr. Biol. 17: 1646-1656.

Guarente, L., and F. Picard, (2005). Calorie restriction--the *SIR2* connection. Cell. 120: 473-482.

Haber, J. E., (2012). Mating-type genes and MAT switching in *Saccharomyces cerevisiae*. Genetics. 191: 33-64.

Hecht, A., T. Laroche, S. Strahl-Bolsinger, S. M. Gasser, and M. Grunstein, (1995). Histone H3 and H4 N-termini interact with SIR3 and SIR4 proteins: a

molecular model for the formation of heterochromatin in yeast. Cell. 80: 583-92.

Huberts, D. H., J. González, S. S. Lee, A. Litsios, G. Hubmann, *et al*., (2014). Calorie restriction does not elicit a robust extension of replicative lifespan in *Saccharomyces cerevisiae*. Proc. Natl. Acad. Sci. U S A. 111: 11727-11731.

Imai, S., C. M. Armstrong, M. Kaeberlein, and L. Guarente, (2000). Transcriptional silencing and longevity protein Sir2 is an NAD-dependent histone deacetylase. Nature. 403: 795-800.

Jazwinski, S. M., (1990). An experimental system for the molecular analysis of the aging process: the budding yeast *Saccharomyces cerevisiae*. J. Gerontol. 45: B68-B74.

Jiang, W., S. Wang, M. Xiao, Y. Lin, L. Zhou, *et al*., (2011). Acetylation regulates gluconeogenesis by promoting PEPCK1 degradation via recruiting the UBR5 ubiquitin ligase. Mol. Cell. 43: 33-44.

Kaeberlein, M., K. K. Steffen, D. Hu, N. Dang, E. O. Kerr, *et al.*, (2006). Comment on "*HST2* mediates *SIR2*-independent life-span extension by calorie restriction". Science. 312: 1312.

Kaeberlein, M., K. T. Kirkland, S. Fields, and B. K. Kennedy. (2004). Sir2-independent life span extension by calorie restriction in yeast. PLoS Biol. 2: E296.

Kaeberlein M., M. McVey, and L. Guarente, (1999). The *SIR2/3/4* complex and *SIR2* alone promote longevity in *Saccharomyces cerevisiae* by two different mechanisms. Genes Dev. 13: 2570-2580.

Kaeberlein, M., and R. W. Powers 3rd, (2007). Sir2 and calorie restriction in yeast: a skeptical perspective. Ageing Res. Rev. 6: 128-140.

Kaeberlein, M., R. W. Powers 3rd, K. K. Steffen, E. A. Westman, D. Hu, *et al.*, (2005). Regulation of yeast replicative life span by TOR and Sch9 in response to nutrients. Science. 310: 1193-1196.

Kang, W. K., Y. H. Kim, H. A. Kang, K. S. Kwon, and J. Y. Kim, (2015). Sir2 phosphorylation through cAMP-PKA and CK2 signaling inhibits the lifespan extension activity of Sir2 in yeast. eLife. 4: e09709.

Kellis, M., B. W. Birren, and E. S. Lander, (2004). Proof and evolutionary analysis of ancient genome duplication in the yeast *Saccharomyces cerevisiae*. Nature. 428: 617-624.

Klar, A. J., J. N. Strathern, J. R. Broach, and J. B. Hicks, (1981). Regulation of transcription in expressed and unexpressed mating type cassettes of yeast. Nature. 289: 239-44.

Klass, M. R., (1977). Aging in the nematode *Caenorhabditis elegans*: major biological and environmental factors influencing life span. Mech. Ageing Dev. 6: 413-429.

Koubova, J., and L. Guarente, (2003). How does calorie restriction work? Genes Dev. 17: 313-321.

Książek, K., (2010). Let's stop overlooking bacterial aging. Biogerontology. 11: 717-723.

Kueng, S., M. Oppikofer, and S. M. Gasser, (2013). SIR proteins and the assembly of silent chromatin in budding yeast. Annu. Rev. Genet. 47: 275-306.

Landry, J., A. Sutton, S. T. Tafrov, R. C. Heller, J. Stebbins, *et al*., (2000a). The silencing protein SIR2 and its homologs are NAD-dependent protein deacetylases. Proc. Natl. Acad. Sci. U S A. 97: 5807-5811.

Landry, J., J. T. Slama, and R. Sternglanz, (2000b). Role of NAD(+) in the deacetylase activity of the SIR2-like proteins. Biochem. Biophys. Res. Commun. 278: 685-690.

Lawrence, J. F., (1987). Recent developments in derivatization for the chromatographic determination of food additives. J. Chromatogr. Sci. 125: 444-452.

Leaver, I. H. and F. G. Lennox, (1965). STUDIES ON THE PHOTO DEGRADATION OF TRYPTOPHAN. Photochemistry and Photobiology. 4: 491–497.

Lee, S. E., F. Pâques, J. Sylvan, and J. E. Haber, (1999). Role of yeast *SIR* genes and mating type in directing DNA double-strand breaks to homologous and non-homologous repair paths. Curr. Biol. 9: 767-770.

Leigh, E. G. Jr., (2010). The group selection controversy. J. Evol. Biol. 23: 6-19.

Lin, S. J., P. A. Defossez, and L. Guarente, (2000). Requirement of NAD and *SIR2* for life-span extension by calorie restriction in *Saccharomyces cerevisiae*. Science. 289: 2126-2128.

Lin, S. J., M. Kaeberlein, A. A. Andalis, L. A. Sturtz, P. A. Defossez, *et al.*, (2002). Calorie restriction extends *Saccharomyces cerevisiae* lifespan by increasing respiration. Nature. 418: 344-348.

Lindstrom, D. L., and D. E. Gottschling, (2009). The mother enrichment program: a genetic system for facile replicative life span analysis in *Saccharomyces cerevisiae*. Genetics. 183: 413-422.

Lin, Y. Y., J. Y. Lu, J. Zhang, W. Walter, W. Dang, *et al.*, (2009). Protein acetylation microarray reveals that NuA4 controls key metabolic target regulating gluconeogenesis. Cell. 136: 1073-1084.

Liu, T. Y., A. E. Dodson, J. Terhorst, Y. S. Song, and J. Rine, (2016). Riches of phenotype computationally extracted from microbial colonies. Proc. Natl. Acad. Sci. U S A. 113: E2822-E2831.

Longo, V. D., (2003). The Ras and Sch9 pathways regulate stress resistance and longevity. Exp. Gerontol. 38: 807-811.

Longo, V. D., E. B. Gralla, and J. S. Valentine, (1996). Superoxide dismutase activity is essential for stationary phase survival in *Saccharomyces cerevisiae*. Mitochondrial production of toxic oxygen species *in vivo*. J. Biol. Chem. 271: 12275-12280.

Longo, V. D., G. S. Shadel, M. Kaeberlein, and B. Kennedy, (2012). Replicative and chronological aging in *Saccharomyces cerevisiae*. Cell Metab. 16: 18-31.

Longo, V. D., and P. Fabrizio, (2012). Chronological aging in Saccharomyces cerevisiae. Subcell. Biochem. 57: 101-121.

Loo, S., and J. Rine, (1994). Silencers and domains of generalized repression. Science. 264: 1768-1771.

Lu, S. P., and S. J. Lin, (2011). Phosphate-responsive signaling pathway is a novel component of NAD+ metabolism in Saccharomyces cerevisiae. J. Biol. Chem. 286: 14271-14281.

Lu, S. P., M. Kato, and S. J. Lin, (2009). Assimilation of endogenous nicotinamide riboside is essential for calorie restriction-mediated life span extension in *Saccharomyces cerevisiae*. J. Biol. Chem. 284: 17110-17119.

Mair, W., and A. Dillin, (2008). Aging and survival: the genetics of life span extension by dietary restriction. Annu. Rev. Biochem. 77: 727-754.

Martínez-Redondo, P., and A. Vaquero, (2013). The diversity of histone versus nonhistone sirtuin substrates. Genes Cancer. 4: 148-163.

Maruyama, Y., T. Ito, H. Kodama, and A. Matsuura, (2016). Availability of Amino Acids Extends Chronological Lifespan by Suppressing Hyper-Acidification of the Environment in *Saccharomyces cerevisiae*. PLoS One. 11: e0151894.

McCay, C. M., M. F. Crowell, and L. A. Maynard, (1935). The effect of retarded growth upon the length of life span and upon the ultimate body size. Nutrition. 5: 155-171.

McCord, R., M. Pierce, J. Xie, S. Wonkatal, C. Mickel, *et al*., (2003). Rfm1, a novel tethering factor required to recruit the Hst1 histone deacetylase for repression of middle sporulation genes. Mol. Cell. Biol. 23: 2009-2016.

Medvedik, O., D. W. Lamming, K. D. Kim, and D. A. Sinclair. (2007). *MSN2* and *MSN4* link calorie restriction and TOR to sirtuin-mediated lifespan extension in *Saccharomyces cerevisiae*. PLoS Biol. 5: e261.

Mei, S. C., and C. Brenner, (2015). Calorie restriction-mediated replicative lifespan extension in yeast is non-cell autonomous. PLoS Biol. 13: e1002048.

Moazed, D., A. Kistler, A. Axelrod, J. Rine, and A. D. Johnson, (1997). Silent information regulator protein complexes in *Saccharomyces cerevisiae*: a SIR2/SIR4 complex and evidence for a regulatory domain in *SIR4* that inhibits its interaction with SIR3. Proc. Natl. Acad. Sci. U S A. 94: 2186-2191.

Mortimer, R. K., and J. R. Johnston, (1959). Life span of individual yeast cells. Nature. 183: 1751-1752.

Nevoigt, E., and U. Stahl, (1997). Osmoregulation and glycerol metabolism in the yeast *Saccharomyces cerevisiae*. FEMS Microbiol. Rev. 21: 231-241.

Ohashi, K., S. Kawai, and K. Murata, (2013). Secretion of quinolinic acid, an intermediate in the kynurenine pathway, for utilization in NAD+ biosynthesis in the yeast *Saccharomyces cerevisiae*. Eukaryot. Cell. 12: 648-653.

Oliva, J., T. Garde-Cerdán, A. M. Martínez-Gil, M. Salinas, and A. Barba, (2011). Fungicide effects on ammonium and amino acids of Monastrell grapes. Food chemistry. 129: 1676-1680.

Orlandi, I., D. Pellegrino Coppola, M. Strippoli, R. Ronzulli, and M. Vai, (2016). Nicotinamide supplementation phenocopies *SIR2* inactivation by modulating carbon metabolism and respiration during yeast chronological aging. Mech. Ageing Dev. 6374: 30092-30096.

Piper, M. D., and A. Bartke, (2008). Diet and aging. Cell Metab. 8: 99-104.

Proctor, B. L., (1983). Recent developments in mass spectrometry for the analysis of complex mixtures. Annu. Rev. Pharmacol. Toxicol. 23: 171-192.

Rine, J., and I. Herskowitz, (1987). Four genes responsible for a position effect on expression from *HML* and *HMR* in *Saccharomyces cerevisiae*. Genetics. 116: 9-22.

Rine, J., J. N. Strathern, J. B. Hicks, and I. Herskowitz, (1979). A suppressor of mating-type locus mutations in *Saccharomyces cerevisiae*: evidence for and identification of cryptic mating-type loci. Genetics. 93: 877-901.

Rogina, B., and S. L. Helfand, (2004). Sir2 mediates longevity in the fly through a pathway related to calorie restriction. Proc. Natl. Acad. Sci. U S A. 101: 15998-16003.

Rose, M. R., (1991). *Evolutionary biology of aging*. Oxford University Press, New York.

Rose, M. R., T. Flatt, J. L. Graves, L. F. Greer, D. E. Martinez, *et al.*, (2012). What is Aging? Front. Genet. 3: 134.

Rusche, L. N., A. L. Kirchmaier, and J. Rine, (2003). The establishment, inheritance, and function of silenced chromatin in *Saccharomyces cerevisiae*. Annu. Rev. Biochem. 72: 481-516.

Sanchez, P.C., (2008). *Philippine Fermented Foods: Principles and Technology*. The University of The Philippines Press, Quezon City.

Sandmeier, J. J., I. Celic, J. D. Boeke, and J. S. Smith, (2002). Telomeric and rDNA silencing in *Saccharomyces cerevisiae* are dependent on a nuclear NAD(+) salvage pathway. Genetics. 160: 877-889.

Santos, J., C. Leão, and M. J. Sousa, (2012). Growth culture conditions and nutrient signaling modulating yeast chronological longevity. Oxid. Med. Cell. Longev. 2012: 680304.

Schleit, J., B. M. Wasko, and M. Kaeberlein, (2012). Yeast as a model to understand the interaction between genotype and the response to calorie restriction. FEBS Lett. 586: 2868-2873.

Shou, W., J. H. Seol, A. Shevchenko, C. Baskerville, D. Moazed, *et al*., (1999). Exit from mitosis is triggered by Tem1-dependent release of the protein phosphatase Cdc14 from nucleolar RENT complex. Cell. 97: 233-244.

Shrivastav, M., L. P. De Haro, and J. A. Nickoloff, (2008). Regulation of DNA double-strand break repair pathway choice. Cell Res. 18: 134-147.

Singh, J., and A. J. Klar, (1992). Active genes in budding yeast display enhanced in vivo accessibility to foreign DNA methylases: a novel in vivo probe for chromatin structure of yeast. Genes Dev. 6: 186-196.

Slator, A., (1908). XXI.--Studies in fermentation. Part II. The mechanism of alcoholic fermentation. Journal of the Chemical Society, Transactions. 93: 217-242.

Smith, D. L. Jr., J. M. McClure, M. Matecic, and J. S. Smith, (2007). Calorie restriction extends the chronological lifespan of *Saccharomyces cerevisiae* independently of the Sirtuins. Aging Cell. 6: 649-662.

Smith, J. S., C. B. Brachmann, I. Celic, M. A. Kenna, S. Muhammad, *et al.*, (2000). A phylogenetically conserved NAD+-dependent protein deacetylase activity in the Sir2 protein family. Proc. Natl. Acad. Sci. U S A. 97: 6658-6663.

Smith, J. S., and J. D. Boeke, (1997). An unusual form of transcriptional silencing in yeast ribosomal DNA. Genes Dev. 11: 241-254.

Steakley, D. L., and J. Rine, (2015). On the Mechanism of Gene Silencing in *Saccharomyces cerevisiae*. G3 (Bethesda). 5: 1751-1763.

Straight, A. F., W. Shou, G. J. Dowd, C. W. Turck, R. J. Deshaies, *et al*., (1999). Net1, a Sir2-associated nucleolar protein required for rDNA silencing and nucleolar integrity. Cell. 97: 245-256.

Taormina, G., and M. G. Mirisola, (2014). Calorie restriction in mammals and simple model organisms. Biomed. Res. Int. 2014: 308690.

Tatar, M., (2009). Can we develop genetically tractable models to assess healthspan (rather than life span) in animal models? J. Gerontol. A. Biol. Sci. Med. Sci. 64: 161-163.

Thrower, D. A., and K. Bloom, (2001). Dicentric chromosome stretching during anaphase reveals roles of Sir2/Ku in chromatin compaction in budding yeast. Mol. Biol. Cell. 12: 2800-2812.

Thurtle, D. M., and J. Rine, (2014). The molecular topography of silenced chromatin in *Saccharomyces cerevisiae*. Genes Dev. 28: 245-258.

Tissenbaum, H. A., and L. Guarente, (2001). Increased dosage of a *sir-2* gene extends lifespan in *Caenorhabditis elegans*. Nature. 410: 227-230.

Tsukamoto, Y., J. Kato, H. Ikeda, (1997). Silencing factors participate in DNA repair and recombination in *Saccharomyces cerevisiae*. Nature. 388: 900-903.

Valdés-Hevia, M. D., R. de la Guerra, and C. Gancedo, (1989). Isolation and characterization of the gene encoding phosphoenolpyruvate carboxykinase from *Saccharomyces cerevisiae*. FEBS Lett. 258: 313-316.

Valencia, M., M. Bentele, M.B. Vaze, G. Herrmann, E. Kraus, *et al*., (2001). *NEJ1* controls non-homologous end joining in *Saccharomyces cerevisiae*. Nature. 414: 666-669.

van Maris, A.J., D. A. Abbott, E. Bellissimi, J. van den Brink, M. Kuyper, *et al*., (2006). Alcoholic fermentation of carbon sources in biomass hydrolysates by *Saccharomyces cerevisiae*: current status. Antonie Van Leeuwenhoek. 90: 391-418.

Vaquero, A., M. B. Scher, D. H. Lee, A. Sutton, H. L. Cheng, *et al*., (2006). SirT2 is a histone deacetylase with preference for histone H4 Lys 16 during mitosis. Genes Dev. 20: 1256-1261.

Wade, J. T., D. B. Hall, and K. Struhl, (2004). The transcription factor Ifh1 is a key regulator of yeast ribosomal protein genes. Nature. 432: 1054-1058.

Wasko, B. M., D. T. Carr, H. Tung, H. Doan, N. Schurman, *et al*., (2013). Buffering the pH of the culture medium does not extend yeast replicative lifespan. F1000Res. 2: 216.

Wątroba, M., and D. Szukiewicz, (2016). The role of sirtuins in aging and age-related diseases. Adv. Med. Sci. 61: 52-62.

Wei, M., P. Fabrizio, J. Hu, H. Ge, C. Cheng, *et al.*, (2008). Life span extension by calorie restriction depends on Rim15 and transcription factors downstream of Ras/PKA, Tor, and Sch9. PLoS Genet. 4: e13.

Weinberger, M., A. Mesquita, T. Caroll, L. Marks, H. Yang, *et al.*, (2010). Growth signaling promotes chronological aging in budding yeast by inducing superoxide anions that inhibit quiescence. Aging (Albany NY). 2: 709-726.

Werner-Washburne, M., E. Braun, G. C. Johnston, and R. A. Singer, (1993). Stationary phase in the yeast Saccharomyces cerevisiae. Microbiol. Rev. 57: 383-401.

White, J., (1955). Effect of seeding rate and sugar concentration on yeast growth and fermentation in aerated glucose worts. Journal of the Institute of Brewing. 61: 146-150.

Wilson, J. M., V. Q. Le, C. Zimmerman, R. Marmorstein, and L. Pillus, (2006). Nuclear export modulates the cytoplasmic Sir2 homologue Hst2. EMBO Rep. 7: 1247-1251.

Wolfe, K. H., and D. C. Shields, (1997). Molecular evidence for an ancient duplication of the entire yeast genome. Nature. 387: 708-713.

Xie, J., M. Pierce, V. Gailus-Durner, M. Wagner, E. Winter, *et al.*, (1999). Sum1 and Hst1 repress middle sporulation-specific gene expression during mitosis in Saccharomyces cerevisiae. EMBO J. 18: 6448-6454.

Zahn, J. M., S. Poosala, A. B. Owen, D. K. Ingram, A. Lustig, *et al.*, (2007). AGEMAP: a gene expression database for aging in mice. PLoS Genet. 3: e201.

Zhang, Y., C. Luo, K. Zou, Z. Xie, O. Brandman, *et al.*, (2012). Single cell analysis of yeast replicative aging using a new generation of microfluidic device. PLoS One. 7: e48275.

Zhu, M., J. Miura, L. X. Lu, M. Bernier, R. DeCabo, *et al.*, (2004). Circulating adiponectin levels increase in rats on caloric restriction: the potential for insulin sensitization. Exp. Gerontol. 39: 1049-1059.

Zill, O. A., and J. Rine, (2008). Interspecies variation reveals a conserved repressor of alpha-specific genes in *Saccharomyces* yeasts. Genes Dev. 22: 1704-1716.